AN INVESTIGATION OF FISCHER-TROPSCH REACTION FOR SYNTHESIS OF HYDROCARBONS AND ALCOHOLS

Thesis submitted in accordance with the requirement of Cardiff University for the degree of Doctor of Philosophy

Sarwat Iqbal

2009

ProQuest LLC
789 East Eisenhower Parkway
P.O. Box 1346
Ann Arbor, MI 48106-1346

DECLARATION

This work has not previously been accepted in substance for any degree and is not concurrently submitted in candidature for any degree.

Signed ..... (Candidate) Date 14.09.2009

STATEMENT 1

This thesis is being submitted in partial fulfillment of the requirements for the degree of PhD

Signed ..... (Candidate) Date 14.09.2009

STATEMENT 2

This thesis is the result of my own independent work/investigation, except where otherwise stated. Other sources are acknowledged by explicit references.

Signed ..... (Candidate) Date 14.09.2009

STATEMENT 3

I hereby give consent for my thesis, if accepted, to be available for photocopying and for inter-library loan, and for the title and summary to be made available to outside organizations.

Signed ..... (Candidate) Date 14.09.2009

STATEMENT 4: PREVIOUSLY APPROVED BAR ON ACCESS

I hereby give consent for my thesis, if accepted, to be available for photocopying and for inter-library loans **after expiry of a bar on access previously approved by the Graduate Development Committee.**

Signed ..... (Candidate) Date 14.09.2009

Abstract

Fischer Tropsch (FT) technology as a source of alternate fuels is unique. The FT products are of excellent quality and their environmental properties are valuable in increasing drive towards cleaner fuels. There was surge of interest in FT in the thirties and fifties (during the Second World War) and now again in last couple of years.

Fischer Tropsch technology has a disadvantage of broad product spectrum. There is strong requirement of improvement in the optimization of reaction in order to get a maximum yield of high value commercial products, mainly high value molecular weight products, alcohols and short chain hydrocarbons. Most of the investigations reported in this thesis have dealt with study and possible modifications in the preparation and reaction conditions of previously studied $CoMnO_x$ catalyst. Co-precipitation method for preparation of this catalyst has been studied in detail. Precipitation by variable pH has been found to be better than constant pH. pH, ageing time of precipitates and temperature of precipitation mixture are very important parameters which affect the selectivity pattern of products. This selectivity pattern was found to be further influenced by reaction temperature and pressure during CO hydrogenation reaction.

An improvement in the selectivities for CO hydrogenation reaction has been developed using a modified co-precipitated Co/Mn oxide catalyst. This modification was achieved by using two different metal promoters. i.e., Potassium and ruthenium. Addition of these promoters has influenced the catalytic properties in a variety of ways as was observed from characterization and reaction results. Addition of small quantity of potassium

(0.15%), and ruthenium (0.1%) promoters shifted the product spectrum to long chain hydrocarbons along with decrease in methane selectivity.

Further improvements in catalytic activity and selectivity were made by addition of two different types of activated carbons (wood and peat shell) into Co/Mn catalyst. Co and Mn impregnated on wood peat carbon were found to be highly selective for high molecular weight hydrocarbons along with low selectivity of CO_2 compared with pure $CoMnO_x$ catalyst. An increase in concentration of metals with these carbons showed an increase in selectivity of CO_2. One particular catalyst system of iron and manganese was studied with peat and wood carbons and was found to be highly selective for CO_2 formation.

Alcohols, an important product of FT reaction are a good substitute to motor fuel which can enhance the octane number and can reduce the environmental pollution. Cobalt molybdenum sulphide is a patented catalyst system for alcohols synthesis. Present study has investigated the influence of transition metal promoters on selectivity pattern of this catalyst. Ti, Ni and Zr metals have been used as promoters. Addition of Ni and Ti into $CoMoS_2$ have shown good catalytic activity but the major product was CO_2. Zr addition has shown less CO_2 and more hydrocarbons. Pure $CoMoS_2$ catalyst was found to be better for synthesis of higher alcohols.

To my mother

ACKNOWLEDGEMENTS

I would like to express my sincere gratitude to the following people who helped me in completion of my studies.

My academic supervisor Prof. Graham Hutchings for giving me this opportunity to work in his group and for his guidance and encouragement throughout this project.

My industrial supervisor Dr. Khalid Karim (SABIC) for his keen interest in the project providing continued support and advice.

Mr. Tahir Hussain and Dr. Saleh. A Al-Sayari (SABIC) for their useful suggestions and input.

Dr.Thomas Davies for his assistance. His invaluable efforts were especially appreciated in completion of this work.

Dr. Albert Carley, for providing much help and inspiration, in particular for XPS analysis.

Dr. Stuart Taylor and Dr. Jonathan Bartley for always being there to help me in research as well as many other difficult situations.

Alun, John, Steve, Richard and Mal, without whom my research would have been much more difficult- thanks for all reactor work and trouble-shooting.

My parents, for their endless love, motivation and understanding.

Finally, I would like to acknowledge SABIC for financial support.

CONTENTS

Contents

Contents

Contents

LIST OF TABLES

List of Tables

List of Tables

LIST OF FIGURES

LIST OF ABBREVIATIONS

BET – Brunaur, Emmett, Teller (surface area)

EDX – Energy Dispersive X-ray Spectroscopy

FID – Flame Ionization Detector

FT – Fischer-Tropsch Synthesis

GHSV – Gas Hourly Space Velocity

SEM – Scanning Electron Microscopy

SF – Sulz-Flory Distribution

TCD – Thermal Conductivity Detector

TPR – Temperature Programme Reduction

XPS – X-ray Photoelectron Spectroscopy

XRD – X-ray Powder Diffraction

Chapter 1

Introduction

1.1 Aims and Objectives

The objective of this research project was synthesis of high value products from the reaction of synthesis gas over a suitable catalyst.

Fischer-Tropsch (FT) products consist of mixture of low and high molecular weight products. A large amount of resources is used in the separation of products formed in F-T reaction. Therefore synthesis of a catalyst with an improved selectivity for high value products is of commercial importance. High molecular weight waxes can be hydrocracked down to valuable products. The market for the speciality wax products is small compared to the markets for lubricant based oils and very much smaller than the

market for distillates that are produced by hydrocracking the wax. Medium molecular weight products can be used as liquid transport fuels. Low molecular weight products can be divided into low and high value products. Methane is a highly favourable product in Fischer Tropsch (F-T) reaction and can be obtained in 100% selectivity. But it is of minor value and is sold as town gas. Low molecular weight (C_2-C_4) olefins are extremely useful products for petrochemical industry and can also be oligomerized to a very good quality diesel. The market for the use of ethane and propane to produce plastics in petrochemical industry is large. They command significantly higher prices than fuels. Butene is also useful petrochemical feed stock. C_3 together with the C_4 paraffins may be sold as liquefied petroleum gas. In addition to hydrocarbons, various oxygenated products are formed in FT reaction. Alcohols are considered as potential substitute for motor fuels because of their environmental friendly behaviour.

Initial development of catalyst in the present study was based on findings of Hutchings *et al.* [1-4] using $CoMnO_x$ catalyst for synthesis of hydrocarbons. Further some studies were done for alcohols formation using $CoMoS_2$ catalyst.

1.2 Heterogeneous Catalysis

Heterogeneous catalysis has influenced our lives greatly in the 20th century. In 1908, the German chemist Fritz Haber succeeded in synthesizing ammonia by feeding N_2 and H_2 at high pressure over an osmium catalyst. Carl Bosch and Alwin Maittasch picked this discovery and tested over 2500 different materials until they found an iron-based compound active enough to serve as a commercial catalyst. The Haber-Bosch ammonia

synthesis has become an important chemical process worldwide through which nitrogen fixation provided mankind with a much-needed fertilizer.

In 1930s there was development of three important types of refinery catalysts, for hydrocarbon cracking, alkylation and dehydrogenation. Heterogeneous catalysis played a major role in warfare, using new cracking and alkylation catalysts. The Allied forces produced higher octane aviation fuel which gave their aircraft superior performance over the Messerschmitt in the famous battle of Britain.

Another important catalytic process which emerged was the Fischer-Tropsch synthesis. Germany and Japan had an abundance of coal, but no reliable source of petroleum. The Co/Fe-catalyzed Fischer-Tropsch process converted coal to syngas. Further reaction of syngas gave a liquid mixture which was rich in C_5-C_{11} olefins and paraffins. South Africa also used this process for converting coal to compensate for its shortage of a petroleum supply. Fischer Tropsch-type processes are now back in demand as governments seek sulfur-free fuels and alternatives to petroleum [5].

1.3 History of Fischer-Tropsch (FT) reaction (CO hydrogenation)

The history of this process started in early 1900s, when Sabatier and Senderens discovered that synthesis gas (CO/H_2) can be converted to methane over reduced cobalt and nickel catalysts at atmospheric pressure and temperatures from 200 to 300°C [6]. Badische Anilin and Soda Fabrik (BASF) followed this work in 1913. They took out two patents [7] on the synthesis of oxygenates using cobalt and osmium catalysts at high pressure. In 1923 Franz Fischer and Hans Tropsch of the Kaiser Wilhelm Institute at Ruhr discovered that alkalized iron catalysts at high pressure (100 to 150 atmospheres

and 400 to 450°C) can produce an oily liquid mixture consisting of oxygenated compounds [8]. The same catalyst was reported to be active for the production of linear hydrocarbons at low pressure, but these catalysts deactivated rapidly [9, 10] and a search was started for an improved catalyst. Fischer and Tropsch observed an enhancement in the selectivity of hydrocarbons by using a combination of iron and zinc oxide [11, 12]. This discovery started an intensive research for metal catalysts for the production of commercial Fischer Tropsch catalyst which is active at low pressure. Early results showed that high pressure was unsuitable for the synthesis of higher hydrocarbons so the catalytic tests were conducted at low pressures. The choice of atmospheric operating pressures were satisfactory for cobalt and nickel catalysts but was not suitable for iron catalysts which operate best in the range 7-30 atmospheres. As a result, the development of practical iron catalysts was delayed for many years. Initial experiments showed that nickel was unsuitable because of its rapid deactivation and high methanation reaction. Later this research was switched to cobalt because of the poor yields and rapid deactivation trends of iron catalyst. In 1934 Ruhrchemie AG achieved the first Fischer – Tropsch plant license using a cobalt thorium oxide catalyst. Eighteen plants were licensed for this process in Germany, Japan, France and Manchuria until 1945 in order to supplement limited petroleum resources. World War II destroyed most of the German plants and the remainings were forced to shut down for several years. At that time there was a decline of interest in the Fischer – Tropsch process in Europe because of an increase in coal prices. After World War II a programme was funded by U.S.Bureau of mines because of the fear for the shortage of petroleum. Various test facilities were constructed by using the reports from German plants. Fixed bed reactors were developed

by two German firms, Ruhrchemie and Lurgi (Arbeitgemeinschaft), using a precipitated iron catalyst. This catalyst was aimed to produce high yield of waxes. Later several companies in USA developed fluidized bed reactors (Standard Oil and Hydrocarbon Research Inc.) with Kellogg Co. with a circulating entrained catalyst version of the reactor [13]. Interest in these processes was decreased by the discovery of immense reserves of petroleum in Middle East in later 1940s and mid 1950s. The plants in US could not compete with the low oil price and were subsequently closed [14].

The most important event in further developments of coal liquefaction was commissioning of a plant in 1955 by South African Coal, Oil and Gas Corporation (SASOL). This plant has been in commercial operation ever since. The plant incorporated both the fixed bed (Arbeitgemeinschaft) reactors and Synthol reactors (Kellogg). Iron based catalysts along with various promoters are used in both reactors.

In 1973, the OPEC embargo increased oil prices and it was realized that crude oil supplies could become limited in future. This realization renewed an interest in synthetic fuel and coal along with other alternatives like wind, water, solar, geothermal and nuclear resources. A lot of effort was put into researching the Fischer-Tropsch synthesis process which already existed as a proven method for the synthesis of fuels and chemicals from coal. The United States exerted a leading role in this research. In 1981, the investment in synfuel research in the US began to suffer and declined to a minimal level in late 1980s. Other nations reduced their investments in alternative energy resources. However, there has been a renewal of interest in the Fischer – Tropsch reaction after the current Gulf oil crisis.

The Fischer – Tropsch process is an indirect method for the formation of products using synthesis gas (derived from coal). Coal can be converted into liquid fuels and chemicals using various direct methods e.g. Pyrolysis (coal decomposition to liquids) and the Bergius hydrogenation reaction (where hydrogen gas and an organic solvent are reacted with the coal to produce methane and liquid hydrocarbons). It has been estimated that 80% of the global energy consumption depends on fossil fuels, which include oil, natural gas and coal. These fuels are unsustainable and estimated availabilities at current rate of production are: 40 years for oil, 65 years for natural gas and 155 years for coal. In contrast to the limited resources, world demands for energy, particularly for oil, are increasing markedly because of the growing population and the world development. More than 60% of the oil is consumed in the transportation sector in forms of gasoline, diesel and jet fuel. The transportation industry is expected to remain highly dependent on oil in the future [15]. The limited natural reserves of oil will drive the world rapidly to peak production and consumption, after which a permanent shortage of oil can be expected. Hence, an alternative route for generating transportation fuel is highly desirable. The Fischer Tropsch (FT) process is one of the processes that are being developed [16] to offer a solution to this problem. The quality of the feed products formed along with a non-crude oil feedstock suggests the FT process should play an important role in the worldwide energy supply in the coming decades [17]. The FT synthesis for the CO hydrogenation to linear C_{2+} hydrocarbons continues to attract considerable research attention [18].

1.4 Preparation of Synthesis gas

Synthesis gas also called as syngas consists of a mixture of carbon monoxide and hydrogen. Syngas can be prepared from coal gasification ($C + H_2O \leftrightarrow CO + H_2$) which involves a thermal balance between the endothermic reactions of carbon with steam and carbon dioxide and the exothermic reaction of carbon with oxygen. Many additional processes occur in the gasifiers e.g., coal devolatilization (coal → char + volatile), water gas shift and methanation reactions [19]. Several other methods are used for the synthesis of syngas which are detailed in table 1.1.

Table 1.1 Syngas generation processes

Process	Equation	
Coal gasification	$C + H_2O \leftrightarrow CO + H_2$	(1.1)
Steam reforming of methane	$CH_4 + H_2O \leftrightarrow CO + 3H_2$	(1.2)
CO_2 reforming of methane	$CH_4 + CO_2 \leftrightarrow CO + 2H_2$	(1.3)
Methane partial oxidation	$CH_4 + \frac{1}{2}O_2 \leftrightarrow CO + 2H_2$	(1.4)
Autothermal reforming	$2CH_4 + \frac{1}{2}O_2 + H_2O \leftrightarrow 2CO + 5H_2$	(1.5)

The technology used to prepare the synthesis gas can be divided into two main categories, gasification and reforming. Gasification is a general process for conversion of solid or heavy liquid feedstock to synthesis gas and reforming is used for conversion of gaseous or light liquid feedstock to synthesis gas.

Coal gasification is an old method for the production of syngas from coal. During gasification, the coal is mixed with oxygen and steam while also being heated and pressurized. During the reaction, oxygen and water molecules oxidize the coal into carbon monoxide while also releasing hydrogen gas.

Steam reforming of hydrocarbons is the dominating process for the production of hydrogen and carbon monoxide. Steam reforming is often used in combination with various and oxygen or air-blown partial oxidation processes for production of synthesis gas.

1.5 Product distribution

Low selectivity to the desired products is the limitation of F-T reaction. Product distribution from CO hydrogenation has been explained through various theoretical models which can fit and rationalize the distribution of products obtained from F-T catalysts [20-22]. These theoretical models are based on the following assumptions:

(1) Chain growth proceeds via a polymerization process, with growth occurring predominantly in single- carbon increments. (2) The probabilities of increase in chain length and of termination are independent of the length of the oligomer chain attached to the surface. Anderson [23] has derived an analytical function which is similar to the distribution function derived by Schulz and Flory. Anderson – Schulz – Flory (ASF) equation was based on the assumption that the FT synthesis is a polymerization process [24].

$$\frac{W_n}{n} = \frac{(1-\alpha)^2}{\alpha}\alpha^n \qquad (1.6)$$

Where n is the carbon number, Wn is the weight fraction of products with carbon number n, and α is the chain growth probability factor which can be defined as follows:

$$\alpha = \frac{r_p}{r_p + r_t} \qquad (1.7)$$

Where r_p and r_t are the rate of chain growth and rate of chain termination respectively. Both rates are controlled by the reaction conditions and catalyst type. Typical ranges of α on Ru, Co and Fe catalysts were reported as 0.85 – 0.95, 0.70 – 0.80, and 0.50 – 0.70 respectively by Dry [24]. The higher the value of α, the longer the chain length is.

For practical reasons, equation (1.6) is often re-written as:

$$\log\frac{W_n}{n} = n\log\alpha + \log\frac{(1-\alpha)^2}{\alpha} \quad (1.8)$$

A plot of $\log\frac{W_n}{n}$~n is the well-known Schulz-Flory diagram. That gives a linear graph with a slope of $\log\alpha$.

Experimental data that reported deviations from the ASF distribution usually have C_1 yields that are higher than the predicted value and have $C_{>2}$ yield that are lower. The Schulz-Flory equation predicts maximum yields for certain products which are summarize in table 1.2 [25].

Table 1.2 Maximum yields of C_n products from a Schulz-Flory distribution

Product fraction	Maximum selectivity/% by mass
C_1	100
C_2	29
C_2-C_4	57
C_5-C_{11}	48
C_{12}-C_{25}	41

Schulz *et al.* [26] explained the high methane yield by assuming that there was a different catalytic site for the methanation reaction, whereas Dry [24] suggested that heat and mass transfer limitations could result in the thermodynamically favored products. Product distribution is also affected when secondary reactions, such as hydrogenation, isomerization, reinsertion and hydrogenolysis are involved [27-31]. So far, there has been

no single model which could explain all the observed catalytic results. There is an interdependence of selectivities and product distributions are mostly broad.

High selectivity to a single valuable product or narrow distribution of products is always economical. Several attempts are being made in order to develop highly selective systems for syngas conversion to fuels and chemicals. These efforts include modification of F-T catalysts, reactor operating optimization and designs of reactors [32, 33].

1.6 Reactors used in FT synthesis

Design of reactors used in FT synthesis is very closely related to the highly exothermic reactions. Poor removal of heat leads to a temperature built up inside the reactor, which results in high selectivity towards methane. Capital cost for construction, ease of operation, product separation and product selectivity are other important factors to be considered during reactor built up for FT reaction.

There are three common types of reactors developed for FT synthesis: tubular fixed bed reactor, fluidized bed reactor and slurry reactor.

1.6.1 Tubular fixed bed reactor

Figure 1.1 (a) shows tubular fixed bed reactor which is the simplest reactor type. Catalyst is packed inside the reactor tube with syngas flowing from top to bottom. Heat removal is achieved by circulation of cooling medium outside the tubes. The advantage of the fixed bed reactor is ease of operation. But it has low capacities. This type of reactor may experience pressure drop and diffusion limitations along the tubes. The first well studied

commercial reactor, SASOL Arge belongs to the tubular fixed bed reactor type. Shell's Middle Distillate Synthesis (SMDS) in Malaysia uses this reactor type.

1.6.2 Fluidized bed reactor

Fluidized bed reactor is of two types: circulating fluidized reactor (CFB) and fixed fluidized bed (FFB) reactor.

The circulating bed reactor type is shown in figure 1.1 (b). In this type, the catalyst is initially passed down by gravity and then mixed with feed gas and circulated through the reactor zone. The temperature of reaction is maintained with feed gas by cooling medium. After the reaction zone, the mixture of feed gas, products and catalyst is passed to the hopper where products are separated and catalyst loss is replaced by the fresh one. CFB reactor is more complicated in operation however, it provides better control of temperature and a lower pressure drop than a fixed bed reactor. SASOL's synthol reactor is a type of CFB reactor.

Figure 1.1 (c) shows fixed fluidized bed (FFB) reactor. Feed gas is introduced to the reactor from bottom of the reactor and flowing upwards through catalyst bed. The catalyst bed and heat exchanger are suspended inside the reactor. The products are collected from the top of the reactor.Hydrocol at Texas used FFB reactor. Fluidized bed reactor has much higher capacities than that of the fixed bed reactor. However both of these reactors are difficult to scale up than the fixed bed reactor due to the complexity of gas-solid contacting as a function of the reactor diameter.

1.6.3 Slurry Phase reactors

A slurry phase reactor is similar to a FFB reactor except that the catalyst is suspended in a molten FT wax. This reactor is not found to be a competitor for the FFB/CFB systems, since slurry bed reactor is reported to have lower conversion at 320°C. At this temperature the wax is hydrocracked which results in loss of the liquid medium. However, slurry phase reactor does have a major cost advantage for the production of waxes at lower temperatures. Due to a simpler construction the slurry reactor is expected to be approximately 45% cheaper than the same capacity multi tubular unit. A good conversion in the slurry bed can be maintained by regular addition of fresh catalyst. This is of commercial advantage because slurry reactors can be kept online for catalyst replacement. The fixed-bed reactors periodically have to be brought offline for replacement of catalysts. SASOL has decided to operate a demonstration unit in order to fully evaluate the slurry process [33].

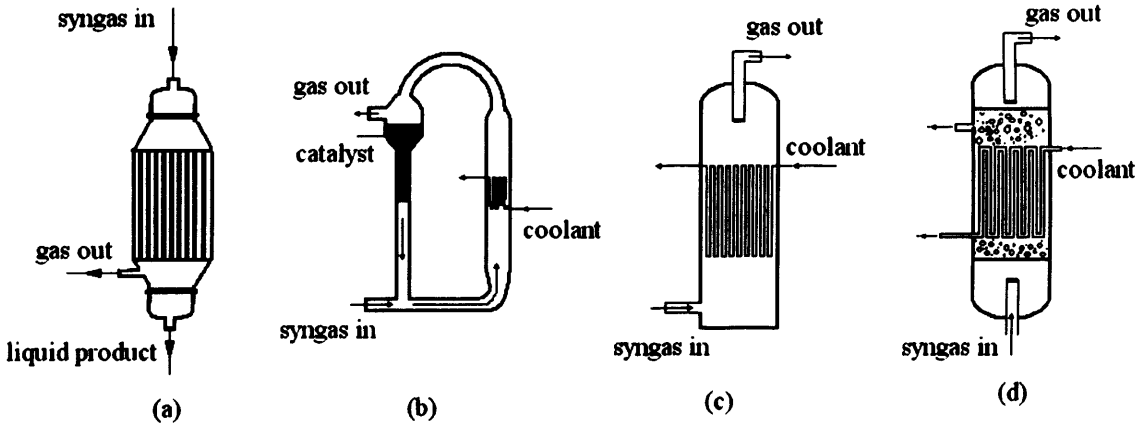

Figure 1.1 FT reactor types a) Tubular fixed bed reactor;b) Circular fluidized bed reactor;c) Fixed fluidized bed reactor;d) Slurry reactor [34]

1.7 CO Hydrogenation - Mechanism

The mechanism of the FT reaction involves the growth of hydrocarbons and oxygenates from the interaction of intermediates derived from CO and H_2. Continuous interaction of monomer with an oligomeric surface species causes chain growth and the final products result from desorption of these species. The mechanism of FT reaction is very complex because of a wide range of products. Various research groups have reviewed the mechanism of hydrocarbon synthesis [16, 35, 36]. Several mechanisms have been proposed for CO hydrogenation reaction which may compete with each other or run in parallel. There are three mechanisms which have been agreed most commonly.

1.7.1 Carbide mechanism

Fisher and Tropsch proposed this mechanism first [37], where the synthesis proceeds by the formation and hydrogenation of metal carbides to give methylene groups which can subsequently be polymerized to yield a broad spectrum of hydrocarbons. This involves dissociation of C-O bond prior to reaction with H_2, which further operates by the insertion of the CH_x group of one M-CH_x species into the M-C bond of another M-CH_x species. This can be presented as follows with simplicity.

CO— > M-CO— > M-C— > M—CH_x— > polymerization

Carbide mechanism was supported by Metterties and Stein [38], Hermann [39] and Olive [40] from homogeneous coordination theory. Laws and Puddephatt [41] have demonstrated ethylene formation by coupling of two methylene groups on a Co cluster. Evidence for CH_2 migration insertion into an M-H bond comes from studies of Carter and Goddard [42]. Saez *et al.* [43] have proposed mechanism for the formation of propene by

bridging two methyles combined with another methyl group on a single Rh atom. These results can provide support to carbide mechanism although the reaction conditions are different compared with FT conditions. There is much evidence [44-46] in favour of the carbide mechanism but it has several flaws. A direct hydrogenation of metal carbide investigated by Kummer *et al.* [47] using labeled ^{14}CO over reduced iron catalyst challenged the carbide mechanism. Their results show that the carbide hydrogenation could be responsible for no more than 8 – 30% of the methane formed. The carbide mechanism could not explain the formation of oxygenated products which is a limitation of carbide mechanism. It is a two or three dimensional polymerization model, with surface carbides combining/inserting in random directions which would lead to larger yield of branched products than observed. It can be concluded that the carbide mechanism cannot fully explain the total product stream.

1.7.2 Hydroxycarbene mechanism

Emmett [48] developed an alternative to the carbide mechanism to explain the product stream in detail. A similar mechanism was proposed by Storch *et al.* [49] where CO is chemisorbed on the metal atoms without dissociation and C-C bond formation occurs by hydroxylcarbene intermediate M-CHOH. The intermediate is formed by the interaction of non-dissociatively adsorbed CO reacting with hydrogen. The intermediate takes part in condensation leading to C-C bond formation and chain growth. Chain termination and desorption of products takes place by hydrogenation of the intermediate to an alcohol. One simple illustration of this mechanism is shown in figure 1.2.

This mechanism can successfully explain the formation of oxygenates and branched products. Various research groups have supported this mechanism [50-53].

Voevodskii [54] suggested a variation of hydroxycarbene mechanism. They proposed formation of carbene species by the hydrogenation of hydroxycarbene intermediate, which then reacted with CO to start chain growth. The mechanistic pathway of this mechanism is illustrated as follows:

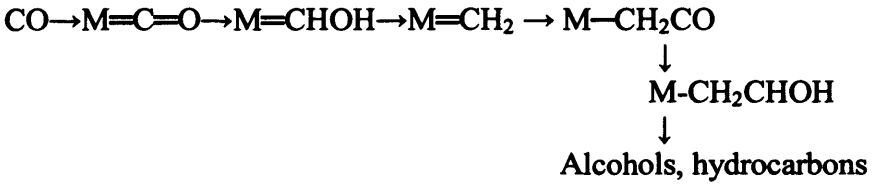

Ekstroom and Lapswzewicz [55] postulated similar mechanism but the carbene undergoes polymerization reaction as was proposed by the carbide mechanism.

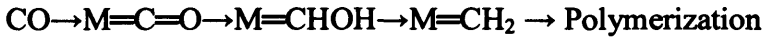

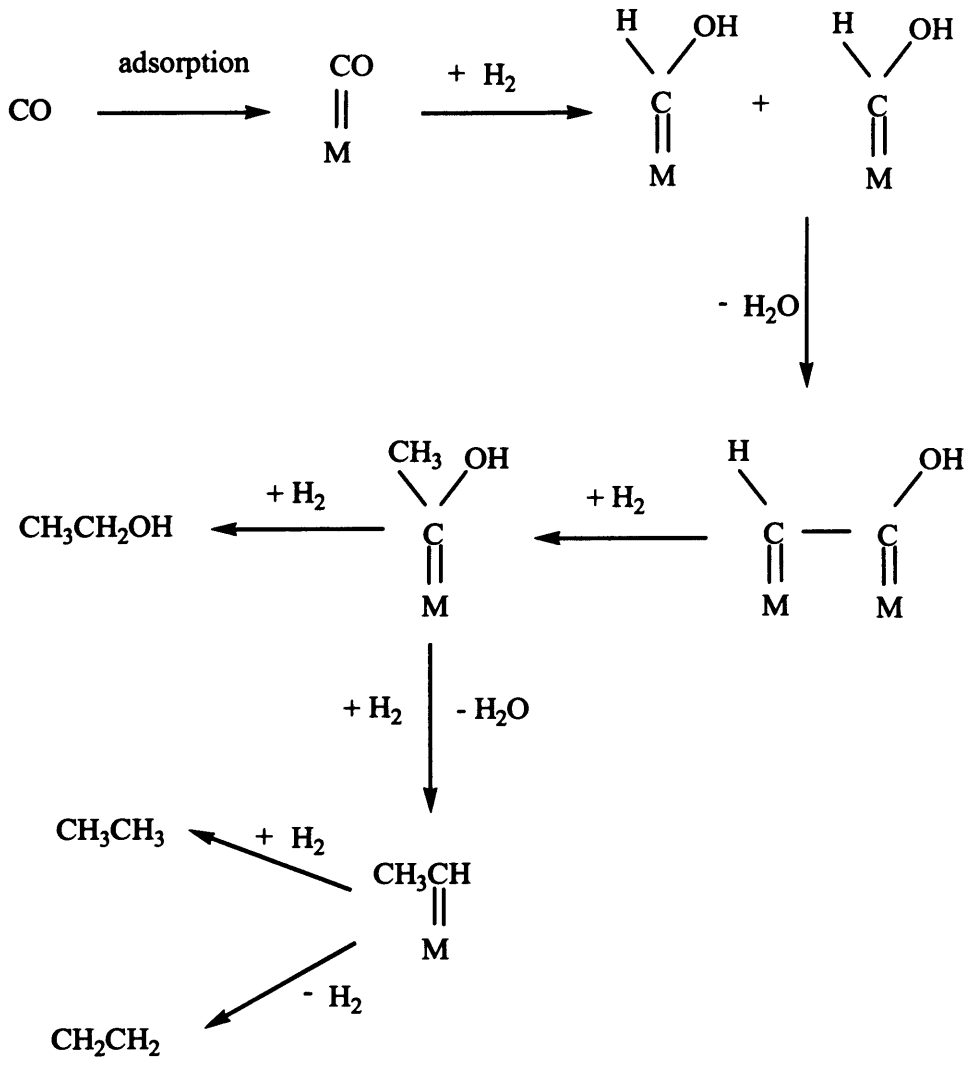

Figure 1.2 The hydroxy-carbene mechanism [34]

1.7.3 CO Insertion mechanism

Pichler and Schulz [56] proposed this mechanism. According to this mechanism the key intermediate is a metal carbonyl M $(CO)_x$ which hydrogenates to $MH(CO)_x$. This is followed by the insertion of a carbonyl group into the M-H bond and subsequent hydrogenation as follows:

$$MH\ (CO)_x \rightarrow MCHO(CO)_{x-1} \rightarrow MCH_3(CO)_{x-1} \rightarrow MCH_3(CO)_x$$

Chain growth is achieved by insertion of CO molecule into metal alkyl bond and subsequent reduction of acyl species.

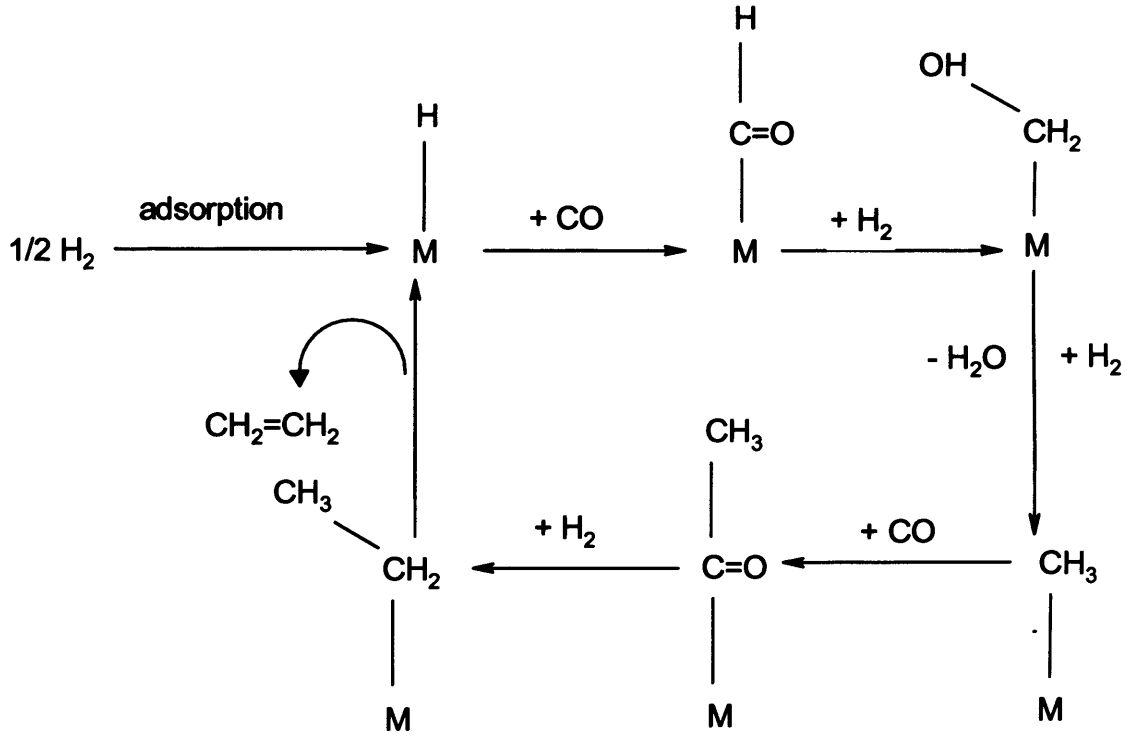

Figure 1.3 The CO insertion mechanism [34]

A large number of products can be obtained following desorption of intermediates. This evidence is supported by various researchers [57-59].

Since the FT reaction is a very complicated catalytic reaction, these mechanisms only provide some possibilities of different routes for the hydrogenation of carbon monoxide. The 'real' mechanism of the CO hydrogenation could be a combination of these routes or maybe is totally different.

1.8 Metal Catalysts used in Fischer - Tropsch (FT) Synthesis

Conversion of syngas into hydrocarbon products requires the presence of suitable metal catalysts. Recent studies emphasize the importance of an active catalyst suitable for the production of hydrocarbons from FTS [60]. The 3d and 4f transition metals (group VIII metals) of the periodic table are particularly suitable for the chemisorption process of CO and H_2 which is the first step of this reaction [61]. Selectivities of various FT catalysts are compared in table 1.3 [62].

Almost all transition metals in group VIII can produce a wide range of products by CO hydrogenation e.g. Pd, Ir, Rh, Os, Ni, Co, Fe, Ru and Pt can produce alcohols and various hydrocarbons. The activity and selectivity of a certain metal catalyst depends on the choice of promoters and supports along with suitable preparation and reaction conditions. Iridium, platinum and palladium exhibit very slight activity and mostly produce alcohols. Rhodium and osmium produce oxygen containing hydrocarbons at high temperatures [63-66]. Ruthenium catalysts can produce paraffins of very high molecular weights. Fe, Co, Ni and Ru are found to be suitable for the production of highest yields of hydrocarbons. Unfortunately, Nickel is found to be unattractive for this process because

of high selectivity to methane. Ru shows very good selectivity for valuable paraffinic waxes but it has been found that world supplies of Ru for the operation of commercial plant would be insufficient in near future. Iron catalyst shows more carburization tendency compared with cobalt. Therefore, cobalt is found to be the most suitable metal for F-T reaction.

Although cobalt is more expensive in comparison with iron but various factors make it economically viable e.g. longer catalyst life time, higher catalytic activity and reproducibility. Titanium, vanadium, chromium and manganese do not find application as the basic metal in F-T catalysts because it is hard to reduce their oxides. But it is found that these metal oxides are important components in F-T catalysts if used as promoters [67-69].

1.9 Cobalt – as an FT catalyst

Cobalt catalyst for FT synthesis was first discovered about 90 years ago. Catalyst technology has advanced from a simple oxide to highly active and highly optimized cobalt catalysts along with various supports and promoters. Advances in cobalt catalyst design can be conveniently discussed in five historical periods:

(1) Discovery (1902-1928), when cobalt catalysts were established as the most active for FT synthesis (2) Commercial development of cobalt and iron catalysts (1929-1928) ,when commercial processes were developed in Germany (3) the iron age (1950-1974),in this age iron catalysts were developed mainly in south Africa and very little work focused on cobalt (4) rediscovery of cobalt (1975-1990) (5) GTL and the return to

cobalt (1991-present),in the (4) and (5) periods cobalt catalysts were rediscovered and developed to commercial application for conversion of natural gas to fuels.

Table 1.3: Typical product selectivity of various FT catalysts

Species	Selectivity
I. Group VIII metals	
Fe	Linear and branched hydrocarbons-alkanes,alkenes and oxygenates
Co	Linear hydrocarbons-alkanes, alkenes
Ni	methane and hydrocarbons
Ru	methane, hydrocarbons, and polyethylene at higher pressures
Rh	C_{2+} oxygenates
Pd	MeOH
Pt	MeOH
II.Mixed Oxides	
Zn oxide	promotes methanol and ethanol formation on Rh
Zr oxide	promotes oxygenate formation on group VIII metals
V oxide	promotes EtOH formation on Rh
Mn oxide	promotes oxygen formation on group VIII metals
Alkali	promotes oxygenate formation on group VIII metals
Th oxide	hydrocarbons, branched alkanes and oxygenates (methanol,$(CH_3)_2O$, branched alcohols
Cr oxide	Methanol and branched alcohols
Cu/Zn	Methanol
$CuCoCr_{0.8}K_{0.09}Ox$	branched higher alcohols
III. Co precipitated nickel based catalysts	
Na: Ni	Methane
Alkali, Mn-Na	Methane + acetaldehyde
IV. Mo-based catalysts	
Mo	hydrocarbons
Alkali-Mo sulphide	C_1-C_5 linear, primary alcohols
Alkali Re-W-Mo	C_1-C_4 alcohols

Various researchers have reported variations in CO hydrogenation activities of supported cobalt catalysts with changes in pretreatment, metal concentration and promoters. Dent and Lin [70] have found the most active catalysts to be Co-Cr_2O_3-kieselguhr and Co-ZrO_2-kieselguhr. Co-MnO-alumina-K_2O has been found to be more selective for light alkenes synthesis. The Gulf patents [71-74] reflect a high level of fundamental understanding of catalyst designs. Iglesia *et al.* [75-78] have reported most important

advances from fundamental studies which lead to a better understanding of relationships between activity and cobalt metal dispersion for supported cobalt catalysts, and effect of precious metal promoters in enhancing reduction of cobalt at lower temperatures along with effect of reaction and readsorption on product selectivity. Goodwin *et al.* [79-85] have reported a relationship of catalysts activity with Zr, La, and Ru promoters.

Cobalt-based FTS catalysts are claimed to have the advantage of a higher conversion rate, high selectivity to paraffins and longer life with considerably clean synthesis gas which leads to higher production rate [86-88]. Supported cobalt metal particles are known to be very active FT synthesis catalysts, because of their high productivity for long chain paraffins. Co-based FT catalysts are prepared usually by impregnation of a porous support such as alumina, silica, titania, or more recently carbon with a solution of a cobalt precursor salt [89-93]. The catalytic performance is known to be a function of both the metal dispersion and the extent of reduction of the oxidic precursor species [94]. The effect of ceria addition on the performance of 10wt. % Co catalysts supported on SiO_2 and Al_2O_3 for Fischer Tropsch synthesis has been investigated by Gheitanchi *et al.* [95]. With the addition of ceria, significant changes in CO conversion and hydrocarbon selectivity are observed. Ceria addition with different loadings to cobalt catalysts enhanced C_5-C_{10} fraction and decreased methane selectivity. Liang *et al.* [96] have reported high yields of light olefins using Co/Mn complex oxides prepared by sol-gel method. Investigations of CO hydrogenation behaviour of iron and cobalt manganese of catalysts indicate that the latter ones exhibit higher activities at lower temperatures with lower methane and higher alkene yields. It has been shown by Ernst *et al.* [97] that the addition of various amounts of cerium oxide modifies significantly the properties of

Co/SiO_2 catalysts in Fischer Tropsch synthesis under pressure, it results in increase in methanation and an orientation of the selectivity towards the C_5-C_{13} fraction at the expense of C_{22+} hydrocarbons while the activity remains almost the same. Addition of Mn to Co catalysts facilitates the reduction of Co_3O_4 and also reduces its particle size [98]. Martinez *et al.* [99] have suggested that a maximum CO conversion is found for the sample with 30 wt. % Co loading supported on SBA-15, the addition of 1 wt. % Re enhances the reducibility of cobalt oxides and increased the catalytic activity. Re also favoured the formation of long chain n-parrafines (C_{10+}) and decreased methane selectivity. Effect of Co catalysts promoted by lanthanum/Al_2O_3 is studied by Ladford *et al.* [100] and this is concluded that, low La contents (up to La/Al = 0.013) promotion on cobalt/alumina has little influence on activity and selectivity of the reduced catalyst in CO hydrogenation. And catalysts with higher loadings of La show a decrease in TOF for CO hydrogenation. And those catalysts prepared by reverse impregnation show a little effect of La on the TOF for CO hydrogenation or selectivity to higher hydrocarbons and olefins. Ernst *et al.* [101] have reported the effect of addition of cerium and lanthanum metals on Co/SiO_2 catalysts. They have adopted sol-gel preparation technique. Addition of cerium and lanthanum enhances methane selectivity along with increase in C_{5+} selectivity and decrease in chain growth probability α. Singleton *et al.* [102] have patented a highly stable cobalt/alumina catalyst doped with lanthanum oxide and barium oxide (in the range of 1% and 5%) that has shown an improvement in thermal stability of the catalyst and enhances the activity. Wanchun *et al.* [103] have patented a catalyst comprising of cobalt, rhenium supported on titania along with boron and phosphorus for the production of C_{12+} hydrocarbons. This has been observed that addition of a very small

amount of phosphorus into cobalt supported catalysts increases CO conversion and C_2 - C_4 selectivity and decreases the C_{5+} oil selectivity [104]. The effect of zirconia addition has been studied by Moradi *et al.* [105]. They have reported an increase in selectivity of higher hydrocarbons by loading zirconium on Co/SiO_2 catalyst.

Mazzone and Fernandes [106] have concluded after a detailed investigation of reaction conditions that conversion of syngas increases with increase in H_2: CO ratio. As the H_2: CO ratio approaches 2 the amount of syngas converted to hydrocarbons (FTS) and water increases. As conversion increases, the water gas shift (WGS) reaction increases its rate due to the production of more water by the FTS reaction. They have also reported that hydrogen is responsible for the termination of hydrocarbon chains into paraffins.As such an increase in the H_2:CO feed ratio will increase the partial pressure of H_2 in the reaction media and thus increases the termination rate into paraffins, reducing the amount of olefins produced by the reaction. At low H_2: CO ratios, the fraction of olefins production is at its maximum since the amount of hydrogen is small enough not to produce great quantities of paraffins. As the H_2:CO ratio increases the termination into paraffin increases and the ratio of olefin to paraffins tends to zero. An increase in the total pressure reduces CO conversion and increases the hydrocarbon yield (about 2 to 25% for each 10 atm increase). This happens because the rate of the FT reaction is directly proportional to the total pressure; the rate of the WGS is not directly affected by the total pressure, but coupled to the H_2O partial pressure, which depends on the conversion level.

Wang *et al.* [107] have studied the influence of La loading on Zr-Co/activated carbon catalysts for FTS. They have observed an increase in CO conversion from 86.4% to

92.3% when low La loading (La=0.2 wt. %) was added into the Zr-Co/activated carbon catalyst.

1.10 Catalyst Promoters

Catalyst promoters play an important role in obtaining a high selectivity to a single product. Promoters are doping agents added to catalyst materials in small amounts in order to improve their activity and selectivity [108]. Promoter elements can be divided into two types on the bases of their action. *Structural Promoters* affect the formation and stability of the active phase of a catalyst material. Metal oxides which are difficult to reduce belong to this category. e.g., Al_2O_3, ThO_2 and MgO [67, 109]. Second type is *Electronic promoters* which directly affect the elementary steps involved in each turnover on the catalyst. Electronic promoters affect the local electronic structure of an active metal mostly by adding or withdrawing electron density near the Fermi level in the valence bond of the metal. This results in a modification of the chemisorption properties of active metal.

The main function of structural promoters is to affect the dispersion of cobalt on support [108]. A high Co dispersion results in a high active Co metal surface and an improved catalytic activity. Structural promotion does not influence the product selectivity but it may increase catalyst activity and stability. Promoter elements can be added to the support oxide resulting in a decreased Co compound formation with the support oxide. More specifically, the formation of cobalt nitrate, cobalt silicate or cobalt aluminate should be avoided under reduction conditions. A related problem is the reduction in the support surface area, specially a problem in the case of titania, where the anatase phase is only stable under oxidative regeneration conditions from 400 to 750°C. The addition of Si,

Zr and Ta as promoter elements may avoid surface collapse of the support. The catalytic performance is known to be a function of both the metal dispersion and the extent of reduction of the oxidic precursor species [110].

Some promoter elements can act as an oxidic interface between the supported Co particle and the support oxide leading to an increased stability of cobalt particles against sintering during reduction or oxidative regeneration. The addition of promoter elements may also lead to increase in cobalt dispersion after preparation. In the absence of promoters, relatively large cobalt crystals are formed, whereas, by addition of these additives, smaller supported cobalt particles are made. Panpranot *et al.* [111] have mentioned that small metal particles composed of a promoter element can dissociate hydrogen in the neighborhood of a supported cobalt particle that leads to the formation of atomic hydrogen which may spill over by diffusion to cobalt. This results in an increase in the number of active sites and therefore a higher catalyst activity. Noble metals such as Re, Pt and Ru are known to act in this manner. In contrast to structural promoters electronic effects are less obvious to be detected. Electronic promotion can only occur when there is a direct interaction between the promoter element and cobalt active surface. A beneficial catalytic effect can be obtained if the deposited metal oxides are not blocking all the active cobalt sites, which would lead to decrease in hydrogen or CO chemisorption. A similar effect occurs with the support oxides which is generally known as the 'strong metal-support interaction' or SMSI effect [108, 112, 113]. SMSI effect is observed in metal supported catalysts. Due to the small particle size of catalytic components, their interaction with the oxide support develops during all stages of catalyst preparation, especially during thermal treatments (calcination, reduction). In most cases the adhesion

forces between reduced metal particles and an oxide support are weak, implying surface bonding through van der Walls forces only. It is expected, therefore that the support exerts little influence on the catalytic and the adsorptive properties of small metal particles. The net result of the SMSI is a decrease in hydrogen chemisorption which results in a decreased hydrogenation activity of the catalyst. This results in lower methane and higher olefin yields in the F-T reaction, when compared to non-SMSI catalysts. This effect has been reported by Hutchings *et al.* [114] and Kugler *et al.* [115] as well. Sizes of metal particles on the catalyst support vary from cluster to a few atoms. Particle size has a strong effect on the catalytic properties of metals. Small particles may have properties which deviate from bulk metal surfaces [116, 117]. Bimetallic alloy formation may also influence the activity and selectivity of Co FT catalysts. Depending on the promoter element added to the cobalt cluster alloying might lead to an increased catalyst activity, selectivity and stability. Table 1.4 shows most commonly investigated promoter metal elements in literature [118].

Table 1.4. Overview of the promotion effects displayed by the different elements reported in the literature for the Co Fischer-Tropsch catalytic performances

Promotion type	Promotion mode	Influence on catalyst			Elements which play a role in this promotion effect
		activity	selectivity	stability	
Structural	Support stabilization	+		+	Mg,Si,Zr,Nb,Rh,La,Ta,Re,Pt
	Cobalt glueing	+		+	B,Mg,Zr
	Cobalt dispersion increase	+		+	Ti,Cr,Mn,Zr,Mo,Ru,Rh,Pd,Ce, Re,Ir,Pt,Th
Electronic	Decorating cobalt surface	+	+	+	B,Mg,K,Ti,V,Cr,Mn,Zr,Mo,La, Ce,Gd,Th
	Cobalt alloying	+	+	+	Ni,Cu,Ru,Pd,Ir,Pt,Re
	Water gas shift	+	+		B,Mn,Cu,Ce
Synergistic	Hydrogenation/dehyd rogenation		+		CrO_x and Pt
	Coke burning			+	Ni,Zr,Gd
	H_2S adsorption			+	B,Mn,Zn,Zr,Mo

1.11 Synthesis of alcohols from syngas

There is an increase in interest for alcohol synthesis since last two decades. Alcohols when used as fuel additives, combust more completely than the traditional fuels and do not have the negative impact on the environment as happened to tetra-ethyl lead and methyl tert-butyl ether (MTBE). With the increasingly tighten environmental law, the use of alcohol in fuel industry is receiving more attention.

Methanol

Methanol is one of the most important chemicals ever developed so far. The majority of methanol is produced *via* the syngas route. The process is a very well developed commercial process with high activity and selectivity. Methanol is widely used as primary raw material and solvent in laboratory as well as in pharmaceutical industry. When used in fuel industry to blend with gasoline, methanol causes problems due to its high blending vapor pressure, low water tolerance and low hydrocarbon solubility.

Ethanol

Ethanol is another important chemical. It has a long history of being used in food industry and medical sector. It has also been used in the chemical industry as solvent or reagent as starting material to manufacture detergents, paint and cosmetic products.

The extensive application of ethanol as automotive fuel in fuel industry started in the 1970's and now is the fastest growing sector among all the applications. Currently there is around 30 million cubic meters per year used in the fuel industry, which accounts for 70% of the world ethanol production.

There are various methods that can be used to produce ethanol. The most widely employed two methods are fermentation and catalytic synthesis. Fermentation is using

food e.g. sugar cane, corn as feedstock to produce ethanol, which has been commercially operated in Brazil (sugar cane) and the USA (corn). Currently 95% of fuel ethanol is obtained from fermentation process. The fermentation method is however time consuming and labor intensive.

Another approach to produce ethanol is catalytic synthesis which could be further classified as ethylene hydration (in which ethylene gas reacted with extremely pure water over the surface of a catalyst support impregnated with phosphoric acid) and syngas route. Syngas routes to produce ethanol are similar to the mixed alcohol synthesis; hence it is discussed in the following section.

Higher alcohols

Apart from the interest in ethanol synthesis, higher alcohol synthesis (also called HAS) has been receiving growing attentions. The HAS normally refers to the synthesis of mixture of C_1-C_6 alcohols with the purpose of obtaining high C_{2+} alcohol selectivity. The percentage of higher alcohols for blending to gasoline is estimated to be circa 30 – 45 wt % [119].

Several processes have been developed to synthesize mixed alcohols: the FT synthesis, isosynthesis, oxosynthesis which includes hydroformylation of olefins, homologation of methanol and lower molecular weight alcohols. The FT synthesis via the syngas route is widely recognized technique for this purpose. Since 1980's, there had been several technology developers worked on the HAS. Dow is the first company that developed the HAS technology using molybdenum sulfide based materials. Snamprogetti and Haldor Topsoe developed a HAS process with modified methanol catalyst and started a 12,000 ton/y pilot plant in 1982 [120]. Lurgi built 2 tones per day (TPD) demonstration plants in

1990 based on its HAS process with low pressure methanol synthesis [121]. IFP built its 20 (BPD) pilot plant in Japan [122].

Several companies have shown interests in developing HAS technology. Power Energy Fuels Inc. (PEFI) developed the Ecalene™ mixed alcohol process [123] which is using modified MoS_2 catalyst based on Dow's process. Pearson Technologies has built a 30 ton/day biomass gasification and alcohol production plant in Mississippi emphasizing in producing ethanol product [124].

The final commercialization of HAS technology depends very much on the development and performance of its catalyst. Together with the development in syngas generation technology, mixed alcohol synthesis could play an important role in the next generation of fuel industry.

1.11.1 Catalysts for alcohols synthesis

According to the active metal involved, catalysts used for HAS can be roughly classified into 4 categories: modified methanol synthesis catalyst, the IFP (Institut Français du Pétrole) mixed oxides catalyst, alkali modified cobalt molybdenum catalyst and rhodium based catalyst.

It is commonly accepted that higher alcohol can be synthesized by appropriate modification of methanol synthesis catalysts and catalytic reaction conditions [124, 125]. With the addition of alkali and alkaline-earth, methanol synthesis catalysts favor the formation of higher alcohols and other oxygenates. This type of catalyst mainly includes alkali-doped ZnO/Cr_2O_3 catalyst, alkali-doped $Cu/ZnO/Cr_2O_3$ catalyst and Co, Fe, or Ni modified $Cu/ZnO/Cr_2O_3$ catalyst. Alkali-doped ZnO/Cr_2O_3 catalyst is also called

modified high pressure methanol synthesis catalyst. The other two types of catalysts, alkali-doped $Cu/ZnO/Cr_2O_3$ and Co, Fe, or Ni modified $Cu/ZnO/Cr_2O_3$ catalyst are called modified low pressure methanol synthesis catalyst.

The IFP mixed oxide catalyst is also called modified FT catalyst which mainly consists of mainly oxides of copper and cobalt and a series of elements such as aluminum, chromium, zinc and noble metals [126, 127]. The function of cobalt in the IFP catalyst is different from that in the modified methanol catalyst because small amount of addition significantly affect the catalytic activity.

Molybdenum sulfide based catalysts for alcohol synthesis were first independently discovered by research groups at Dow Chemicals [128-130] and Union Carbide [131]. They reported that molybdenum sulfide catalysts promoted by cobalt and alkali compounds are active for the higher alcohol synthesis.

Molybdenum carbide catalysts were also reported for the formation of alcohols by Leclercq *et al.* [132] and Woo *et al.* [133]. They reported that the formation of alcohols is linked with the surface stoichiometry and to the extent of carburization. Potassium promotion could enhance the selectivity towards C_1-C_7 alcohols [133]. Xiang *et al.* [134] and Ayela *et al.* 135] investigated the addition of cobalt and potassium to the molybdenum carbides system respectively and reported that addition of both leads to high activity and selectivity towards C_{2+} alcohols.

Rhodium based catalyst is another category for higher alcohol synthesis [136]. Rhodium containing catalyst shows good selectivity toward the synthesis of ethanol and other C_2 oxygenates [137]. However, its high price due to limited natural resource makes

commercially application difficult. Hence, study in the rhodium containing catalyst currently is for academic purpose.

In the present study some investigation has been done on synthesis of higher alcohols as well.$CoMoS_2$ has been reproduced under modified and well controlled preparation conditions and is further studied by addition of several metals (e.g. Zr, Ti and Ni) as promoter.

Following this introduction, chapter 2 is experimental which is mainly focused on the catalyst preparation, catalyst characterization, catalytic reaction procedure and data analysis. Effect of various preparation and reaction variables on $CoMnO_x$ has been discussed in chapter 3. An influence of metal promotes (K and Ru) on $CoMnO_x$ catalyst is detailed in chapter 4. Chapter 5 is related to addition of two different types of activated carbon (Wood and peat derived) in cobalt manganese in comparison with an iron manganese catalyst. Chapter 6 is about syngas conversion to alcohols using $CoMoS_2$ catalyst modified with various metal promoters like Ni, Ti and Zr. Chapter 7 concludes all the investigated catalyst systems in present study followed by appendix 1-6 with a detailed description of reactor systems, GC configurations and data evaluation methods.

1.12 References:

[1]. M. van der Riet, G. J. Hutchings, and R. G. Copperthwaite, *J. Chem. Soc. Chem. Commun.*, 1986, **10**, 798.

[2]. R. G. Copperthwaite, G. J. Hutchings, M. van der Riet, and J. Woodhouse, *Ind. Eng. Chem. Res.*, 1987, **26**, 869.

[3]. S. Colley, R. G. Copperthwaite, G. J. Hutchings, and M. van der Riet, *Ind. Eng. Chem. Res.*, 1988, **27**, 1379.

[4]. G. J. Hutchings, M. van der Riet, and R. Hunter, *J. Chem. Soc., Faraday Trans.* 1989, **85**, 2875.

[5]. R. Agrawal, N. R. Singh, F. H. Ribeiro, and A. D. Delgass, *Substantial fuel for the transportation sector.* Proc. Natl. Acad. Sci. USA, 2007, **104**, 4828

[6]. P. Sabatier, J. B. Senderens, and C. B. Hebd. *Séances Acad. Sci.,* 1902, **134**, 514

[7]. BASF: German Patent, 1913, **293,787**

[8]. F. Fischer, and H. Tropsch, *Brennest- Chem.*, 1923, **4**, 276

[9]. F. Fischer, and H. Tropsch, German Patent 1922, **411,216**

[10]. F. Fischer, and H. Tropsch, *Brennest-Chem.*, 1924, **201**, 217

[11]. F. Fischer, and H.Tropsch. German Patent, 1925, **484,337**

[12]. F. Fischer, and H. Tropsch, *Brennest-Chem.*, 1926, **7**, 97

[13]. M. E. Dry, in "*Catalysis – Science and Technology*" Vol.1, J. R. Anderson and M. Boudart, Springer Verlag Berlin 1981, **4**, 159

[14]. R. B. Anderson, in "*Catalysis*" Vol.4 P. H. Emmet, Van Nostrand-Reinhold, New Jersey, 1956

[15]. B. P Statistical Review of World Energy, 2006

[16]. J. P. Hindermann, G. J. Hutchings, and A. Kiennemann, *Catal. Rev. Sci. Eng.*, 1993, **35**, 1

[17]. G. L. Bezemer, P. B. Radstake, U. Falke, H. Oosterbeek, H. P. C. E. Kuipers, A. J. Van Dillen, and K. P. de Jong, *J. Catal.*, 2006, **237**, 152

[18]. M. E. Dry, *Appl. Catal. A.*, 1996, **138**, 319

[19]. P. Courty, and P. Chaumette. *Eng. Prog.*, 1987, **7**, 23

[20]. G. Henrichi-Olive, and S. Olive, Angew. *Chem. Int. Ed. Engl.*, 1976, **15**, 136

[21].C. N. Satterfield, G. A. Huff, H. G. Stenger, and R. J. Madon, *Ind. Eng. Chem. Fundam.*, 1985, **24**, 450

[22]. C. N. Satterfield, and G. A. Huff, *J. Catal.*, 1982, **73**, 187

[23]. R. B. Anderson, in "*Catalysts for the Fischer-Tropsch synthesis*", Vol. 4, Van Nostrand Reinhold, New York 1956

[24]. M. E. Dry, *J. Mol. Catal.*, 1982, **17**, 133

[25]. S. E. Colley "*Hydrogenation of carbon monoxide over modified cobalt-based catalysts*", PhD Thesis, University of Witwatersrand, 1991

[26]. H. Schulz, E. van Steen, and M. Claeys, in '*Selective hydrogenation and dehydrogenation*', DGMK, Kassel, Germany, 1993

[27]. S. Novak, R. J. Madon, and H. Suhl, *J. Catal.*, 1982, **77**, 141

[28].E. Iglesia, S. C. Reyes, R. J. Madon, and S. L. Soled, in "*Advances in Catalysis*" , Vol. 39, Academic Press, New York, 1993, 221

[29]. E. W. Kuipers, C. Scheper, J. H. Wilson, and H. Oosterbeek, *J. Catal.*, 1996, **158,** 288

[30]. E. W. Kuipers, I. H. Vinkenburg, and H. Oosterbeek, *J. Catal.*, 1995, **152,** 137

[31]. C. L. Bianchi, and V. Ragaini, *J. Catal.*, 1997, **168**, 70

[32]. D. L. King, J. A. Cusumano, and R. L. Garten, *Catal. Rev. - Sci. Eng.*, 1981, **23**, 233

[33]. M. E. Dry, *Catal. Today.*, 1990, **6**, 183

[34]. Y. Zhao "*On the investigation of alcohol synthesis via the Fischer Tropsch reaction*", PhD Thesis, University of Cardiff, 2007

[35]. A. A. Adesina, *Appl. Catal.,* 1996, **138**, 345

[36]. B. H. Davies, *Fuel Proc. Technol.*, 2001, **71**, 157

[37]. F. Fischer, and H. Tropsch, *Brennstoff Chem.*, 1926, **7**, 97

[38]. E. L. Metterties, and J. Stein, *J. Chem. Rev.*, 1979, **79**, 479

[39]. W. A. Hermann, *Chem. Int. Ed. Engl.*, 1982, **21**, 117

[40]. G. Henrici-Olive, and S. Olive in 'The *chemistry of the metal carbon bond'* Vol.3, Hartley and Patai, J. Wiley and Sons, 1985

[41]. W. J. Laws, and R.J. Puddephatt, *J. Chem. Soc. Chem. Commun.*, 1984, **2**, 116

[42]. E. A. Carter, and W. A. Goddard, *J. Am. Chem. Soc.*, 1987, **109**, 579

[43]. I. M. Saez, N. J. Meanwell, B. F. Taylor, B. E. Mann, and P. M. Maitlis, *J. Chem. Soc. Chem. Commun.*, 1987, **5**, 361

[44]. D. Bianchi, L. M. Tau, and C. O. Bennett, *J. Catal.*, 1983, **84**, 358

[45]. A. T. Bell, *Catal. Rev. - Sci. Eng.*, 1981, **23**, 203

[46]. P. M. Loggenberg, L. Carlton, R. G. Copperthwaite, and G. J. Hutchings, *J. Chem. Soc. Chem. Commun.*, 1987, **8**, 541

[47]. J. T.Kummer, T. W. de Witt, and P. H. Emmett, *J. Am. Chem. Soc.*, 1948, **70**, 3632

[48]. P. H. Emmett, Lecture No. 4, "*Catalytic Processes Utilizing CO and H_2*", Oak Ridge National Laboratory, 1974

[49]. H. Storch, N. G. Golumbic, and R. B. Anderson, in "*The Fischer-Tropsch and related synthesis*" J. Wiley and sons, New York, 1951

[50].W. K. Hall, R. J. Kokes, and P. H. Emmett, *J. Am. Chem. Soc.*, 1957, **79**, 2983

[51].W. K. Hall, R. J. Kokes, and P. H. Emmett, *J. Am. Chem. Soc.*, 1960, **82**, 1027

[52]. V. Ponec, *Catalysis*, 1981, **5**, 49

[53]. A. Raje, and B. H. Davies, in: "*J.J. Spivey Ed., Catalysis*". The Royal Soc. Chem., Cambridge, 1996, **12**, 52

[54]. V. V. Voevodskii in: M. Van der Riet, "*Carbon monoxide hydrogenation with transition metal oxide supported cobalt and iron catalysts*", PhD Thesis, University of Witwatersrand, 1988

[55]. A. Ekstroom, and J. A. Lapswzewicz, *J. Phys. Chem.*, 1987, **91**, 4514

[56]. H. Pichler, and H. Schulz, *Chem. Ing. Tech.*, 1970, **42**, 1162

[57]. G. Henrichi-Olive, and S. Olive, *Chem. Int. Ed. Engl.*, 1976, **15**, 136

[58]. C. K. Rofer-De Poorter, *Chem. Rev.*, 1981, **81**, 447

[59]. S. L. Brown, and S. G. Davies, *J. Chem. Soc. Chem. Commun.*, 1986, **1**, 84

[60]. G. Jacobs, J. A. Chaney, P. M. Patterson, T. K. Das, J. C. Maillot, and B. H. Davies, *J. Synch. Rad.*, 2004, **11**, 414

[61]. S. A. Hedrick, S. S. C. Chuang, A. Pant, and A. G. Dastidar, *Catal. Today.*, 2000, **55**, 249

[62]. M. A. Vannice, *J. Catal.*, 1975, **37**, 462

[63]. M. A. Vannice, *J. Catal.*, 1976, **40**, 129

[64]. M. A. Vannice, *J. Catal.*, 1975, **37**, 449

[65]. M. A. Vannice, *J. Catal.*, 1979, **50**, 278

[66]. S. E. Colley, R. G. Copperthwaite, G. J. Hutchings, and M. Van der Riet, *Ind. Eng. Chem.*, 1988, **27**, 1339

[67]. J. Venter, M. Kaminsky, G. L. Geoffrey, and M. A.Vannice, *J. Catal.*, 1987, **103**, 450

[68]. E. Tronconi, C. Christiani, N. Ferlazzo, P. Forzatti, P.L. Villa , and I. Pasquon. *Appl. Catal.*, 1987, **32**, 285

[69]. A. L. Dent, and M. Lin, *Am. Chem. Soc. Adv. Chem. Series.*, 1979, **178**, 47

[70]. T. B. Kobylinski, U.S.Patent, 1978, **4,088,671**

[71]. C. B. Kibby, and T. P. Kobylinski, U.S.Patent, 1985, **4,492,774**

[72]. H. Beuther, C. L. Kibby, T. P. Kobylinski, and R. B. Pannell, U.S. Patents, 1983, **4, 413,064**, 1985, **4,493,905**, 1986, **4,605,680**, 1986, **4,613,624**

[73]. T. P. Kobylinski, C. L. Kibby, R. B. Pannell, and E. G. Eddy, U.S. Patents, 1986, **4,605,676**, 1986, **4,605,679**

[74]. E. Iglesia, S. L. Soled, and R. A. Fiato, *J. Catal.,* 1992, **137**, 212

[75]. E. Iglesia, S. L. Soled, R. A. Fiato, and G.H. Via, *J. Catal.*, 1993, **145**, 345

[76]. E. Iglesia, S. L. Soled, and J. Baumgartner, *J .Catal.*, 1995, **153**, 108

[77]. E. Iglesia, *Appl. Catal.*, 1997, **161**, 59

[78].S. Eri, J. G. Goodwin ,G. Marcelin, and T. Riis, U.S. Patents, 1989, **4,880,763**, 1989, **4,801,573** , 1992, **4,857,599** , 1992, **5,116,879**

[79]. S. Vada, B. Chen, and J. G. Goodwin, *J. Catal.*, 1995, **153**, 224

[80]. S. Ali, B. Chen, and J. G. Goodwin, *J. Catal.*, 1995, **157**, 25

[81]. G.J. Haddad, B.Chen, and J. G. Goodwin, *J. Catal.*, 1996, **160**, 43

[82]. K. Kogelbauer, J. G. Goodwin, and R. Oukaci, *J. Catal.,* 1996, **160**, 125

[83]. A. R. Belambe, R. Oukaci, and J. G. Goodwin, *J. Catal.*, 1997, **166**, 8

[84]. R. Oukaci, A. H. Singleton, and J. G. Goodwin, *Appl. Catal.,* 1999, **186**, 129

[85]. J. J. Li, G. Das, T. Zhang, and Y. Davies, *Appl. Catal.,* 2002, **236**, 67

[86]. C. H. Bartholomew, in *"Studies in surface science and catalysis"* 2003, **163**, 2884

[87]. G. Jacobs, K. Chudhari, D. Sparks, Y. Zhang, B. Shi, R. Spicer, T. K. Das, J. Li, and B. H. Davies, *Fuel.,* 2003, **82**, 1251

[88]. E. Iglesia, *Appl. Catal.,* 1997, **161**, 59

[89]. Y. Q. Zhuang, M. Claeys, and E. V. Steen, *Appl. Catal.,* 2006, **301**, 138

[90]. A. A. Mirzaei, R. Habibpour, M. Faizi, and E. Kashi, *Appl. Catal.,* 2006, **301**, 272

[91]. F. Morales, F. M. F. de Groot, O. L. G. Gijzeman, A. Mens, O. Stephan, and B. M. Weckhuysen, *J. Catal.*, 2005, **230**, 301

[92]. P. A. Chernavskii, *Kinet. Catal.*, 2005, **46**, 634

[93]. J. S. Girardon, A. S. Larmontov, L.Gengembre, P. A. Chernavskii, A. Griboval-Constant, and A. Y. Khodakov, *J. Catal.,* 2005, **230**, 339

[94]. R. Gheitanchi, A. A. Khodadadi, M. Taghizadeh, and Y. Mortazavi, *React. Kinet. Catal. Lett.,* 2006, **88,** 225

[95]. Q. Liang, K. Chen, W. Hou, and Q. Yan, *Appl. Catal.,* 1998, **166**, 191

[96]. B. Ernst, L. Hilaire, and A. Kiennemann, *Catal. Today.,* 1999, **50**, 425

[97]. D. Das, G. Ravichandran, and D. K. Chakrabarty, *Appl. Catal.,* 1995, **131**, 335

[98]. A. Martinez, C. Lopez, F. Marquez, and I. Diaz, *J. Catal.,* 2003, **220,** 486

[99]. S. J. Ledford, H. M. Houlla, P. Andrew, and M.H. David, *J. Phys. Chem.*, 1989, **50**, 6770

[100]. B. Ernst, A. Kiennemann, and P. Chaumette, ILERCSI-ECPMURA CNRS 1498

[101]. A. H. Singleton, Energy International Corporation [US/US], 135 William Way Pittsburg, PA 15328 (US)

[102]. C. Wenchun, M. Kamel, M. Manzer, and E. Leo, Subramanian, Munirpallam A.2001, (Kennett Sq., PA) 09/314811

[103]. B. C. Murchison, 1985, (Midland, MI) 06/550852

[104]. G. R. Moradi, M. M. Basir, A. Taeb, and A. Kiennemann, *Catal. Commun.*, 2003, **4**, 27

[105]. L. C. A. Mazzone, and F.A.N. Fernandes, *Lat. Am. Appl. Res.*, 2006, **36**, 141

[106]. T. Wang, Y. Ding, Y. Lu, and L. Lin, *J. Nat. Gas. Chem.*, 2008, **17**, 153

[107]. B. Cornils, W. A. Herrmann, R. Schlogl, and C. H. Wong, in "*Catalysis from A to Z", A* concise encyclopedia, Wiley-VCH, Weinheim

[108]. M. E. Dry, T. Schingingles, and C. S. Botha, *J. Catal.*, 1970, **17**, 341

[109]. J. S. Girardon, A.S. Larmontov, L. Gengembre, P. A. Chernavskii, A. Griboval-Constant, and A.Y. Khodakov, *J. Catal.*, 2005, **230**, 339

[110]. J. Panpranot, J.G. Goodwin, and A. Sayari, *Catal. Today.*, 2002, **77**, 269

[111]. S. J.Tauster, S.C. Funk, and R. L. Garten, *J. Am. Chem. Soc.*, 1978, **100**, 170

[112]. K. I. Hadjiivanov, and D.G. Klissurski, *Chem. Soc. Rev.*, 1996, **25**, 61

[113]. G. J. Hutchings, *S. Afr. J. Chem.*, 1986, **34**, 65

[114]. E. L. Kugler, *Prep__ Am.Chemi, Soc. Div. Pet. Chem.*, 1980, **25**, 564

[115]. D. L. King, *J. Catal.*, 1978, **51**, 397

[116]. C. S. Kellner, and A.T. Bell, *J. Catal.*, 1982, **75**, 251

[117]. http://igitur-archive.library.uu.nl/dissertation/2006-0906-201148/c2.pdf

[118]. J. C. Slaa, J. G. Van Ommen, and J.R.H. Ross, *Catal. Today.*, 1992, **15**, 129

[119]. H. B. M. Olayan, *Eng. Prog.*, 1987, **7**, 9

[120]. A. H. El Sawy, NTIS. DE90010325. SAND89-7151, 1990, Mitre Corporation

[121]. A. J. Lucero, R. E. Klepper, W. M. O'Keefe, and V. K. Sethi, *Prepr. Symp. - Am. Chem. Soc., Div. Fuel, Chem.*, 2001, **46**, 413

[122]. U.S. Department of Energy, National Renewable Energy Laboratory, 2006 NREL/SR-510-39947

[123]. K. Klier, *Adv. Catal.*, 1982, **31**, 243

[124]. K. Smith, and R.B. Anderson, *J. Catal.*, 1984, **85**, 428

[125]. A. Surgier, US Patent, 1974, **3787332**

[126]. A. Surgier, US Patent, 1975, **3899577**

[127]. G. J. Quarderer, and K. A. Cochran, European Patent, 1984, **0,119,609**

[128]. R. R. Stevens, European Patent, 1986, **0,172,431**

[129]. C. B. Murchison, M. M. Conway, R. R. Stevens, and G. J. Quarderer, Proc. 9th Int. Congr. Catal., Calgary, 1988, **2**, 626

[130]. N. E. Kinkade, European patents, 1985, **0,149,255** and **0,149,256**

[131]. L. Leclercq, A. Almazouari, M. Dufour, and G. Leclercq, in: "*The Chemistry of Transition Metal Carbides and Nitrides*", S.T. Oyama (Ed.), Blackie, Glasgow, 1996, 345

[132]. H. C. Woo, K.Y. Park, Y.G. Kim, I. Nam, J. S. Chung, and J. S. Lee, *Appl. Catal.*, 1991, **75**, 267

[133]. M. Xiang, D. Li, H. Qi, W. Li, B. Zhong, and Y. Sun, *Fuel.*, 2007, **86**, 1298

[134]. E. C. Alyea, D. He, and J. Wang, *Appl. Catal.*, 1993, **104**, 77

[135]. M. Ichikawa "Agency of Industrial Science and Technology", early disclosure, No. 85 - 32731, 1985, **2**, 19

[136]. S.C. Nirula, 1994, PEP Review no. 85-1-4, SRI International, Meno Park, CA.

Chapter 2

Experimental

2.1 Catalyst Preparation

There are several methods for the preparation of catalysts and each catalyst can be prepared through different routes. Impregnation, coprecipitation and deposition precipitation are three important methods for catalyst preparation which are widely used in industry. There are various preparation variables involved in these methods which affect the morphology and activity of catalysts. e.g. heat treatment is important in impregnation; pH, temperature and ageing time affect the nature of catalyst in precipitation and deposition precipitation methods.

Most of the catalysts going to be discussed in this thesis have been prepared by these three methods. In the preparation of few catalysts the impregnation method has been used in combination with coprecipitation for the deposition of promoters with catalyst precursor prepared by coprecipitation to give the required level of doping. Table 2.1 lists details of the starting reagents which have been used mainly in this study.

Table2.1 Reagents used in catalyst preparation

$Co(NO_3)_3.6H_2O$	98%	Aldrich
$Mn(NO_3)_2.4H_2O$	97%	Fluka
Ammonia	35%	Fisher
Activated carbon	-	Norit
Potassium acetate	99%	Aldrich
Titanium (IV) oxide acetyl acetone	99%	Aldrich
Zirconyl nitrate	99%	Aldrich
Nickel nitrate	99%	Aldrich
$(NH_4)_6Mo_7O_{24}\cdot 4H_2O$	-	Sigma Aldrich
20% wt $(NH_4)_2S$ in H_2O	-	Aldrich
$Co(CH_3CO_2)_2\cdot 4H_2O$	98+%	Sigma Aldrich
CH_3COOH	>99%	Fischer
K_2CO_3	>99%	Fischer
bentonite clay	-	Aldrich
sterotex® lubricant	-	Abitec
ruthenium (III) nitrosyl nitrate	-	Aldrich
solution in dilute nitric acid	-	Aldrich

2.1.1 Co-precipitation

The co-precipitation is a commonly used technique for the preparation of catalysts. In this method two or more metal compounds are precipitated simultaneously giving a homogeneous mixture. This method has been approved as an extremely reproducible method of preparation if the experiment is performed under carefully controlled conditions (e.g. temperature, pH and flow rate of precipitating agents and metal solutions). The obtained precipitates follow different steps (ageing, washing, drying,

calcination and reduction) to give a final catalyst with homogeneous distribution of active metal components. This method can successfully be used for the large scale production of catalysts [1].

There is a main disadvantage associated with this method of preparation which is very high chemical cost because of the large mass loss that occurs during the derivation of final product from the reagents. Co-precipitation method has been observed as the best technique for catalyst preparation in this research and it facilitated a homogeneous preparation of reproducible catalysts on laboratory scale.

It has been observed during this research that co-precipitation requires proper control of all preparation variables and steps. Most important variables to be controlled are rate of addition of different solutions, rate of stirring, pH, temperature of precipitation and ageing time. These factors affect the reproducibility of catalyst affecting the final structure and activity of catalyst. In this study only nitrates of cobalt and manganese were used and the precipitating agent was always ammonia (various other precipitating agents were tried but ammonia has been found as the best precipitating agent). During heat treatment -NO_3 and NH_3 decompose to high area oxides avoiding poisoning effects [2]. Warm distilled water was used for all dilutions or washings to minimise impurities. Filtration was done in a preheated funnel in order to avoid a change in the metal ratio induced by the cooling of precipitation mixture during filtration process.

In this study two different methods have been employed for co-precipitation of $CoMnO_x$ catalyst.

1. simultaneous mixing of two metals salts solutions with precipitating agent in which flow rates of both(nitrate solutions and precipitating agent) were kept constant for precipitation at a single constant pH and

2. Introduction of precipitating agent in the mixed metals salts solution in which flow rate of precipitating agent was kept constant and pH of precipitation mixture was varied

Method 2 was found better for this particular catalyst in which pH of the precipitation mixture was varied. Both methods have been detailed in the following paragraphs.

i) Preparation of cobalt manganese oxide catalysts by coprecipitation at constant pH

100 ml each of Co and Mn 1M solutions (prepared from the nitrate salts) were premixed and heated to 70°C. The NH_3 precipitating solution (200ml of 5.6M NH_3 solution) was also preheated to 70°C. Both reagents (mixed metal salts solutions and NH_3 solution) were combined together in the reaction vessel at 70°C at a combined pumping rate of 6.7ml/min (3.3 ml/min NH_3 solution, 3.3 ml/min metals solution). The reagents were combined a reaction vessel (70°C) containing 100 ml of water (necessary for submerging the pH probe) and reacted at constant pH of 8.30 +/- 0.01. The duration of reaction was ca.1h and it yielded 500 ml of solution containing the co-precipitated catalyst. This solution was filtered through a preheated funnel (using wide mesh filter paper to enable a rapid filtration) and washed (using 500ml of warm distilled water).

After washing the catalyst was dried (110°C) over night (16h) giving a material denoted as catalyst precursor which was calcined at 500°C for 24h to get a final catalyst.

ii) Preparation of cobalt manganese oxide catalysts by coprecipitation at variable pH

100 ml each of Co and Mn 1M solutions (prepared from the nitrate salts) were premixed and heated to 80°C in a round bottom flask. Ammonium hydroxide solution (5.6M/l) preheated at 80°C was added to the nitrate solution, which was continuously stirred whilst the temperature was maintained at 80°C. pH was varied from 2.80 to 8.0. The precipitates were first filtered and then washed several times with warm distilled water. The precipitates were then dried at 110°C for 16h to give a material denoted as the catalyst precursor which was subsequently calcined in static air in the furnace (500°C, 24h) to give the final catalyst.

2.1.2 Impregnation

Impregnation is very well known and simple process for catalyst preparation on industrial scale. In this method solutions of metals salts precursors are added to the pores of support followed by subsequent drying for the removal of solvent. Drying has to be carried out in a way so that the impregnated component remains within the pore system and does not migrate to the exterior surface. If this stage is done correctly, the support has crystallites of the impregnated component in the interstices of pores [2].

There are two types of impregnation divided on the bases of the amount of added volume of the solutions, wet impregnation and incipient wetness impregnation. In wet impregnation the volume of metals salt solution is larger than pore volume of support. However, in incipient wetness impregnation method the amount of added solutions is equal to or less than the pore volume of support.

All the doped catalysts were prepared by impregnation method. The main advantages of this technique are that the metal is deposited directly on the exposed surface of catalyst due to which most of the active metal is exposed directly to the reagent gases. This is opposite to the catalysts prepared by coprecipitation or deposition precipitation methods where the active metal gets distributed uniformly through whole surface of the catalyst. Catalyst preparation by this method is very rapid and reproducible and there is less waste of expensive metal components. The disadvantage of this method is the limited amount of material which can be incorporated in a support.

In this study incipient wetness impregnation has been adopted for deposition of metals dopants on the surface of cobalt manganese oxide catalysts.

The detailed procedure for deposition of metal dopants on surface of catalysts by incipient wetness impregnation method is detailed as under:

2.1.2.1 Deposition of metal promoters on the surface of cobalt manganese oxide catalysts

Pore volume of catalyst precursor (uncalcined material) of cobalt manganese oxide was measured by slowly adding distilled water in a weighed quantity of catalyst precursor, until it was in a mouldable form between paste and solution state. It was observed that 1.6g of precursor needs 1.10ml of distilled water.

Catalyst precursor was impregnated with calculated amounts of metal promoters reagents dissolved in measured volume of distilled water. The resulting slurry was dried at 110°C

for 16h followed by calcination at 500°C for 24h. All the doped catalysts detailed in chapter 4 have been prepared by this method.

2.1.3 Deposition Precipitation

Deposition-precipitation is a technique for catalyst preparation in which metal particles are deposited on the surface of a support by precipitation in such a way that nucleation is prevented in the bulk of solution. This procedure enables deposition of finely divided active metal components on the surface of a support. In this method higher loadings of active metal precursors are achieved on the surface of support compared with impregnation.

In this study deposition precipitation method has been adopted for the deposition of cobalt and manganese on activated carbon. The detailed procedure is given as under:

2.1.3.1 Preparation of cobalt/iron and manganese supported/combined catalysts with activated carbon by deposition precipitation method

Aqueous solutions of Cobalt nitrate hexahydrate/iron nitrate nonahydrate and Manganese nitrate tetrahydrate were mixed and preheated in a round bottom flask at 80°C. Weighed quantity of activated carbon was added in this mixture of solutions. Ammonium hydroxide solution (5.6M) preheated at 80°C was added to the nitrate solution, which was continuously stirred whilst the temperature was maintained at 80°C. pH was varied from 4.80 to 8.0. The precipitates were first filtered and then washed several times with warm distilled water. The precipitates were then dried at 110°C for 16h to give a material

denoted as the catalyst precursor which was subsequently calcined in tube furnace (500°C,24h) under continuous flow of helium to give the final catalyst.

This procedure was adopted for preparation of all Co/Fe and Mn catalysts combined with activated carbon which are discussed in chapter 5.

2.1.4 Catalysts preparation for alcohols

2.1.4.1 Preparation of alkali-promoted cobalt molybdenum sulfide catalysts for syngas conversion to alcohols

Alkali-promoted cobalt molybdenum sulfide catalysts (Co-MoS_2/K_2CO_3) were prepared as follows. A solution of $(NH_4)_2MoS_4$ was prepared by dissolving $(NH_4)_6Mo_7O_{24}\cdot 4H_2O$ (15g) into $(NH_4)_2S/H_2O$ (106 ml, 20%) with stirring (340-343K, 1h). A solution of the cobalt compound was prepared by dissolving Co $(CH_3CO_2)_2$ (10.5g) in distilled water (200 ml). The two solutions were then added simultaneously drop-wise into a well-stirred solution of aqueous acetic acid solution (30%) at 328K. The solution was vigorously stirred (1h, 328 K) and the resultant black solution was filtered and dried at room temperature in a fume cupboard overnight. The dried sample was heated under nitrogen (1h, 773 K ramping rate 25K/min), giving a grey-black product. This product was then ground and mixed with K_2CO_3, bentonite clay and sterotex® lubricant in a weight ratio of 66/10/20/4 (10% K_2CO_3) unless otherwise indicated.

This method was adopted for preparation of $CoMoS_2$ catalysts which are discussed in chapter 6.

2.2 Analysis of products

The residual gaseous product was analyzed by on-line gas chromatography (FID and TCD), and liquids were analyzed by off-line gas chromatography. The detailed description of gas chromatography used in this study is discussed in appendix 3 (for syngas to alcohols) and appendix 6 (for syngas to alkenes).

2.2.1 Gas Chromatography

Chromatography is the collective term for a family of techniques capable to produce data for the composition of chemical mixtures. Gas Chromatography is one of the most extensively used techniques amongst the analytical methods. This technique specifically involves a sample being vaporized and injected into the head of the chromatographic column. The sample is transported through the column by the flow of inert, gaseous mobile phase. The column itself contains a stationary phase which is adsorbed onto the surface of an inert solid.

2.2.1.1 Instrumental components

Gas chromatograph (GC) mainly consists of following components:

i. Carrier gas
ii. Sample injector port
iii. Columns
iv. Detectors
v. Data acquisition system

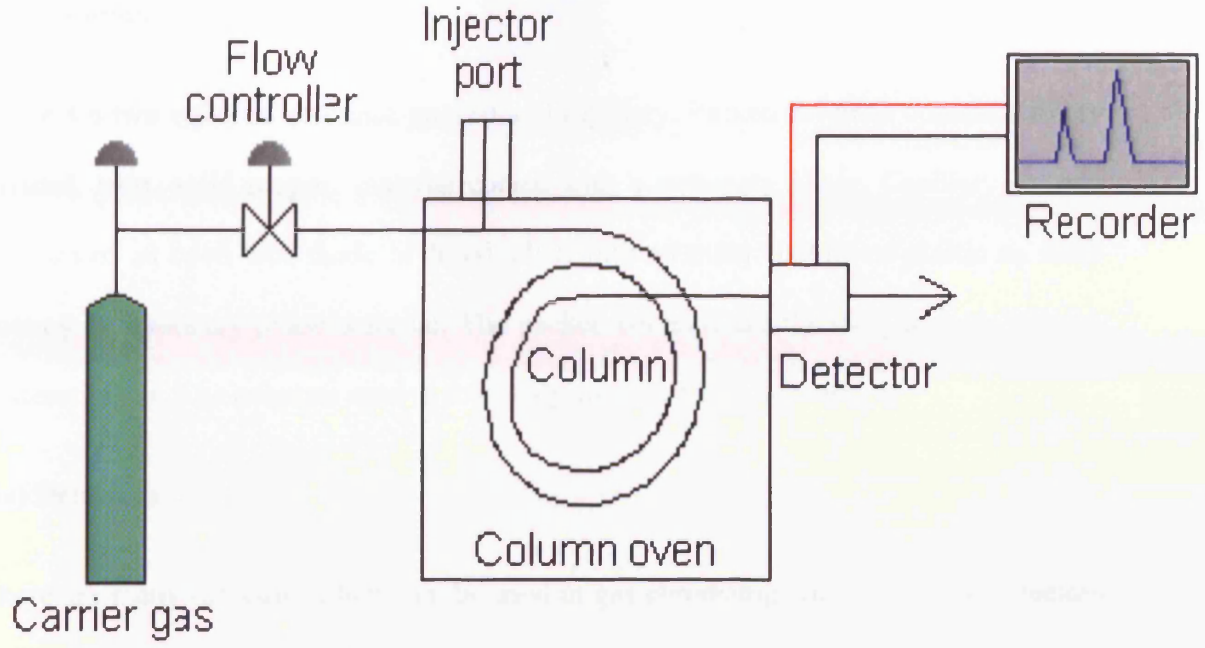

Fig.2.1 Diagram of a gas chromatograph system

(i) Carrier gas

The carrier gas flows through column in order to promote the elution of components from the mixture of chemicals. The carrier gas must be inert. Commonly used include helium, argon and carbon dioxide. The choice of carrier gas is often dependent on the type of detector which is being used. The carrier gas system also contains a molecular sieve to remove water and other impurities.

(ii) Sample Injection port

Injection port is the point where sample is introduced in the GC. High temperature of the injector port vaporizes the mixture (if not in gas phase) and the gas components are swept into the column by mobile phase.

(iii) Columns

There are two types of columns, packed and capillary. Packed columns contain a finely divided, inert, solid support material coated with a stationary phase. Capillary column consists of an open tube made of fused silica with an outer coating of plastic an inner coating of stationary-phase material. The packed columns are the most popular column systems in use. The columns used in this study are detailed in appendix 6.

(iv) Detectors

There are many detectors which can be used in gas chromatography. Different detectors will give different types of selectivity.

a. Thermal conductivity detector (TCD)

TCD is a chemical specific detector. This detector senses changes in the thermal conductivity of the column effluent and compares it to a reference flow of carrier gas.TCD consists of an electrically heated filament in a temperature-controlled cell. Under normal conditions there is a stable heat flow from the filament to the detector body. When an analyte elutes and the thermal conductivity of the column effluent is reduced, the filament gets heated up and changes resistance. This change in resistance is often sensed by a Wheatstone bridge circuit which produces a measurable voltage change. The column effluent flows over one of the resisters while the reference flow is over a second resistor in the four-resister circuit. The TCD detects all molecules, not just hydrocarbons, so it is commonly used for fixed gas analysis (O_2, N_2, CO, CO_2, H_2S, NO, NO_2).

b. Flame Ionization Detector (FID)

FID is one of the many methods to analyze materials coming off of the GC column. A stainless steel jet is constructed in FID. The carrier gas from column flows through the jet mixes with hydrogen and burns at the tip of FID. There is metal collector electrode located at the side of flame. Hydrocarbons ionized in the flame are attracted to this electrode and the resulting electron current is amplified by an electrometer amplifier. FID is sensitive to almost all hydrocarbons.

(v) Data Acquisition

Computer based systems are extensive tools for the analysis of data from data systems. The raw data can be plotted to form the chromatograms in variable scales of retention and the response axis.

2.3 Catalytic testing

CO hydrogenation for syngas to alkenes was carried out using six fixed-bed laboratory reactors, which enabled testing of catalysts under identical experimental conditions. The detailed description of these reactors is given in appendix 4. A single bed reactor was used for evaluation of few catalysts which is detailed in appendix 1.

CO hydrogenation for syngas to alcohols was carried out in high pressure alcohols reactor which has been detailed in appendix 2.

2.4 Calculations

Gas chromatographic data was corrected for the derivation of final data using method of calculations detailed in appendix 5.

2.5 Surface and Bulk Characterization

2.5.1 BET Surface Area Measurements

Surface area is an important characteristic capable of affecting the quality and utility of materials. For this reason it is important to determine and control this factor accurately. The most common and widely used technique for the estimation of surface area is BET (Brunauer, Emmett and Teller) method. BET equation is based on the extension of the Langmuir model for monolayer molecular adsorption. There is an assumption that adsorption of first layer takes place in an array of surface sites with same energy. Molecules in the first layer act as sites for multilayer adsorption which approaches infinite thickness as $p \rightarrow p_o$.

$$\frac{p}{V(p_0 - p)} = \frac{1}{V_m C} + \frac{C-1}{V_m C} \bullet \frac{p}{p_0} \qquad (2.1)$$

BET equation

Where

Where p and p_0 are the equilibrium and saturation pressure respectively, V is the volume of gas adsorbed at pressure p, V_m is the volume of gas required to form a monolayer and C is a constant related heat of adsorption.

Based on experimental results, equation (2.1) can be plotted as $\frac{p}{V(p_0 - p)}$ versus $\frac{p}{p_0}$. The slope and intercept of the BET plot are equal to $\frac{C-1}{V_m C}$ and $\frac{1}{V_m C}$ respectively. With the monolayer volume V_m known, the surface area can be obtained by:

$$A_s = \frac{V_m}{22414} N_A \sigma \qquad (2.2)$$

Where N_A is the Avogadro number and σ is the area of one nitrogen molecule (generally accepted as 0.162 nm^2).

Measurement of the BET surface area was achieved by N_2 physi-sorption at the temperature of liquid nitrogen. Before each measurement, the sample was degassed for 1 h at 393K under N_2 flowing. Measurement was done using Micromeritics ASAP2000 (Gemini). Sample tube (with sample) was first evacuated and the void volume of the apparatus measured using helium. Afterwards the sample tube was immersed into liquid nitrogen, followed by adding nitrogen to start adsorption. Data of pressure drop versus volume of nitrogen adsorbed were then recorded, which could be used to calculate the surface area according to the method described above.

2.5.2 X-ray Diffraction

X-ray Diffraction (XRD) is a versatile, non-destructive technique that reveals detailed information about the chemical composition and crystallographic structure of materials.

Diffraction occurs when electromagnetic radiation impinges on a material with a comparable length scale to the wavelength of radiation. The distances of crystal lattices

are between 0.15-0.4 nm that is within the electromagnetic spectrum of X-ray, which allows diffraction to occur.

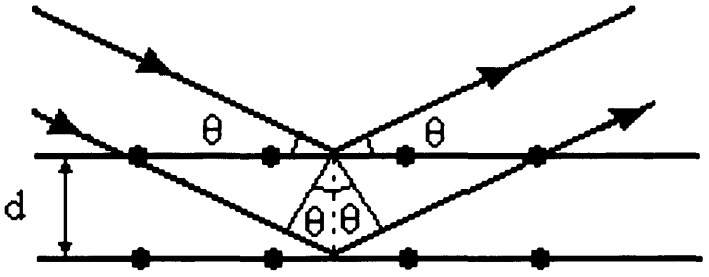

Fig. 2.2 X-Ray beams on a crystal

Figure 2.2 shows a simple illustration of X-ray diffraction. Two X-ray beams with wavelength λ are reflected from two adjacent crystal lattices. The resulting diffraction follows a mathematical correlation called Bragg's law:

$$d = \frac{n\lambda}{2\sin\theta} \qquad (2.3)$$

Where d is the interplanar spacing, θ is the diffraction angle, n is an integer and λ is the wavelength of the radiation. The equation can be applied to both single crystal and crystalline powders due to the random orientation of the crystallites.

XRD is one of the widely used analytical techniques. It offers information on the dimensions and content of the elementary cell, crystallite size and quantities of the phases present. In the powder XRD, a sample contains a large number of randomly oriented crystalline particles, of which those orientated at the Bragg angle θ produce a diffracted beam of angle 2θ.

The powder XRD method was used in this study to characterize catalysts. An Enraf Nonius PSD120 diffractometer with a monochromatic CuKα source operated at 40 keV

and 30 mA was used to obtain intensity and 2θ values. Phase identification was performed by matching experimental patterns to the JCPDS data base.

2.5.3 Temperature Programmed Reduction (TPR)

Temperature programmed reduction (TPR) is the most commonly used analytical technique used to get information on the reduction behavior of metal oxide catalysts. The direct information obtained includes the number of defined peaks in the TPR profile and the corresponding temperature at which these peaks occur. Various properties such as the ease with which species can be reduced, the state of metallic compounds, interactions of metal-metal and metal-support can be obtained from TPR. These characteristics can then be used for the optimization of catalyst pretreatment.

In TPR, a reducible catalyst or catalyst precursor is exposed to a flow of a reducing gas mixture (typically nitrogen or argon containing few volume percent of hydrogen), while the temperature is increased linearly. The rate of reduction is continuously followed by measuring the composition of the reducing gas mixture at the outlet of the reactor. The experiment permits the determination of the total amount of hydrogen consumed, from which the degree of reduction and thus the average oxidation state of the solid material after reduction process can also be determined [3].

A TPDRO 1100 series (Thermo Electron Corporation) was used to perform the TPR measurements. Typical measurement was performed by sandwiching a sample (0.03 g) with quartz wool in a quartz reactor tube. The sample was out-gassed by heating at 393K for 60 minutes in a stream of Ar (15 cm^3/min). After cooling down to ambient

temperature, Ar was switched to a gas mixture made of 10% H_2/Ar. A cold trap containing a mixture of liquid nitrogen and iso-propanol was used to trap water that was produced from the reduction of the metal oxide. The gas mixture (20 cm^3/min) flowed through the reactor, followed by an increase of temperature at 5K/min from ambient to 1273K and then returned to ambient. The consumption of hydrogen during the reaction was recorded by a TCD detector, giving intensity as function of temperature.

2.5.4 X-ray Photoelectron Spectroscopy (XPS)

XPS, is one of the most frequently used techniques in catalysis, as it provides information on the elemental composition, the oxidation state of elements and, dispersion of one phase over another.

XPS is based on the photoelectric effect, whereby an atom absorbs a photon of energy, $h\nu$, after which a core or valence electron with binding energy E_b is ejected with kinetic energy.

$$E_k = h\nu - E_b - \varphi \qquad (2.4)$$

Where:

E_k = the kinetic energy of the photoelectron h is the plank's constant, v is the frequency of the existing radiation,E_b is the binding energy of the photoelectron with respect to the Fermi level of the sample and φ is the work function of the spectrometer.

In XPS, the intensity of photoelectrons is measured as a function of their kinetic energy.

XPS can be used to analyze the composition of samples because a set of binding energies is characteristic for an element. Binding energies are not only element-specific but also contain chemical information, because the energy levels of core electrons depend slightly on the chemical state of the atom.

An XPS spectrometer contains an X-ray source – usually Mg Kα (1253.6 eV) or Al Kα (1486.3 eV) and an analyzer which is mostly hemispherical in design. In the entrance tube, the electrons are retarded or accelerated to a value called the 'pass energy' at which they travel through the hemisphere filter. Behind the energy filter is the actual detector, which consists of an electron multiplier which amplifies the incoming photoelectrons to measurable current. The resolution of XPS is determined by the line width of the X-ray source, the broadening due to the analyzer and the natural line width of the level. These three factors are related as follows:

$$(\Delta E)^2 = (\Delta E_X)^2 + (\Delta E_{an})^2 + (\Delta E_{nat})^2 \qquad (2.5)$$

where:

ΔE is the width of a photoemission peak at half-maximum, ΔE_X is the line width of the X-ray source, ΔE_{an} is the broadening due to the analyzer and ΔE_{nat} is the natural line width.

The instrument used was Kratos Axis Ultra-DLD photoelectron spectrometer. Samples were run using a monochromatic aluminium x-ray source (hv=1486.6ev). Kratos charge neutralization system was used to minimize sample charging. All high resolution spectra were run at pass energy of 40ev whilst survey spectra were run at energy of 160ev.

2.5.5 Scanning Electron Microscopy (SEM)

The scanning electron microscopy (SEM) is a type of electron microscope that images the sample surface by scanning it with a high-energy beam of electrons. The electrons interact with the atoms that make up the sample producing signals that contain information about the sample's surface topography and composition. A beam of electrons is produced at the top of the microscope by an electron gun. The electron beam follows a vertical path through the microscope which is held within vacuum. The beam travels through electromagnetic fields and lenses, which focus the beam down towards the sample. The energy exchange between the electron beam and the sample results in the emission of secondary electrons and electromagnetic radiation, which can be detected to produce an image. The electrons are detected by scintillator-photomultiplier device and the resulting signal is rendered into a 2-dimensional intensity distribution that can be viewed and saved as an image. The brightness of the signal depends on the number of secondary electrons reaching the detector. If the beam enters the sample perpendicular to its surface the activated region is uniform about the axis of the beam and a certain number of electrons 'escape' from within the sample. The escape distance of one side of the beam decreases with an increase in angle of incidence resulting in the emission of more secondary electrons.

The analysis was performed using a Zeiss Evo-40 series scanning electron microscope.

2.5.6 Energy Dispersive X-ray Spectroscopy (EDX)

Energy Dispersive X-ray Spectroscopy is an analytical technique used for the elemental analysis of a sample. An electron beam of 10-20 Kev energy strikes the surface of a

conducting sample. The incident beam excites an electron in inner shell, prompting its ejection resulting in the formation of an electron hole within the atom's electronic structure. An electron from an outer, high energy shell fills the hole and the excess energy is released in the form of an x-ray.

The EDX detector measures the number of emitted x-rays versus their energy. The energy of the x-ray is characteristic of the element from which x-ray was emitted. The EDX detector converts the energy of each individual x-ray into a voltage signal of proportional size. This is achieved through a three stage process. Firstly the x-ray is converted into a charge by an ionization of atoms in the semiconductor crystals. Secondly this charge is converted into the voltage signal by the field effect transmitter preamplifier. Finally the voltage signal is input into the pulse processor for measurement. The output from the preamplifier is a voltage ramp where each x-ray appears as a voltage step on the ramp. In traditional EDX analysis in the SEM the spatial resolution is limited to around one micron by the interaction volume of the beam within the sample.

The equipment used was a Zeiss Evo-40 series SEM in conjunction with INCAx-sight EDX detector.

2.6 References

1. US Patent, **4605639**

2. *"Catalyst Handbook"* Martyn V. Twigg 1989, **38**

3. "*Handbook of heterogeneous catalysts*" G. Ertl and H. Knozinger, J. Weikamp 1997, **3**, 1080

4. W. A. Dietz, *J. Gas Chrom*, 1967, 68

5. O. Mikes, Ref. therein, M. Van der Riet "*Carbon Monoxide Hydrogenation with Transition Metal Oxide Supported Cobalt and Iron Catalysts*", PhD Thesis, University of Witwatersrand, 1988

Chapter 3

Effect of preparation conditions on the catalytic performance of $CoMnO_x$ catalysts for CO hydrogenation

3.1 Introduction

As discussed in chapter 1, the development of a suitable catalyst for the synthesis of selective products through Fischer Tropsch reaction is commercially attractive. There has been renewed interest in recent years in selective production of petrochemical feedstocks such as ethylene, propylene and butylenes (C_2-C_4 olefins) directly from synthesis gas [1-8]. Whatever the operating conditions, the FT reaction always produces a wide range of hydrocarbons and oxygenated products.

Methane, an unwanted product, is always present and its selectivity can vary from as low as about 1% up to 100%. At the other end of the product stream, the selectivity of longer chain linear waxes can vary from zero to over 70%. The intermediate carbon number products between the two extremes are only produced in limited amounts. Thus it seems to be impossible to produce, on a carbon number basis, more than about 18% C_2,about 16% C_3,about 42% gasoline/naphtha (C_5 to 200°C BP) and about 20% diesel fuel (200 to 320°C) [9].

The range of carbon number products can be varied by altering the operating temperature, the type of catalyst, the amount or type of promoter present, the feed gas composition, the operating pressure or the type of reactor used. Whatever the process conditions, there is always a clear interrelationship between all of the products formed.

An approach to improve the selectivity of the classical FT process for conversion of syngas to hydrocarbons involves the use of a bifunctional catalyst system containing a metal catalyst (FT catalyst) combined with a support. The FT reaction with cobalt-based catalysts has been studied extensively [10-15] and it has been shown that cobalt-based catalysts are superior to other metal catalysts typically iron-based catalysts. Co-Mn catalysts favour olefins formation [16, 17] more than the other Co-based bimetallic catalysts. The Co-Mn catalysts are mainly composed of metallic cobalt particles dispersed on MnO [18].

There was growing interest in manganese oxide during the 1970s for the synthesis of light alkenes [19- 21]. Many catalysts were patented during this time for the synthesis of light alkenes from iron and manganese oxide catalysts that demonstrated high selectivity

for C_2-C_4 alkenes. This early work brought about the realization that manganese oxide could be used for the promotion of light alkenes selectivity with iron catalysts and this resulted in a diverse range of research established on the basis of this system. The addition of manganese to Co catalysts has been proved to bring about a significant increase in the formation of light alkenes and a decrease in methane selectivity [22-29]. Manganese as a promoter can improve the dispersion of the Co active component and suppresses carbon chain growth as well as deep hydrogenation of primary FT products, leading to high selectivity of lower alkenes.

Van der Riet [30] has reported the best results so far with $CoMnO_x$ catalysts for the direct synthesis of light alkenes from syngas. He has observed C_3 hydrocarbons as the major product with comparatively low C_1 and C_2 selectivities. The total C_3 selectivity increased with increasing conversion which was achieved by increasing temperature or pressure whilst C_1 and C_2 remain low. For example for a $CoMnO_x$ catalyst with Co/Mn = 1:1 at 220°C, at conversions of ca.40 mole %, C_3 selectivities of ca.20 mass % were reported with a corresponding CH_4 selectivity of 7-8.5 mass %. This catalyst was stabilized after ca.120h.

Ground pelletelised catalysts consisting of a co-precipitated mixture of cobalt and a partially reducible manganese oxide gave excellent yields of olefins from synthesis gas [31-34]. These investigations were carried out in micro reactors and it was found that only small amounts of carbon dioxide appeared in the products. Copperthwaite *et al.* [33] attributed the formation of carbon dioxide to the oxidation of carbon monoxide using $CoMnO_x$ catalysts. The same catalyst has however been shown to be an excellent water gas shift (WGS) catalyst [35] at higher reaction temperatures (300-400°C).

Keyser *et al.* [36] undertook an investigation 10 years afterwards to establish the performance of the cobalt/manganese oxide catalyst for the conversion of carbon monoxide with hydrogen under conditions favouring the formation of gaseous, liquid and solid (i.e. wax) hydrocarbons. The catalyst required a fairly long stabilization period and produced an industrially viable product stream. They observed a significant water gas shift (WGS) reaction activity under Fischer Tropsch synthesis conditions (2100 kPa, 220°C). The WGS activity increased with increasing manganese oxide content but decreased with an increase in pressure from 600 to 2100 kPa. The yield of olefin was most favourable at short reaction times (time on stream) but decreased significantly as a result of hydrogenation at long reaction times. They have also reported the effect of pressure variation on selectivity of olefins. A lower olefin yield was observed at high pressure of syngas.

Co-Mn catalysts have been investigated intensively for their higher selectivity to lower molecular weight olefins [37, 38] but the present studies have been focussed mainly on the improvement of the preparation method and the characterization of the catalysts. The effect of a wide range of preparation variables on the structure and morphology of precipitated cobalt manganese catalyst for FT synthesis has been studied. These variables include the molar ratio of Co: Mn, precipitate ageing time, pH and temperature of precipitation, and choice of precipitation agents. Optimum preparation conditions have been decided on the basis of the catalytic results. The effects of reaction variables (reaction temperature and pressure) have also been studied in order to define the best reaction conditions for further studies. Particular attention has been paid to collect all liquids and waxes to get a full mass balance along with gas phase data.

3.2 Catalyst preparation and pre-treatment

All catalysts going to be discussed in the following sections were prepared by coprecipitation according to the methods detailed in chapter 2. All of these catalysts were reduced under pure hydrogen at 400°C for 16h before reaction with syngas. Detailed reaction conditions are given along with results.

3.3 Effect of preparation conditions

The effect of a range of preparation variables at the precursor stage of cobalt manganese oxide catalysts has been investigated and the optimum preparation conditions are identified with respect to catalytic activity for the CO hydrogenation.

It is important to mention that there is considerable variation in the catalytic activity of $CoMnO_x$ catalysts and they require ~ 100 h to become stabilized. Hence, all the catalysts discussed in this chapter were stabilized for 80-100 h.

3.3.1 Effect of constant and variable pH on the coprecipitation of $CoMnO_x$

3.3.1.1 Catalyst preparation at constant pH

Initial catalyst preparation was done by coprecipitation of cobalt and manganese nitrates heated at 70°C with ammonium hydroxide solution preheated at 70°C at pH of 8.30 as detailed in chapter 2. All efforts were made to control pH in the range of +/-0.01 as this is an important factor for $CoMnO_x$ catalyst [30]. The temperature of coprecipitation affects the metal ratio in the catalyst which has a subsequent effect on the catalytic activity; thus the temperature of precipitation mixture was adjusted to 70°C and a buchner

funnel was heated in the oven prior to filtration process in order to avoid uncontrolled precipitation, particularly of manganese species. Precipitation was done in the sealed reaction vessel and there was minimal contact of oxygen in order to avoid the oxidation of manganese species. The whole slurry consisted of a homogeneous mixture of precipitates and there was no appearance of black particles indicating oxidation of manganese. All tubes of short size were used for the flow of mixed nitrates solutions and ammonia solutions in order to avoid the temperature fluctuation. Large pore size filter paper (Whatman filter paper no.14) was used for very quick filtration and due to its ability to retain a larger portion of the precipitated catalyst. Percent yield of most of these catalysts was 40-50%.

Catalytic tests were carried out in single bed reactor detailed in chapter 2. In a typical experiment the catalyst (2 g, 0.6-0.85 mm) was reduced with H_2 (GHSV = 300 h^{-1}, 400°C, atmospheric pressure) in a fixed bed stainless steel reactor. A mixture of $CO/H_2/N_2$ (47.5: 47.5: 5) was allowed to react over the reduced catalyst at a GHSV = 300 h^{-1} at pressure of 6 bar. Liquid products were collected in a trap held at 20°C and analyzed by off-line gas chromatography, and the residual gaseous product was analyzed by on-line gas chromatography (FID and TCD).

3.3.1.1.2 Results

3.3.1.1.2.1 Testing results of catalysts calcined in different furnaces

Two different types of furnaces (tube furnace and muffle furnace) were used for the calcination of catalysts. Catalysts calcined in the muffle furnace showed better catalytic results compared with the results of the same catalyst calcined in the tube furnace. Therefore, all catalysts discusses in this chapter were calcined in the muffle furnace.

Comparison of the CO hydrogenation results for catalysts calcined in the two different furnaces are shown in table 3.1.

Table 3.1 CO hydrogenation over $CoMnO_x$ catalysts calcined in two different furnaces

	Tube furnace	Muffle furnace
Calcination temp. (°C)	500	500
Calcination time (h)	24	24
Ramping rate (°C/min)	50	50
Conversion of CO	22.4	9.4
Selectivity / wt% (normalized using mass balance)		
CH_4	11	8.5
C_2H_4	0.2	1.8
C_2H_6	2	2.4
C_3H_6	2.5	9
C_3H_8	3	2
C_4	3	4.8
C_{5+}	72.4	69

Reaction conditions: Catalyst wt = 2g,Time online 126h, 220°C, 6 Bar, CO/H_2 (1:1 mol ratio), GHSV = 300 h^{-1} C_{5+} = Gaseous, liquid and solid C_5-C_9 + liquid oxygenates

Interestingly the apparatus used to calcine a catalyst can have a marked effect on its activity. Calcination in a tube furnace was carried out under static air. Flowing or circulating air may induce different properties in a material. The catalyst calcined in the

tube furnace was good in catalytic activity with high conversion but the selectivity to alkenes was very low. On the other hand the catalyst calcined in the muffle furnace showed very good selectivity to light alkenes particularly ethylene and propylene although conversion was low under similar reaction conditions.

Catalyst calcined in tube furnace was found to be more active for CO conversion with lower selectivity to alkenes. On the other hand catalyst calcined in muffle furnace was highly selective to formation of alkenes although CO conversion was low.

3.3.1.1.2.2 Characterization for catalysts calcined in different furnaces

(i) BET surface area

The surface areas of $CoMnO_x$ solids obtained with calcination in different furnaces were measured using the BET method. For catalysts calcined in the tube furnace, the BET surface area was 15 m^2/g, whereas for the catalyst calcined in the muffle furnace the BET surface area was 9 m^2/g. The increase in surface area of the catalyst calcined in tube furnace may result in a more active material leading to an enhancement in CO conversion.

(ii) XRD

The XRD pattern of catalyst calcined in the muffle furnace is compared with the XRD pattern of catalyst calcined in the tube furnace in figure 3.1. Both catalysts show typical mixed spinel oxide structure of $CoMnO_x$ along with some phases of Mn_3O_4. There is no major difference between the XRD patterns of catalysts calcined in the different furnaces.

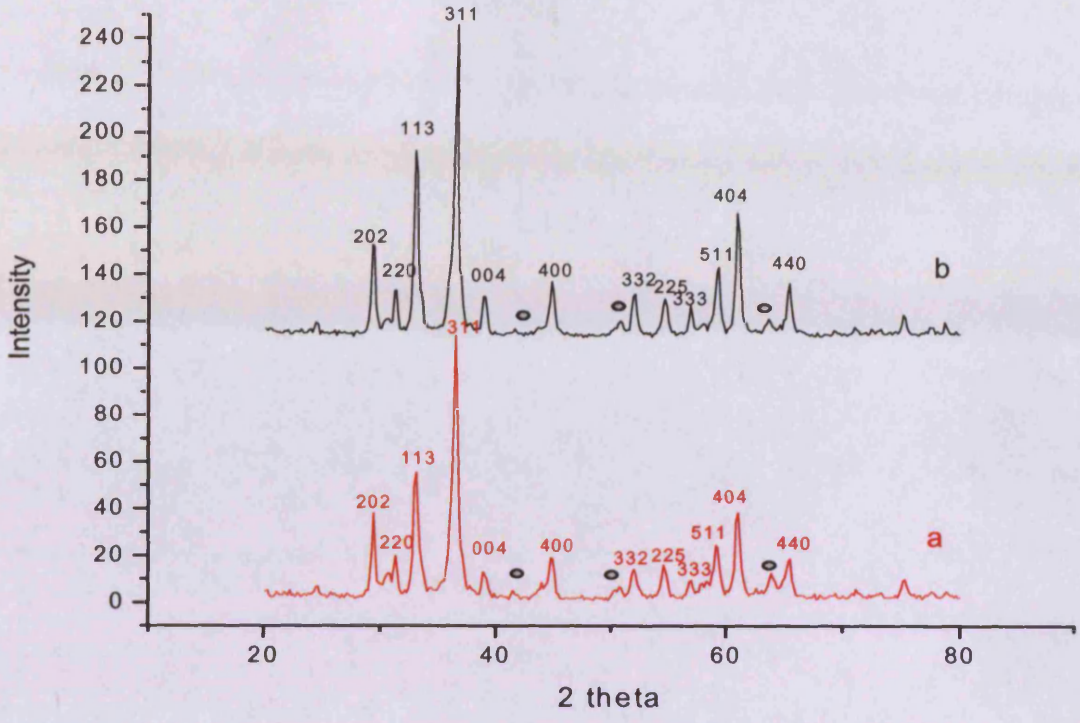

Figure 3.1 XRD pattern of catalysts (a) calined in muffle furnace (b) calcined in tube furnace (○) Mn_3O_4

3.3.1.2 Catalysts preparation at variable pH

One catalyst was prepared using the method of variable pH described in chapter 2 under the section 2.1.1 of catalyst preparation at variable pH. The metal nitrate precursors were premixed rather than co-fed and the precipitant was added to the mixed metals solutions at temperature of 70°C.Precipitates were filtered, washed and dried at 110°C for 16h followed by calcination in muffle furnace at 500°C for 24h.

3.3.1.2.1 Results

3.3.1.2.1.1 Testing results of catalyst prepared at variable pH

CO hydrogenation results for catalyst prepared at variable pH are presented in table 3.2.

Table 3.2 CO hydrogenation over a $CoMnO_x$ catalyst prepared by the variable pH method

Calcination temperature (°C)	500
Calcination time (h)	24
Conversion of CO (%)	10.1
Selectivity / wt% (normalized using mass balance)	
CH_4	9.1
C_2H_4	4.4
C_2H_6	2.3
C_3H_6	13
C_3H_8	2.6
C_4	9
C_{5+}	59.1

Reaction conditions: Catalyst wt = 2g,Time online 92 h, 220°C, 6 Bar, CO/H_2 (1:1 mol ratio), GHSV = 300 h^{-1} C_{5+} = Gaseous, liquid and solid C_5-C_9 + liquid oxygenates

A comparison of catalysts prepared by the constant pH method presented in table 3.1 (under calcination in the muffle furnace) with data presented in table 3.2 shows that the catalyst prepared by variable pH method is better with respect to alkenes selectivity, especially ethylene and propylene.

This is not in agreement with the observations made by M.Van der Riet [30]. The difference in selectivity of catalysts prepared at constant and variable pH can be attributed to the precipitation of cobalt and manganese at different pH values. Cobalt precipitates at lower pH value than Mn. Constant pH preparation results in the formation of a material precipitated at a single pH but the variable pH method gives a material precipitated at different range of pH values from 2 to 9 which may result in more sequential precipitation of metal species resulting in different activity and selectivity. On

the bases of these results the variable pH method was selected as the best one for the investigation of further preparation variables.

3.3.1.2.1.2 Characterization of catalyst prepared at variable pH

(i) XRD

Figure 3.2 shows the XRD patterns of catalyst prepared by the variable pH method. This catalyst shows a typical (Co, $Mn)_2O_4$ spinel structure between $MnCo_2O_4$ (cubic) and Mn_3O_4 (tetragonal). The catalyst prepared by co precipitation using the variable pH method is different with respect to peak shapes in comparison with the catalyst prepared at constant pH. Most of the peaks were broader compared with the catalyst prepared at constant pH.

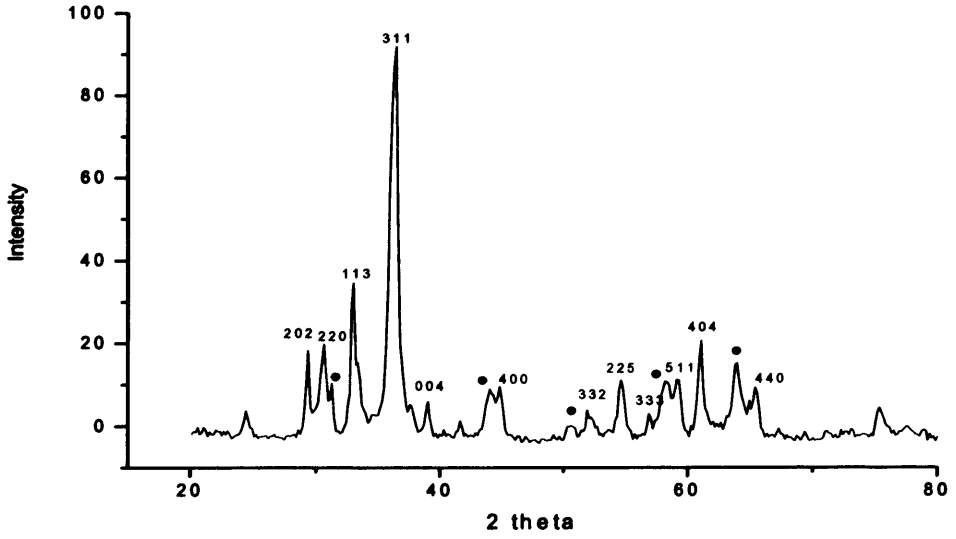

Figure 3.2 XRD pattern for catalyst prepared by variable pH method (○) Mn_3O_4

(ii) BET

The surface area of the catalyst prepared by the variable pH process was $10m^2/g$ which is similar to the catalyst prepared at constant pH. These results show that pH variation results in slightly different bulk structure but it does not affect the surface of catalyst.

3.3.2 Effect of variation of metals ratios (Co and Mn)

3.3.2.1 Results

3.3.2.1.1 Testing results of catalysts prepared with variation of metal ratios (Co: Mn)

Five new batches of catalysts were prepared with different ratios of cobalt and manganese metals in the starting solutions, using the variable pH method of precipitation.

All the experiments reported in the following paragraphs were done in the 6-bed reactor detailed in chapter 2. The catalyst (0.5 g, 0.6-0.85 mm) was reduced with H_2 (GHSV = 600 h^{-1}, 400°C, atmospheric pressure). A mixture of $CO/H_2/N_2$ (47.5: 47.5: 5) was allowed to react over the reduced catalyst at a GHSV = 600 h^{-1} at pressure of 6 bar. Liquid products were collected in a trap held at 20°C . Table 3.3 shows a comparison of catalytic data for catalysts prepared with different Co: Mn ratios.

The catalyst prepared with a 1:1 ratio (Co: Mn) showed better selectivity to light alkenes along with less methane. Catalysts prepared with metal ratios of Co: Mn = 1:1.3 and Co: Mn = 1.3:1 have comparable activity and selectivity with the catalyst prepared with 1: 1 which shows similar nature of all three catalysts. On the other hand the catalysts prepared

with highest ratios of both metals (Co: Mn = 1:1.5 and Co: Mn = 1.5:1) are slightly different in their activity and selectivity.

Table 3.3 CO hydrogenation of catalysts prepared with different ratios of metals

	Metal ratios (Co:Mn)				
	1.5:1	1.3:1	1:1	1:1.3	1:1.5
Conversion of CO	16	13	12.9	14	17
Selectivity / wt% (normalized using mass balance)					
CH_4	15	16	12.7	13	14.3
C_2H_4	2.1	4.1	5	4.8	2.4
C_2H_6	7	5	5.5	5	8
C_3H_6	16	22	21	19	18
C_3H_8	3.6	5	4.5	4	4.9
C_4	11	17	16	15.4	13
C_{5+}	41	29	34	36	37
Alcohols	1.9	1.5	1.2	3.3	2

Reaction conditions: Catalyst wt = 0.5g,Time online 88h, 220°C, 6 Bar, CO/H_2 (1:1 mol ratio), GHSV = 600h^{-1} C_{5+} = Gaseous, liquid and solid C_5-C_9 + liquid oxygenates, alcohols=C_1-C_3 in gas phase

Mirzaei *et al.* [39] reported a marked enhancement in the selectivity to light alkenes with an increase in the manganese concentration. Van der Riet [30] observed an increase in methane yield with increase in concentration of cobalt ratio and a decrease in the selectivity to alkenes, while increasing the concentration of manganese increased propylene selectivity and decreased the selectivity to methane. But the ratios of cobalt and manganese were changed with a wide range by both researchers while the results presented in table 3.3 are from the catalysts in which the metal ratios were varied in a narrow range from 1 to 1.5. It can be speculated that a small variation in metal ratios may not be enough to affect the catalytic activity and selectivity as was also apparent from the characterization results of these catalysts which are discussed below.

3.3.2.1.2 Characterization of catalysts prepared by variation of metal ratios (Co: Mn)

(i) BET

Table 3.4 Surface area analysis of catalysts prepared with different ratios of metals

Metal ratios (Co:Mn)				
1.5:1	1.3:1	1:1	1:1.3	1:1.5
BET(m^2/g)				
11	6	6	5	9

Catalysts with the highest ratios of cobalt and manganese (both Co: Mn=1.5:1 and Co: Mn=1:1.5) show higher surface areas but there is no apparent difference in the surface area of catalysts prepared by variation of metal ratios between 1 and 1.3. This trend of surface area values shows that the variation of metal ratios was not enough to affect the catalysts morphology.

(ii) XRD

Figure 3.3 shows a comparison of catalysts prepared with different metal ratios. All these catalysts show a typical (Co, $Mn)_2O_4$ spinel structure between $MnCo_2O_4$ (cubic) and Mn_3O_4 (tetragonal). It is apparent that a change in metal ratios does not make any marked difference in the bulk structure of catalysts. Mirzaei *et al.* [39] reported the appearance of Co_3O_4 (cubic), $CoMnO_3$ (rhombohederal) and (Co, Mn) (Co, $Mn)_2O_4$ (tetragonal) phases in the catalyst with a 1:1 ratio of cobalt and manganese. But they observed additional peaks of Mn_2O_3 (cubic) and Mn_5O_8 (monoclinic) phases for catalysts prepared with Co: Mn = 1:6. Co_3O_4 (cubic), $CoMnO_3$ (rhombohederal) and (Co, Mn)$(Co,Mn)_2O_4$ (tetragonal) were more obvious for catalysts prepared with Co:Mn =3:1. Present studies did not show the appearance of any additional peaks of cobalt and manganese which means that a slight variation in metal ratios (1 to 1.5) may not be enough to affect the bulk structure of

the catalyst. This observation also explains the catalytic activity of these catalysts which is not considerably different because of no big difference in the bulk structure of catalysts.

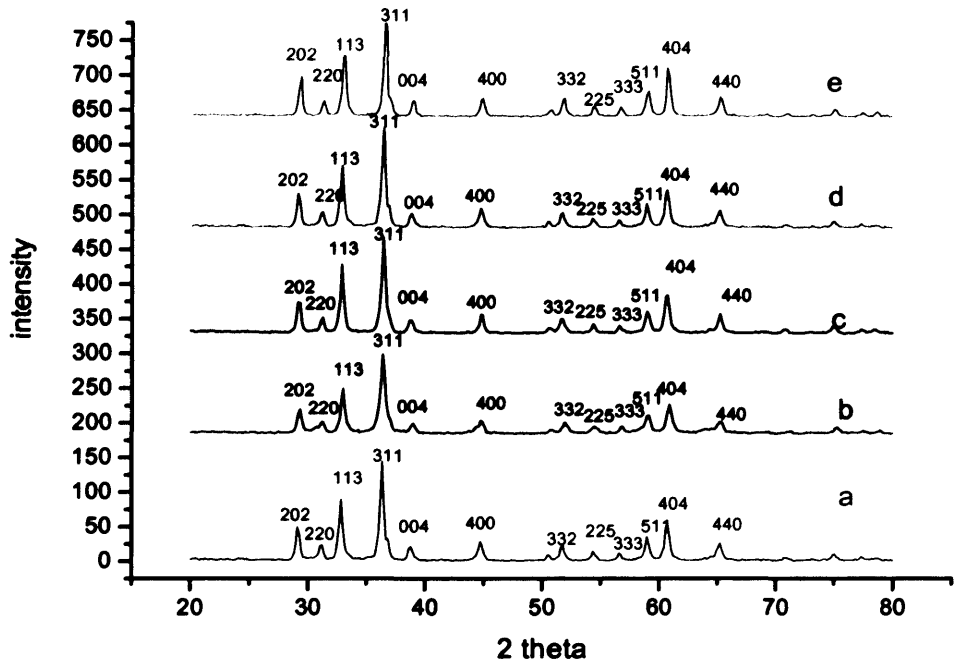

Figure 3.3 XRD pattern for the catalysts prepared with different ratios of metals (a) Co/Mn=1/1,(b) Co/Mn=1.5/1,(c)Co/Mn =1.3/1,(d)Co/Mn=1/1.3,(e)Co/Mn =1/1.5

It is apparent from table 3.3 that the catalyst prepared with a 1:1 ratio of cobalt to manganese was best with respect to selectivity of light alkenes and methane. So this ratio was chosen for further study of the variation of preparation variables.

3.3.3 Effect of temperature variation

Three new batches of catalysts were prepared by taking equivalent metal solutions (Co: Mn = 1:1) and using the variable pH method of precipitation. The temperature of precipitation mixture was varied from 60-80°C.

3.3.3.1 Results

3.3.3.1.1 Testing results of catalysts prepared by variation of temperature

Table 3.5 shows testing results for catalysts prepared at different temperatures of precipitation. There is a remarkable increase in catalytic activity and selectivity with an increase in temperature of the precipitation mixture. The catalyst prepared 80°C was best with respect to both catalytic activity and selectivity. Mirzaei *et al.* [39] have reported a decline in selectivity to ethylene and propylene at 85°C and there is more selectivity for both products at 70°C compared with catalysts prepared at 35 and 50°C, along with a slight decrease in CO conversion with an increase in temperature from 35 to 80°C. Maiti *et al.* [40] also reported 70°C as the best precipitation temperature showing a remarkable effect of temperature on the catalytic activity and selectivity of the catalyst. 70°C was reported as the best temperature of coprecipitation by Van der Riet [30] as well. But the present studies have shown 80°C as the best temperature of precipitation.

Table 3.5 CO hydrogenation of catalysts prepared at different temperatures

	Temperature of precipitation mixtures (°C)		
	60	70	80
Conversion of CO	12	16	19
Selectivity / wt% (normalized using mass balance)			
CH_4	16.5	15	18
C_2H_4	1.3	2.3	2
C_2H_6	5.6	7	10
C_3H_6	13	16	18
C_3H_8	6	5	7
C_4	11	13	13.9
C_{5+}	44	40	28.5
Alcohols	2.3	1.5	3

Reaction conditions: Catalyst wt = 0.5g,Time online 96h, 220°C, 6 Bar, CO/H_2 (1:1 mol ratio), GHSV = 600h^{-1} C_{6+} = Gaseous, liquid and solid C_6-C_9 + liquid oxygenates, alcohols=C_1-C_3 in gas phase

3.3.3.1.2 Characterization of catalysts prepared by variation of temperature

(i) XRD

Figure 3.4 shows a comparison of catalysts prepared at different temperatures of precipitation. All catalysts show the typical (Co, $Mn)_2O_4$ spinel structure between $MnCo_2O_4$ (cubic) and Mn_3O_4 (tetragonal) along with new phases of Mn_3O_4 presented by ○. There is also the appearance of one new phase presented by □ in the catalyst prepared at 80°C and 60°C. Catalyst prepared at 80°C shows less intense peaks. The appearance of Mn_3O_4 phases (○) at higher temperature along with slight broadening in peaks can be related to different activity and selectivity of catalyst prepared at 80°C.

The appearance of additional phases of Mn_3O_4 at higher temperature is in agreement with the results reported by Mirzaei *et al.* [39]. They have observed the appearance of additional phases of manganese oxide with an increase in temperature: Mn_5O_8 (monoclinic) along with (Co, $Mn)_2O_4$ which has been reported to be the best catalyst with respect to activity and selectivity. They have also reported broader peaks for the catalysts prepared at higher temperature (70°C) of precipitation, relating them to the best catalytic activity of catalyst prepared at higher temperature.

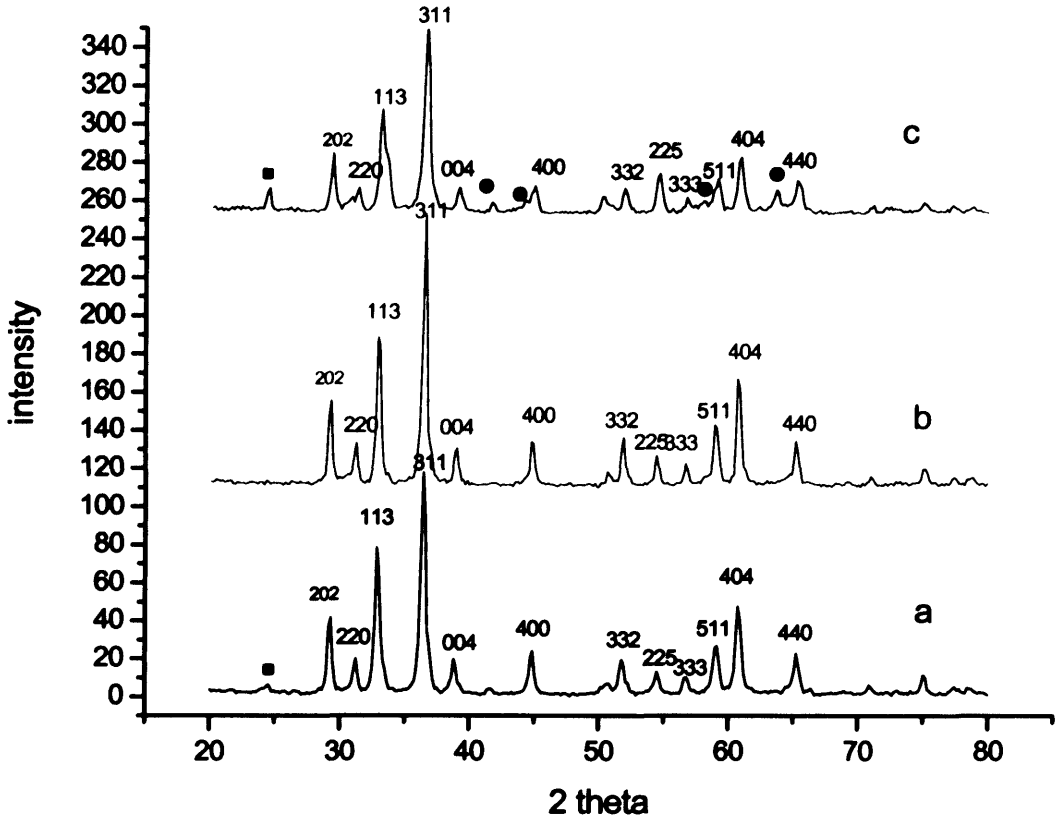

Figure 3.4 XRD pattern for the catalysts prepared at different temperatures of precipitation (a) 60°C, (b)70°C, (c) 80°C (□) New phases, (○) Mn_3O_4

(ii) BET

There is no apparent difference in the surface area of catalysts prepared at different precipitation temperatures as shown in table 3.6.

Table 3.6 Surface area analysis of catalysts prepared at different temperatures

Temperature of precipitation (°C)		
60	70	80
BET (m^2/g)		
8	9	10

3.3.4 Effect of pH variation

The final pH of precipitation mixture was varied from 7-9 during preparation of the $CoMnO_x$ catalyst with Co/Mn = 1/1, at 80°C using 5.6M ammonium hydroxide solution as precipitant using the variable pH method of precipitation.

3.3.4.1 Results

3.3.4.1.1 Testing results of catalysts prepared by variation of pH

Table 3.7 presents catalytic testing results for catalysts prepared by the variable pH method with pH values of 7, 8 and 9 respectively. The catalyst material prepared at a pH value of 8.0 showed very good activity and selectivity with respect to alkenes. There was a slight difference in the selectivity of the catalyst prepared at a pH of 9 and 8, with the activity of the latter being higher. The catalyst prepared at a pH of 7 was good with respect to selectivity to propylene compared with those prepared at pH of 9 and 8, but the methane selectivity was highest for this material.

Table 3.7 CO hydrogenation of catalysts prepared by variation of pH

	Final pH value of precipitation mixtures		
	7	8	9
Conversion of CO (%)	16	19	9
Selectivity / wt% (normalized using mass balance)			
CH_4	16	13	11
C_2H_4	2	1.9	5
C_2H_6	8	7.2	5
C_3H_6	18.5	17.2	17.5
C_3H_8	4.5	4	5
C_4	13	12.5	12.9
C_{5+}	29.5	37	32
Alcohols	1.9	1.8	1.2

Reaction conditions: Catalyst wt = 0.5g,Time online 90h, 220°C, 6 Bar, CO/H_2 (1:1 mol ratio), GHSV = 600h^{-1} C_{5+} = Gaseous, liquid and solid C_5-C_9 + liquid oxygenates, alcohols=C_1-C_3 in gas phase

Mirzaei *et al.* [39] have studied the effect of different values of pH and they have concluded pH 8.3 as the optimum value using sodium carbonate as the precipitating solution.

3.3.4.1.2 Characterization of catalysts prepared by variation of pH

(i) BET

Table 3.8 Surface area analysis of catalysts prepared by variation of pH

Final pH of precipitation mixture		
7	8	9
BET (m^2/g)		
7	9	6

Catalyst prepared with pH = 8 shows higher surface area compared with catalysts prepared with 7 and 9 pH values.

(ii) XRD

Figure 3.5 presents a comparison of XRD patterns for catalysts prepared at different pH values. There is the appearance of few peaks of manganese oxide Mn_3O_4 (°) along with typical $(Co, Mn)_2O_4$ spinel structure in the catalyst prepared at pH = 8. Most of the phases of mixed spinels were missing in the catalysts prepared at pH of 7. Catalyst prepared at pH 8 showed broader peaks in comparison with catalysts prepared at pH 7 and 9. Although the selectivity with respect to ethylene was low for catalyst prepared at pH of 8 but it was more active for CO conversion with almost similar selectivity to propylene. Therefore, pH=8.0 was selected as the best parameters for further investigations.

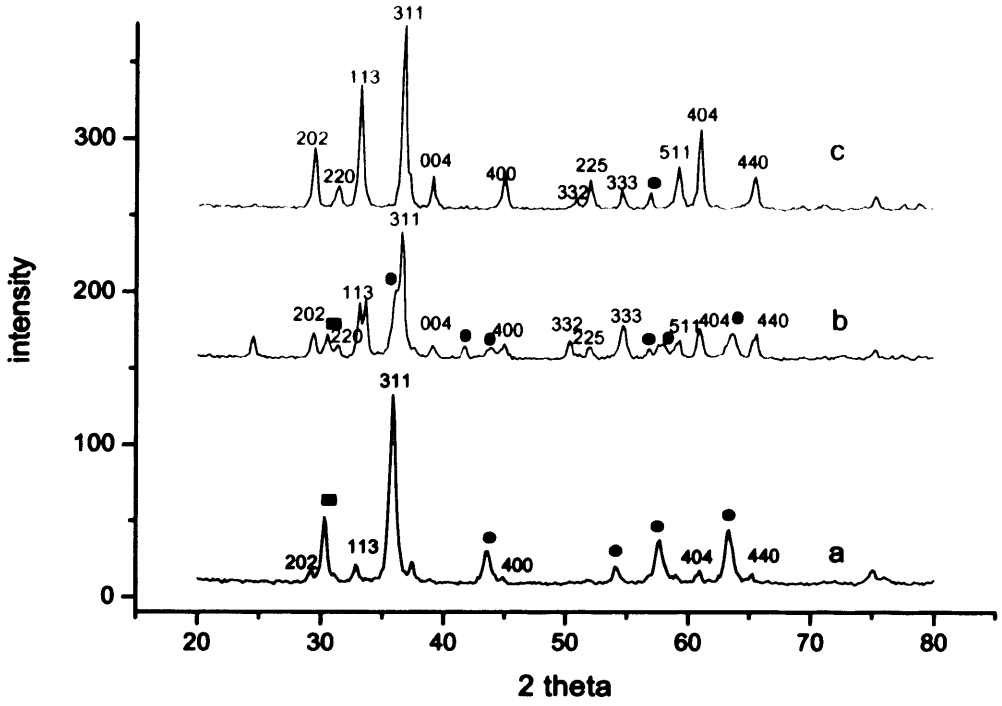

Figure 3.5 Comparison of catalysts prepared at different final values of pH (a) pH =7,(b) pH =8 (c) pH =9 (o) Mn_3O_4

pH 8 was selected for further study of the variation of preparation variables.

3.3.5 Effect of variation of precipitating agents

3.3.5.1 Results

3.3.5.1.1 Testing results of catalysts prepared by variation of precipitating agents

Three different precipitating agents (ammonium bicarbonate, ammonium hydroxide and sodium carbonate) 5.6M each were used for the preparation of catalysts with a Co/Mn ratio = 1/1, at 80°C and using the variable pH precipitation method with a final pH = 8.

Interestingly sodium carbonate presented (table 3.9) very good activity with respect to CO conversion and high selectivity of ethylene maintaining low methane selectivity. The similar effect of carbonate precipitating agents on FT reaction has already been reported by Diffenbach and Fauth [41]. The factors responsible for the high ethylene selectivity of the sodium carbonate precipitated catalysts remained unidentified.

Table 3.9 CO hydrogenation of the catalysts prepared with different precipitants

	Precipitating agents		
	Sodium carbonate	Ammonium hydroxide	Ammonium bicarbonate
Conversion of CO	25	16	21
Selectivity / wt% (normalized using mass balance)			
CH_4	15.6	14	18
C_2H_4	10.1	2.4	1.15
C_2H_6	4.3	7	9
C_3H_6	5	18.4	14
C_3H_8	5.2	5.4	8.01
C_4	6.4	13	11
C_{5+}	50.7	38.4	42.4
Alcohols	2	1.3	1.8

Reaction conditions: Catalyst wt = 0.5g,Time online 86h, 220°C, 6 Bar, CO/H_2 (1:1 mol ratio), GHSV = 600h^{-1} C_{5+} = Gaseous, liquid and solid C_5-C_9 + liquid oxygenates, alcohols=C_1-C_3 in gas phase

Dry and Oosthuizen [42] found that the catalyst basicity increased with sodium content and there was a decrease in methane selectivity with an increase in surface basicity. Sodium in combination with manganese can produce stable FT catalysts with high selectivity to light olefins and a suppressed quantity of methane [43].

An *et al.* [44] have reported a negative effect of residual sodium on FT synthesis (which is not observed in the present studies). This effect was observed because of sodium remaining in the catalyst if the catalyst precursor was insufficiently washed after precipitation. The residual sodium inhibits the extent of carburization and poisons the FTS reaction.

A comparison of precipitating agents in table 3.9 shows ammonium hydroxide to be the best precipitating agent. Van der Riet [30] also reported ammonium hydroxide as the best precipitant. We chose ammonium hydroxide as precipitating agent for further investigation of ageing time.

3.3.5.1.2 Characterization of catalysts prepared by variation of precipitating agents

(i) XRD

Figure 3.6 presents a comparison of XRD patterns for catalysts prepared with three different precipitating agents. Almost all phases of the typical (Co, $Mn)_2O_4$ spinel structure are present in these catalysts. Interestingly the catalyst prepared with sodium carbonate shows difference in peak intensities and shapes. All typical phases of mixed Co, Mn spinel oxides are present in this catalyst.

There are some additional phases of manganese oxide (Mn_3O_4) phases along with some new phases (□, which could not be identified) in the catalyst prepared with ammonium hydroxide and ammonium bicarbonate which are absent in the catalyst prepared with sodium carbonate. Presence of additional manganese oxide phases may be responsible for the different selectivity pattern.

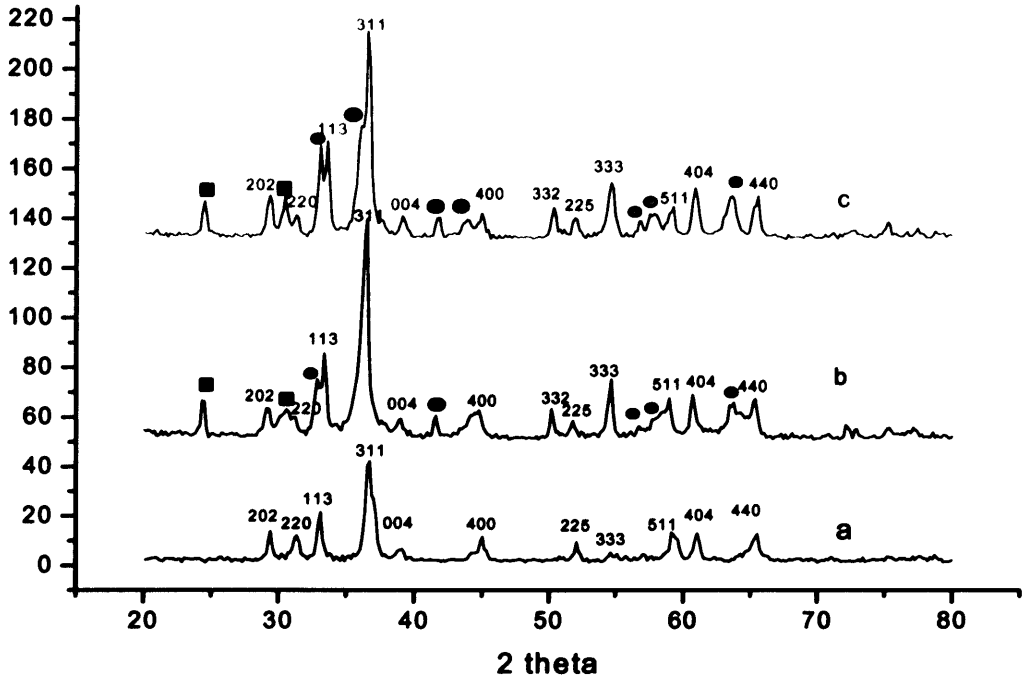

Figure 3.6 XRD comparison of catalysts prepared with different precipitants (a) Sodium carbonate (b) Ammonium bi carbonate (c) Ammonium hydroxide (○) Mn_3O_4 (□) new phases

(ii) BET

Table 3.10 BET surface areas of catalysts prepared with different precipitating agents

Precipitating agents		
Na_2CO_3	NH_4HCO_3	NH_4OH
BET (m^2/g)		
9	7	5

The catalyst prepared with ammonium hydroxide showed lowest surface area. The surface area of the sodium carbonate precipitated catalyst was much higher than the ammonium bicarbonate precipitated catalyst.

(iii) SEM

Figures 3.7 (a) and (b) present a comparison of SEM micrographs of catalysts prepared with sodium carbonate and ammonium hydroxide. The catalyst prepared with sodium carbonate has more well defined spherical particles in combination with small square shaped particles. Catalysts prepared with ammonium hydroxide showed a nonuniform surface structure with various particles of large grains embedded in the form of aggregates.

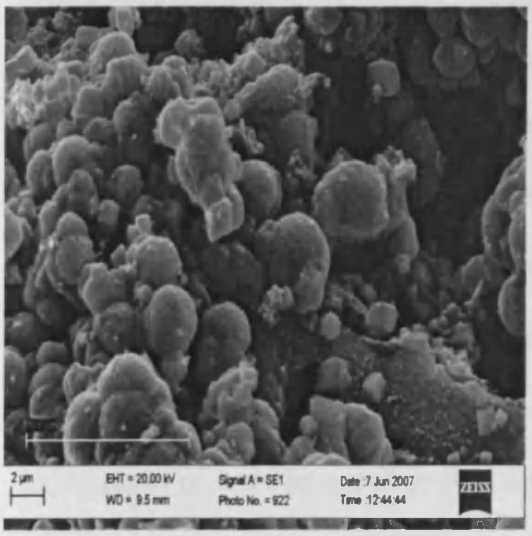

(a) Sodium carbonate

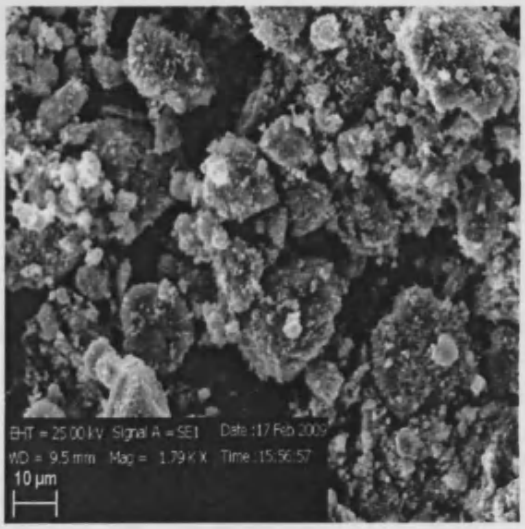

(b) Ammonium hydroxide

Figure 3.7SEM of the catalyst prepared with different precipitants

3.3.6 Effect of variation of ageing time

3.3.6.1 Results

3.3.6.1.1 Testing results of catalysts prepared by variation of ageing time

Ageing of precipitates for different time intervals has been found to be an important parameter in the stabilization of catalysts. Hutchings *et al.* [45-53] have demonstrated the importance of ageing time with respect to catalyst activity for the oxidation of CO by mixed copper manganese oxides and mixed copper zinc oxides. Mirzaei *et al.* [54, 55] have also studied the effect of ageing time on catalytic performance of mixed iron cobalt oxide catalysts for syngas conversion to light alkenes. In all these studies it has been observed that the ageing of precipitates obtained by coprecipitation leads to phase changes towards thermodynamically stable forms. In the present study the effect of catalyst precursor ageing on the morphology and catalytic activity of cobalt, manganese oxide has been studied for the hydrogenation of CO. A series of mixed cobalt manganese oxide catalysts were prepared by the co-precipitation method (Co/Mn=1:1, 80°C, variable pH=8) with a range of ageing times 0 (unaged), 0.5, 2 and 5h for the precipitate under similar conditions. The catalysts were calcined for 24h at 500°C. The effect of ageing time on catalytic performance is shown in table 3.11. These results show a considerable variation in the catalytic performance of catalysts after the ageing process. The catalyst aged for 0 h shows highest activity with lowest selectivity to methane among the series of aged catalysts, along with high selectivity to ethylene and propylene. The catalyst aged for 0 h was also found to be more selective to C_{6+} products with a lower selectivity to methane. After half an hour ageing the catalyst shows similar activity with slight

variation in the selectivity. The catalyst aged for half an hour is more selective to propene but shows more methane compared with catalyst aged for 0 h. The catalyst aged for 2h was least active with respect to CO conversion although it was highly selective towards alcohols. The catalyst aged for 5h has been found to be more selective towards methane. The catalyst aged for half an hour has been reported to be more active for CO conversion to light alkenes [39].

Table 3.11 CO hydrogenation of catalysts aged for different time intervals

	Ageing time(h)			
	0	0.5	2	5
Conversion of CO	16	15.63	10.36	12.5
Selectivity / wt% (normalized using mass balance)				
CH_4	14	17	18.5	23.9
C_2H_4	2.4	1.8	2.13	2
C_2H_6	7	9.9	9.65	12
C_3H_6	18.4	21.15	20.1	19.7
C_3H_8	5.4	9.4	10	9.32
C_4	13	13.1	14	13.3
C_{5+}	38.4	23	18.6	17.2
Alcohols	1.3	4.7	6.79	2.4

Reaction conditions: Catalyst wt = 0.5g,Time online 92h, 220°C, 6 Bar, CO/H_2 (1:1 mol ratio), GHSV = 600h^{-1} C_{5+} = Gaseous, liquid and solid C_5-C_{22} + liquid oxygenates, alcohols=C_1-C_3 in gas phase

The difference in selectivity of catalysts aged for longer times (2 and 5h) can be explained on the basis of further precipitation of metals during the ageing process. There was a considerable decrease in pH of the precipitation mixture during ageing of 2h and 5h catalysts which shows more precipitation of metals which may have an effect on the relative ratio of cobalt and manganese in final catalyst. Hutchings *et al.* [45, 46] have reported a decrease in the catalytic activity of $CuMnO_x$ catalysts for ageing periods of 1-5h.

3.3.6.1.2 Characterization of catalysts prepared by variation of ageing time

(i) XRD

Figure 3.8 shows XRD pattern of $CoMnO_x$ catalysts aged for different time intervals.

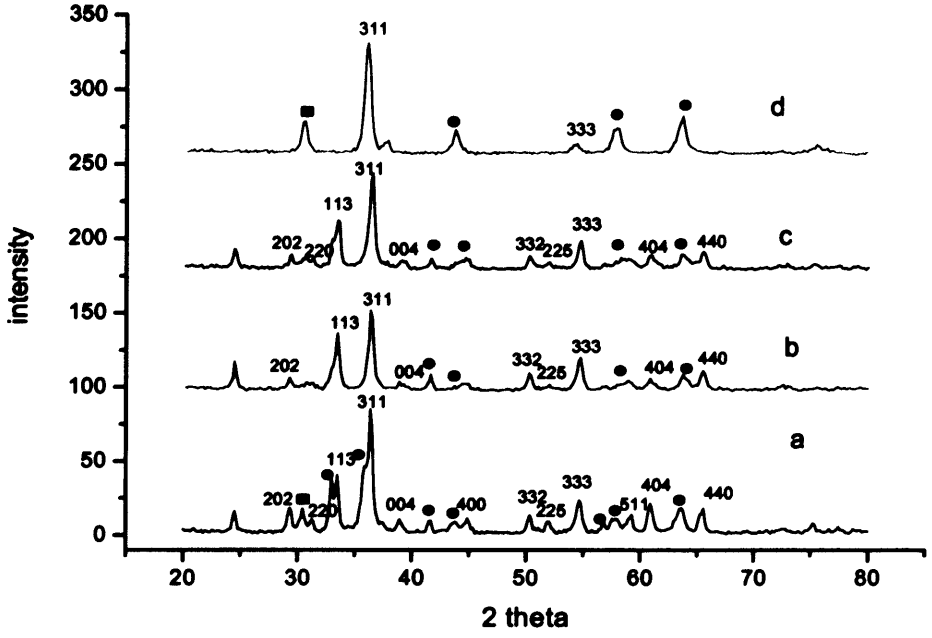

Figure 3.8 Comparison of XRD of catalysts aged at different time intervals (a) unaged (b) 0.5h(c)2h(d)5h(○) Mn_3O_4(□) unidentified phases

The best catalytic activity and selectivity with respect to light alkenes along with less methane was found for unaged catalyst and this catalyst was a mixed spinel oxide along with additional phases of manganese oxide (Mn_3O_4) represented by small circles (○). Some new phases (represented by small rectangle) also appear which could not be identified. Most of these phases are present in the catalyst aged for half an hour but the peaks get sharper with an increase in ageing time. Some phases of mixed spinel oxide disappear in the catalyst aged for 5h and some phases are highly crystalline. An increase

in crystallinity of these mixed oxide phases can be related to different activity and selectivity during CO hydrogenation. Mn_3O_4 phases are present in this catalyst which are more intense and crystalline, a new phase starts appearing next to the phase 311. Similar observations have been reported earlier [39, 56] regarding XRD changes with increase in ageing time from 0 to 5h and the catalysts with more crystallinity were found to be less active and selective during the CO hydrogenation reaction.

(ii) BET

Table 3.12 presents the BET surface areas for catalysts aged for different time intervals. There is a decrease in surface area after calcination, and all these catalysts show almost similar values of surface area. The catalyst aged for 5 h has the lowest surface area and was least active in CO hydrogenation.

Table 3.12 BET of aged catalysts (0 to 5h)

Catalysts	Surface area (m^2/g)	
	Before calcination	After calcination
Unaged	12	9
(0.5h ageing)	11	7
(2h ageing)	9	8
(5h ageing)	8	6

(iii) XPS

Table 3.13 shows the XPS results for catalysts aged for different times. The catalyst aged for 5h has a completely different metal ratio compared with other two catalysts aged for half an hour and 2 hours. It (5h) has more cobalt and less manganese while other catalysts (0.5 and 2h) have more manganese and less cobalt.

Table 3.13 XPS results for aged samples

Ageing time	Heat treat	Co/Mn
30min	Uncalcined	0.55
30min	calcined	0.43
2h	Uncalcined	0.6
2h	calcined	0.47
5h	Uncalined	2.04
5h	Calcined	1.2

(iv) SEM

Ageing of catalysts for different time intervals has shown a considerable affect on morphology and structure of catalysts as shown in the following figures. SEM images of catalysts aged for different times are shown in figure 3.9. Unaged catalyst in figure 3.9 (a) shows various particles of different shapes and variable sizes.

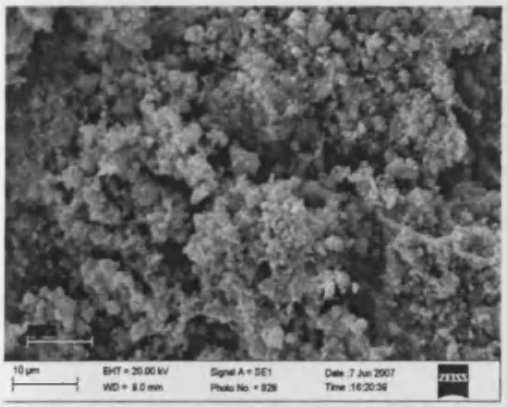

(a) Unaged

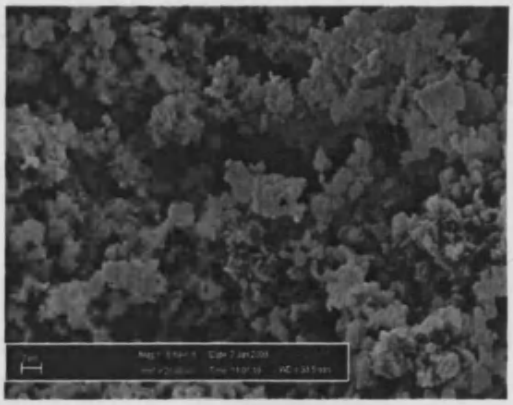

(b) 0.5h ageing

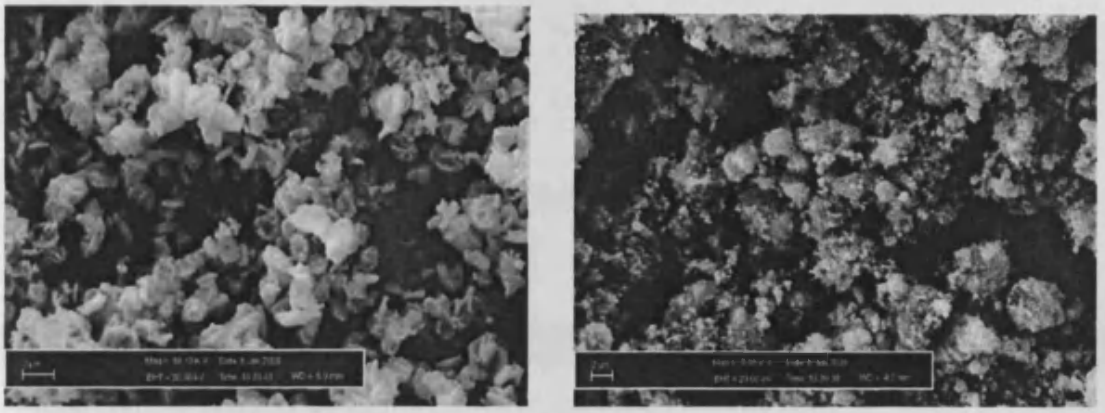

(c) 2h **(d) 5h**

Figure 3.9 SEM image of the catalysts aged for different time intervals

The catalyst aged for half an hour shows well defined particles in the form of regular plates of different sizes along with some needle like structures. The catalyst aged for 2h shows similar plates and larger needle like structures. This shows a growth of particles with an increase in ageing time from 0 to 2h. The SEM micrograph of the catalyst aged for 5h is completely different with different aggregates of particles.

(v) TPR

Figure 3.10 shows TPR profile of catalyst aged for 0h. The TPR of mixed cobalt manganese oxides ($CoMnO_x$) is difficult to interpret due to the large number of possibilities of mixed cobalt and manganese oxidation states resulting from the multi-valency of each element. This catalyst was calcined before TPR so we do not expect nitrates and water contents. First peak appears from reduction of cobalt species Co_3O_4 to CoO and Co metal. It has also been observed that addition of manganese to cobalt system decreases the reducibility of cobalt species [57]. Second peak is attributed to the subsequent reduction of oxides of manganese.

This is difficult to relate the peaks with well defined redox reactions. However, it is expected that the lower temperature peaks more likely correspond to the reduction of Co^{+2} as cobalt has a higher reducibility than manganese in mixed compounds. Manganese oxide, Mn_2O_3, is expected to reduce in one step to MnO. Second peak is attributed to the subsequent reduction of oxides of manganese. The manganese oxide does not reduce to Mn^0 [58].

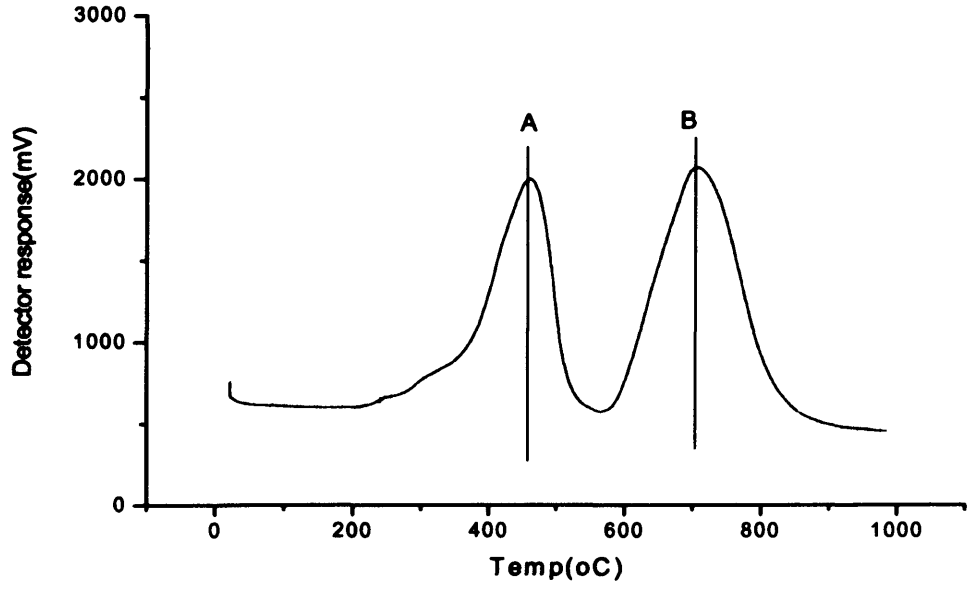

Figure 3.10 TPR profile of $CoMnO_x$ catalyst

Table 3.14 TPR results of $CoMnO_x$ catalyst

T(°C) Peak A	T(°C) Peak B	H_2 Peak 1(μmol/g)	H_2 Peak 2(μmol/g)	H_2abs., peak 1(%)	H_2abs., peak 2(%)
462.4	707.4	3135.28	5090.81	38.20	61.91

3.3.7 Optimum preparation conditions

After a detailed investigation of preparation variables $CoMnO_x$ catalyst was prepared using the following preparation conditions:

Ratio of metals (Co/Mn) =1/1, temperature of precipitation = 80°C, precipitating agent = ammonium hydroxide, molarity of ammonium hydroxide = 5.6M, ageing time = 0h

The catalyst prepared under these conditions was used for the investigation of reaction conditions as discussed below.

3.4. Effect of reaction conditions

The reaction conditions have a marked effect on the catalytic performance. It has been reported by Dry [59] that selectivity on a carbon basis is essentially a function of the probability of chain growth, α.

Control of the product selectivity is therefore to a large extent determined by the factors that influence the value of α. The main factors are the temperature of the reaction, the gas composition and more specifically the partial pressures of the various gases in contact with catalyst inside the reactor. Overall, by manipulating these factors a high degree of flexibility can be obtained regarding the type of product and the carbon range.

For optimization of reaction conditions, in this study the effects of operating conditions such as reaction temperatures and reaction pressure have been examined to investigate the catalyst stability and its performance under different FT conditions.

3.4.1 The influence of operating temperature

An increase in FT operating temperature shifts the selectivity profile to lower carbon number products. Desorption of growing surface species is one of the main chain termination steps and since desorption is an endothermic process so a higher temperature should increase the rate of desorption which will result in a shift to lower molecular mass products.

Table 3.15 Influence of reaction temperature on $CoMnO_x$ catalyst

	Reaction temperature (°C)		
	220	240	270
Conversion of CO	12	36	89
Selectivity / wt% (normalized using mass balance)			
CH_4	16.8	8	3.3
C_2H_4	3.2	0.1	0
C_2H_6	9.1	3	3.2
C_3H_6	28.4	4.5	0
C_3H_8	7.4	6	3.5
C_4	17.6	1	0.7
C_{5+}	14.6	17	5.1
CO_2	tr	51	84
Alcohols	2.6	7	tr

Reaction conditions: Catalyst wt = 0.5g, Time online 96h, 6 Bar, CO/H_2 (1:1 mol ratio), GHSV = $600h^{-1}$, C_{5+} = Gaseous, liquid and solid C_5-C_{22} + liquid oxygenates, alcohols=C_1-C_3 in gas phase, tr=trace amount

An increase in temperature from 220°C to 240°C increased the CO conversion from 12 to 36% as shown in table 3.15. Product stream shifted to an increased selectivity to ethane and propane with lower selectivity to ethylene and propane showing more hydrogenation at high temperature. A further increase in temperature to 270°C showed a tremendous increase in CO_2 and alkane selectivity with high activity, along with no olefins.

As the temperature is increased the system becomes more hydrogenating and the ratio of alkenes to alkanes decreases. Probably for the same reasons the selectivity to alcohols

also decreases with an increase in temperature up to 270°C. The degree of chain branching also increases with an increase in temperature, which can result in higher molecular weight products thus increasing C_{5+} selectivity at high temperature. Van der Riet [30] has observed exactly similar effects on activity and selectivity of $CoMnO_x$ catalysts with an increase in temperature. It is worth mentioning here that the amount of heavy products including wax and liquids increased with an increase in temperature to 270°C.

CO_2 was the most dominant product at high temperature. The very first reaction in FT is the chemisorption of CO at the catalyst surface. There are two possibilities of reaction, either the chemisorbed CO as such inserts into the growing chain leading to subsequent hydrogenation to CH_2 or CO first dissociates to C and O atoms on the surface and the C then hydrogenates to CH_2 which then inserts into growing hydrocarbon chain. In later case the adsorbed oxygen atoms could react with hydrogen atoms and result in water formation (the main by-product of FT reaction). In spite of little or no CO_2 produced on cobalt catalyst at low temperature of reaction, either CO chemisorption does not occur on the catalyst surface or the actual rate of hydrogen reacting with oxygen atoms is much faster than that of CO reacting with OH species. Co catalyst has been reported to be a good water gas shift catalyst at higher temperature [35] resulting in higher CO_2 selectivity. This can be argued that the rate of CO reacting with oxygen atoms is faster at higher temperature compared with hydrogen reacting with oxygen.

Bai *et al.* [60] have demonstrated an increase in alkene selectivity with an increase in temperature for a Fe/Mn catalyst using a slurry phase FT reactor. They have also reported the formation rate of liquids and heavy waxes decreasing with an increase in

temperature from 270 to 300°C. They have observed a slight increase in methane selectivity with an increase in temperature.

Mirzaei *et al.* [61] have reported a significant increase in methane selectivity with increase in temperature from 280 to 450°C for an iron manganese catalyst, obtaining the highest alkene selectivity at 360°C, which remains high at higher temperature. Their studies and results concentrate on the formation of alkenes (C_2-C_4) only without mentioning formation of CO_2 and alkanes.

Everson and Mulder [62] have observed an increase in CO conversion with an increase in temperature for a fixed set of operating conditions and for a fixed bed length with the product stream shifting towards the higher molecular weight hydrocarbons. They have also observed a decrease in alkene to alkane ratio consistent with the present studies.

3.4.2 The influence of reaction pressure

The higher the CO partial pressure the more is the catalyst surface covered by adsorbed monomers. The lower the coverage by partially hydrogenated CO monomers the higher the probability of chain growth is expected to be [61]. Two key steps leading to chain termination are desorption of the growing polymeric chains yielding alkenes, and hydrogenation of the chains to yield alkanes.

Table 3.16 shows the effect of an increase in reaction pressure of syngas on the performance of the $CoMnO_x$ catalyst. There is an increase in CO conversion with an increase in pressure from 3 to 9 bars, and methane selectivity decreased with an increase in pressure. Likewise the propylene to propane ratio increased with an increase in

pressure of syngas. From these results 6 bar pressure was chosen as the best reaction pressure because of the high propylene to propane ratio, with a lower selectivity to methane. Interestingly there is a decrease in alcohol synthesis with an increase in pressure of syngas. Alcohols are also primary FT products just like alkenes, and it could be possible that at least some, if not all, of the alkenes are formed by dehydration of these primary alcohols.

These observations are in agreement with the reported results of syngas pressure variation [59, 61]. Mirzaei *et al.* [61] have reported no significant decrease in CO conversion for a $FeMnTiO_2$ catalyst with an increase in pressure from 1 to 6 bar along with an increase in the selectivity of light alkenes. A tremendous decrease in methane selectivity is reported with an increase in pressure.

An increase in total pressure would generally result in condensation of hydrocarbons which are normally in the gaseous state at atmospheric pressure. Higher pressure would probably lead to the saturation of catalyst pores by liquid reaction products [63]. A different composition of the liquid phase in catalyst pores at high syngas pressures could affect the rate of elementary steps.

Van der Riet [30] reported a decline in catalytic activity of $CoMnO_x$ with an increase in pressure from 5.9 bar to 10.95 bar and the selectivity to hydrocarbons remained unchanged. A further increase in pressure to 211 bar reduced the catalytic activity even more and the selectivity changed appreciably. This has been postulated to be in indication of deactivation of the catalyst at elevated pressures as the result of a structural change e.g. carbide formation or particle disintegration. They have also concluded 6 bar pressure as

the most appropriate pressure for syngas conversion to light alkenes using the $CoMnO_x$ catalyst system.

Table 3.16 Influence of reaction pressure of syngas on $CoMnO_x$ catalyst

	Reaction pressure (bar)			
	1	3	6	9
Conversion of CO	6.1	4.75	12	18.3
Selectivity / wt% (normalized using mass balance)				
CH_4	45	21	16.8	15.3
C_2H_4	3.2	5.3	3.2	3
C_2H_6	1.5	6.5	9.1	8.5
C_3H_6	11.3	21.6	28.4	26
C_3H_8	0.63	7	7.4	5.6
C_4	8	8.5	17.6	18
C_{5+}	16.6	9.5	15.8	17.11
Alcohols	6.2	4	2.6	1.8

Reaction conditions: Catalyst wt = 0.5g, Time online 94h, Temp=220°C 6 Bar, CO/H_2 (1:1 mol ratio), GHSV = $600h^{-1}$ C_{5+} = Gaseous, liquid and solid C_5-C_{22} + liquid oxygenates, alcohols=C_1-C_3 in gas phase

Keyser *et al.* [36] have reported a decrease in olefinic content with an increase in pressure from 6 bar to 211 bar which was correlated with an indirect effect of the corresponding increase in contact time. They have also reported a significant increase in C_{8+} fraction with increase in pressure. Other investigators have reported a decrease in olefin selectivity with an increase in pressure for cobalt catalysts [33, 64, 65].

3.5 Conclusions

The type of furnace affects the surface structure of catalysts, which results in differences in catalytic activity and selectivity. Calcination in a muffle furnace decreases the surface area of the catalyst which decreases the catalytic activity.

The co-precipitation preparation method under constant and variable pH results in different catalytic selectivities. The catalyst prepared by the variable pH method increases

selectivity to ethylene and propylene. Catalysts prepared by both methods do not show any difference in surface area which is related to their similar catalytic activities.

The best preparation conditions for an optimum catalytic performance are 1/1 Co/Mn ratio, at pH 8 and 80°C for 0 h ageing. It has been observed that catalysts with less crystalline mixed spinel oxide structures have good catalytic activity and selectivity. An increase in ageing time increases the crystallinity of the mixed spinel oxide phase and results in a decline in the selectivity to light alkenes. It is clear that the precipitation conditions, especially temperature and pH of precipitation mixture, are of crucial importance and control of these parameters should be incorporated into the experimental design involving co-precipitation for the preparation of mixed metal oxide catalysts.

Reaction conditions also play an important role in controlling the catalytic activity and selectivity. An increase in the temperature of the reaction decreases olefin selectivity and increases the selectivity to alkanes. Methane selectivity increases tremendously with an increase in reaction temperature. Higher temperature increases selectivity to C_{5+} products along with tremendous increase in CO_2 formation.

An increase in reaction pressure at 220°C increases the catalytic activity and decreases methane selectivity. An increase in pressure from 3bar to 9bar decreases the selectivity to ethylene and increases propene selectivity.

The best reaction conditions were 220°C at 6 bar pressure, with molar feed ratio of $CO/H_2 = 1/1$.

3.6 References:

[1]. D. J. Duvenhage and N. J. Coville, *Appl. Catal.*, 1997, **153**, 43

[2]. C. Cabet, A. C. Roger, A. Kiennemann, S. Lakamp and G. Pourroy, *J. Catal.*, 1998, **173**, 64

[3]. L. Sergio, S. L. Gobzalez-Cortes, M. Serbia, A. Rudolfo-Baecher, A. Oliveros, J. Oeozco, B. Fontal, A. J. Mora and G. Delgado, *Reac. Kinet. Catal. Lett.*, 2002, **75**, 3

[4]. F. Tihay, G. Pourroy, M. Richard-Plouet, A.C. Roger and A. Kiennemann, *J. Appl. Catal.*, 2001, **206**, 29

[5]. F. Tihay, A. C. Roger, A. Kiennemann and G. Pourroy, *Catal. Today.*, 2000, **58**, 263

[6]. T. V. Reshetenko, L. B. Avdeeva, A. A. Khassin, G. N. Kustova, V. A. Ushakov, E. M. Moroz, A. N. Shmakov, V. V. Kriventsov, D. I. Kochubey, Y. T. Pavlyukhin, A. L. Chuvilin Z. R. Ismagilov, *Appl. Catal.*, 2004, **268**, 127

[7]. V. A. de la Pen'a O'Shea, N. N. Menéndez, J. D. Tornero and J. L. G. Fierro, *Catal. Lett.*, 2003, **88**, 123

[8]. A. A. Mirzaei, R. Habibpour and E. Kashi, *Appl. Catal.*, 2005, **296**, 222

[9]. M. E. Dry, *Stud. Surf. Sci. Catal.*, 2004, **152**, 211

[10]. C. H. Yang, F. E. Massoth and A. G. Oblad, *Adv. Chem. Ser.*, 1979, **178**, 35

[11]. A. O. Rautavoma and H. S. Van der Baan, *Appl. Catal.*, 1981, **1**, 247

[12]. B. Sarup and B. W. Wojciechowski, *J. Chem. Eng.*, 1989, **67**, 62

[13]. I. C. Yates and C. N. Satterfield, *En. Fuels.*, 1991, **5**, 168

[14]. E. Iglesia, S.C. Reyes, J.R. Madon and S.I. Soled, *Adv. Catal. Relat. Subj.*, 1993, **39**, 221

[15]. C. A. Chanenchuk, I.C. Yates and C.N. Satterfield, *En. Fuels.*, 1991, **5**, 847

[16]. G. P. Vander laan and A. A. C. M. Beenackers, *Catal. Rev. Sci. Eng.*, 1999, **41**, 225

[17]. S. L. González-Cortés, S. M. A. Rodulfo-Baechler, A. Oliveros, J. Orozco, B. Fontal, A. J. Mora and G. Delgado, *React. Kinet. Catal. Lett.*, 2002, **75**, 3

[18]. M. J. Keyser, R. C. Everson and R. L. Espinoza, *Appl. Catal.*, 1998, **171**, 99

[19]. A. G. Ruhrchemie, British Patent GB, 1976, **1,553,361**

[20]. H. Kolbel, and K. D.Tillmetz, US Patent 1977, **4,177,203**

[21]. H. Kolbel, and K. D. Tillmetz, German Patent 1976, **2,507,647**

[22]. J. Barrault, *Stud. Surf. Sci. Catal.*, 1982, **11**, 225

[23]. J. Barrault, C. Forquy, J. Menezo and R. Maurel, *Reac. Kinet. Catal. Lett.*, 1980, **15**, 153

[24]. J. Barrault, C. Forquy and V. Perrichon, *Appl. Catal.*, 1983, **5**, 119

[25]. B. Bussemeier, C.D. Frohning and B. Cornils, *Hydrocarb. Proc.*, 1976, **55**, 105

[26]. B. Bussemeier, C.D. Frohning, G. Horn and W. Kluy, *Chem. Abst.*, 1977, **87**, 41705

[27]. B. Bussemeier, C.D. Frohning, G. Horn and W. Kluy, *Chem. Abst.*, 1977, **86**, 124093

[28]. H. Kölbel and D. K. Tillmetz, *Chem. Abst.*, 1977, **86**, 192342

[29]. H. Kölbel and D. K. Tillmetz, *Chem. Abst.*, 1980, **92**, 146244

[30]. M. Van der Riet, "*Carbon Monoxide Hydrogenation with Transition Metal Oxide Supported Cobalt and Iron Catalysts*", PhD Thesis, University of Witwatersrand, 1988

[31]. M. Van der Riet, G. J. Hutchings, and R. G. Copperthwaite, *J. Chem. Soc. (London), Chem. Commun.*, 1986, **10**, 798

[32]. M. Van der Riet, R. G. Copperthwaite, and G. J. Hutchings, *J. Chem. Soc. (London), Faraday Trans.*, 1987, **83**, 2963

[33]. R. G. Copperthwaite, G. J. Hutchings, M. Van der Riet, and J. Woodhouse, *Ind. Eng. Chem. Res.*, 1987, **26**, 869

[34]. S. E. Colley, R. G. Copperthwaite, G. J. Hutchings, and M. Van der Riet, *Ind. Eng. Chem. Res.*, 1988, **27**, 1339

[35]. F. M. Gottschalk, R. G. Copperthwaite, M. Van der Riet, and G. J. Hutchings, *Appl. Catal.*, 1988, **38**, 103

[36]. M. J. Keyser, R. C. Everson, and R. L. Espinoza, *Appl. Catal.*, 1998, **171**, 99

[37]. B. Bussemeier, C. D. Frohning and B. Cornils, *Hydrocarb. Proc.*, 1976, **105**, 55

[38]. J. L. Zhou, S. R. Yan, Y. D. Guan, X. Y. Huang and Q. J. Zeng, *Proceedings of the Fourth Japan–China Symposium on Coal C_1 Chemistry*, 1993, **5**, 473

[39]. A. A. Mirzaei, M. Faizi, and R. Habibpour *Appl. Catal.*, 2006, **306**, 98

[40]. G. C. Maiti, R. Malessa, U. Lochner, H. Papp, and M. Baerns, *Appl. Catal.*, 1985, **16**, 215

[41]. R. A. Diffencbach, and D. J. Fauth, *J. Catal.*, 1986, **100**, 466

[42]. M. E. Dry, and G. J. Oosthuizen, *J. Catal.*, 1968, **11**, 18

[43]. Q. Xu, D. He, M. Fujiwara, and Y. Souma, *J. Mol. Catal.*, 1997, **120**, L 23

[44]. X. An, B. Wu, W. Hou, H. Wan, Z. Tao, T. Li, Z. Zhang, H. Xiang,Y. Li, B. Xu, and F. Yi, *J. Mol. Catal.*, 2007, **263**, 266

[45]. G. J. Hutchings, A. A. Mirzaei, R.W. Joyner, M. R. H. Siddiqui, and S. H. Taylor, *Catal. Lett.*, 1996, **42**, 21

[46]. G. J. Hutchings, A. A. Mirzaei, R. W. Joyner, M. R. H. Siddiqui, and S. H. Taylor, *Appl. Catal., 1998*, **166**, 143

[47]. S. H. Taylor, G. J. Hutchings, and A. A. Mirzaei, *Chem. Commun.*, 1999, **4**, 1373

[48]. M. Whittle, A. A. Mirzaei, J. S. J. Hangreeves, R. W. Joyner, C. J. Kiely, S. H. Taylor, and G. J. Hutchings, *Phys. Chem. Chem. Commun.*, 2002, **4**, 5915

[49]. A. A. Mirzaei, H. R. Shaterian, R. W. Joyner, J. S. J. Hangreeves, S. H. Taylor, and G. J. Hutchings, *Catal. Commun.*, 2003, **4**, 17

[50]. A. A. Mirzaei, H. R. Shaterian, M. Habibi, G. J. Hutchings, and S. H. Taylor, *Appl. Catal.*, 2003, **253**, 499

[51]. A. A. Mirzaei, H. R. Shaterian, S. H. Taylor, and G. J. Hutchings, *Catal. Lett.*, 2003, **87**, 103

[52]. S. H. Taylor, G. J. Hutchings, and A. A. Mirzaei, *Catal. Today.*, 2003, **84**, 113

[53]. A. A. Mirzaei, H. R. Shaterian, and M. Kaykhaii, *Appl. Surf. Sci.*, 2005, **239**, 246

[54]. A. A. Mirzaei, R. Habibpour, and E. Kashi, *Appl. Catal.*, 2005, **296**, 222

[55]. A. A. Mirzaei, R. Habibpour, M. Faizi, and E. Kashi, *Appl. Catal.*, 2006, **301**, 272

[56]. K. J. Cole, "Copper Manganese based mixed oxides for ambient temperature CO oxidation and higher temperature oxidation reactions", PhD Thesis, Cardiff University, 2008

[57]. F. Morales, E. Smit, F. M. F. Groot, T. Visser, and B. M. Weckhuysen, *J. Catal.*, 2007, **246**, 91

[58]. L. R. Leith and M. G. Howden, *Appl. Catal.*, 1988, **37**, 75

[59]. M. E. Dry, *Stud. Surf. Sci. Catal.*, 2004, **152**, 197

[60]. L. Bai, H. Wei, Y. Wang-Li, Yi. Z. Han, and B. Yhong, *Fuel.*, 2002, **81**, 1577

[61]. A. A. Mirzaei, S. Vahid, and M. Feyzi, *Adv. Phys. Chem.*, 2008, **2009**, 1

[62]. C. R. Everson, and H. Mulder, *J. Catal.*, 1993, **143**, 166

[63]. A. Griboval, A. Y. Khodakov, R. Bechara, and V. L. Zholobenko, *Stud. Surf. Sci. Catal.*, 2002, **144**, 609

[64]. S. E. Colley, "*Hydrogenation of carbon monoxide over modified cobalt-based catalysis*", PhD thesis, University of Witwatersrand, Johannesburg, South Africa, 1991

[65]. H. H. Storch, N. Golumbic, and R. B. Anderson, in "*The Fischer-Tropsch and Related Synthesis*", Wiley, New York, 1951

Chapter 4

The influence of metal promoters in the hydrogenation of carbon monoxide using cobalt manganese oxide catalysts

4.1 Introduction

Classical Fischer Tropsch (FT) synthesis follows a polymerization process for hydrocarbon chain growth giving a broad range of product distribution from methane to waxes [1]. Large proportion of the feedstock consists of unsaturated hydrocarbons, especially those with two to four carbon atoms. These unsaturated light hydrocarbons synthesised from syngas using modified FT catalysts are of great economic interest.

Variation of reaction conditions leads to moderate shifts in the broad product distribution within the constraints of the Schulz-Flory (SF) distribution law [2]. However, high selectivity to a single product or narrow distribution of products requires the development of an improved catalyst. Incorporation of metal promoters and other additives is an approach to the chemical modification of FT catalysts. Catalyst promoters enhance the overall catalytic performances and lifetime if the promoter element is added in an appropriate manner and in a limited range of loading. It is difficult to define the term 'promoter' since there are many different types of promoters and it is often difficult to distinguish between the promoters, the active catalytic component and the carrier. An appropriate definition can be 'a promoter is a substance added to a catalyst in a small amount, which by itself has little or no activity, but it imparts either better activity or selectivity for the desired reaction than is realized without it' [3].

Table 1.3 (in chapter 1), details the beneficial effects of promoters for cobalt catalysts. It is clear from the table that different promoter elements could have multiple modes of promotion action.

Many transition metal oxides have been investigated as potential promoters for Co-based catalysts in FTS [4-30].

Although different promotion functions have been proposed in literature, transition metal oxides have mostly been regarded as electronic promoters, having direct influence on the activity or selectivity of Co sites. This effect is manifested through direct interaction of the supported Co particles with the transition metal oxides. Hence, the transition metal

oxide promoters are thought to be spreading over the cobalt surface in sub-monolayer coverages, modifying the adsorption properties of Co active sites [31].

Early in the nineties, Ruiz *et al.* [10] reported an enhancement in catalyst activities and increased selectivities to alkenes and higher hydrocarbons upon addition of V, Mg and Ce oxides to Co-based FT catalysts. These variations were attributed to electronic effects induced by the metal oxides. Similar results were reported by Bessel [11] using a Cr promoter in Co/ZSM-5 catalysts. Addition of Cr improved the catalyst activity and shifted the selectivity from methane to higher, generally more olefinic hydrocarbons. They suggested an interaction between transition metal oxide and the cobalt oxide as a cause of promotion which inhibits cobalt reduction and improves cobalt dispersion.

Further, Kikuchi *et al.* [12] reported the effect of Cr, Ti, Mn and Mo on the FT performance of catalysts loaded with ultra fine cobalt particles. The addition of these promoters effectively enhanced the catalyst activity, lowered the methane selectivity and increased C_{5+} production. They attributed these effects to a structural promotion, causing a decrease of the cobalt particle size in the catalysts. Another promotion induced by Mn and Mo was reported by the group of Belosludov [19]. They investigated the addition of Mn and Mo to Co-based FT catalysts using computational chemistry. They found that the transition metal oxides under investigation improved the sulphur tolerance of the catalysts.

Effect of two metal promoters (Ru and K) on the catalytic activity of $CoMnO_x$ catalyst will be discussed in this chapter. Different loadings of these metal promoters have been studied along with $CoMnO_x$ catalysts in an attempt to:

– Firstly; further enhance the selectivity towards the commercially viable C_2 and C_3 olefins, and – Secondly; to further suppress methane formation, and thus prevent the loss of an expensive carbon source to a commercially less viable product.

4.2 Experimental

The detailed preparation of catalysts and their testing has been discussed in chapter 2. Briefly, Cobalt manganese oxide catalysts (Co/MnO_x) were prepared by co-precipitation from a solution of mixed nitrates with aqueous ammonia under variable pH from 2.8 to 8 at 80°C. Precipitates were filtered, washed and dried at 110°C. Doping of the catalysts with various metal promoters was achieved by incipient wetness. The doped materials were dried at 110°C for 16h and calcined at 500°C for 24h. The calcined catalysts were pelleted and sieved (0.65-0.85mm). Catalysts (0.5g) were loaded in to six fixed-bed laboratory reactors (Appendix 4). Catalysts were subsequently reduced *in situ* at 400°C for 16h in a hydrogen atmosphere (GHSV = $600h^{-1}$, atmospheric pressure). All catalysts were tested under almost identical reaction conditions (CO/H_2 =1/1, T=220°C, P = 6 bar, and GHSV = $600h^{-1}$). A stabilization period of ~100h after initiation of FT synthesis was allowed before mass balance data collection. Analysis of gas products was determined by on-line gas chromatography capable of analysis of hydrocarbons (FID) and CO, H_2, CO_2, N_2 (TCD detector) as detailed in chapter 2.

Catalysts doped with potassium and ruthenium were prepared and tested according to the method detailed as above and their results will be discussed in the following sections.

4.3 Potassium (K)

The impact of potassium addition on the performance of FTS catalysts has been studied extensively. Potassium is known to promote the formation of olefins and longer-chain hydrocarbons, and the suppression of methane [32-36]. The positive impact of potassium addition on the activity of FT catalysts depends on the level of promotion.

4.3.1 Results

4.3.1.1 Catalytic activity results

The effect of potassium loading on the performance of Co/MnO_x catalysts during the CO hydrogenation is presented in table 4.1. The addition of small quantities of potassium (0.09, 0.1, 0.12, 0.15 wt %) was shown to be enough to affect the performance of these catalysts in a variety of ways. Potassium acetate was used as a salt precursor. Particular attention was given to the selectivity of methane and alkenes to alkane ratio.

Table 4.1 shows that a small variation in potassium concentration with $CoMnO_x$ has a remarkable effect on the activity and selectivity of catalysts during CO hydrogenation. An increase in potassium concentration from 0.09 to 0.1 % drops CO conversion down from 15 to 9.7% along with a decrease in methane selectivity. There is an increase in the selectivity of ethylene with an increase in potassium concentration from 0.09 to 0.1%, but selectivity of propene decreases from 29% to 22%.

Table 4.1 CO hydrogenation over $CoMnO_x$ promoted with various concentrations of potassium

	Concentrations of potassium (wt %)				
	0	0.09	0.1	0.12	0.15
Conversion of CO	12	15	9.7	13	15.5
Selectivity / wt% (normalized using mass balance)					
CH_4	16.8	17.5	13	16.21	14.9
C_2H_4	3.2	3.7	5	2.5	2.5
C_2H_6	9.1	10.4	2.5	8	5.7
C_3H_6	28.4	29.1	22.6	22.9	19.4
C_3H_8	7.4	7.6	3	6.63	6.6
C_4	17.6	14.8	17	14.5	15.4
C_{5+}	14.8	12.7	31	24.1	31
CO_2	tr	tr	tr	tr	tr
Alcohols	2.6	4.3	2	4.5	4.5

Reaction conditions: Catalyst wt = 0.5g,Time online 112h, 220°C, 6 Bar, CO/H_2 (1:1 mol ratio), GHSV = 600 h^{-1} C_{6+} = Gaseous, liquid and solid C_6-C_9 + liquid oxygenates,tr=trace quantity

Further increase in K loading to 0.12% increases CO conversion along with an increase in methane selectivity with a decrease in selectivity of ethylene. But propene selectivity remains similar to 0.1% K loading. Further increase in K loading to 0.15% increases CO conversion along with a decrease in the selectivity of propene. Methane decreases and ethylene remains the same. Colley [2] has studied effect of potassium promoter with $CoMnO_x$ in detail. A drop in CO conversion has been reported with an increase in concentration of potassium from 0.01 to 0.5%. Methane trend was reported to drop down to certain level with increase in K loading and then starts increasing again.

Results presented in table 4.1 show that only low levels (0.09 and 0.1%) of potassium were required to increase olefin selectivities when compared with an unpromoted $CoMnO_x$ catalyst, while an increase in concentration of potassium increased selectivity of higher hydrocarbons.

The amount of potassium required for an optimum catalytic activity depends on the nature of the metals and catalyst support. Miller and Moskovits [36] have concluded that

there must be a sufficient amount of alkali metal to enhance dissociative chemisorption of CO, but there must not be a level such that the hydrogen adsorption is totally reduced. Yang and Oblad [37] have found the alkali effect to approach saturation at 0.2g/100g Fe which is consistent with the low levels of alkali content used for optimum catalytic performance of CoMnOx catalyst.

4.3.1.2 Characterization of catalysts promoted with potassium

(i) BET

Table 4.2 shows surface areas of $CoMnO_x$ catalysts doped with various loadings of potassium.

Table 4.2 Surface area of catalysts promoted with potassium

$CoMnO_x$ +K (%)	Surface area (m^2/g)	
	Before calcination	After calcination
0.00	15	11
0.09	17	9
0.1	14	10
0.12	13	7
0.15	11	8

The BET data from the above table shows that K influences the surface area to some extent. There is decrease in surface area with increase in concentration of alkali content.

These results are consistent with those reported by Dry and Oosthuizen [38] who showed that the alkali promoter decreased the surface area of reduced iron catalysts and that a greater loss in area was recorded the more basic the alkali added. They added alkali promoters in the order between 0 and 2.0/100g Fe.

(ii) XRD

An investigation of XRD pattern of catalysts promoted with different concentrations of potassium and calcined at 500°C for 24h shows presence of typical mixed Co-Mn oxide spinels identified as $(Co,Mn)(Co,Mn)_2O_4$.

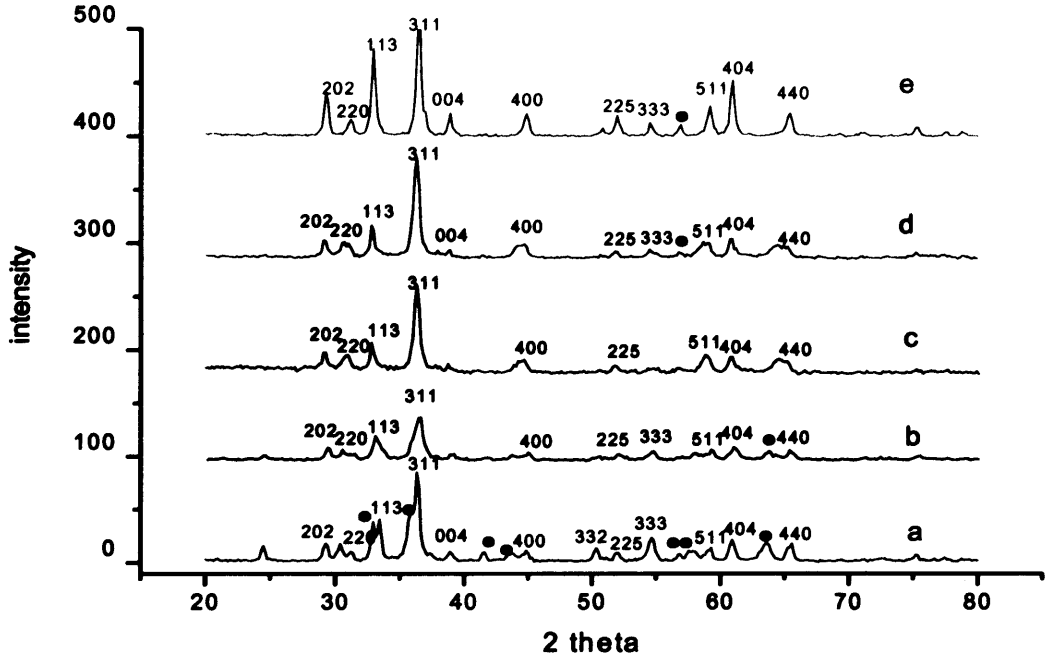

Figure 4.1 XRD comparison of catalysts promoted with potassium, $CoMnO_x$+K (a) 0.00%, (b) 0.09%, (c) 0.1%, (d) 0.12%, (e) 0.15% (○) Mn_3O_4

This comparison presented in figure 4.1 shows that the incorporation of the alkali affected the width of peaks.

A small concentration of potassium e.g. 0.09% does not affect the bulk structure a lot. Most of the phases are similar to pure $CoMnO_x$. There is slight change in the peak intensities and shapes. Further increase in concentration of potassium to 0.1, 0.12 and 0.15% increases the intensity of peaks. $CoMnO_x$ catalyst with 0.15% potassium has

shown highest intensities of all peaks. This catalyst was different in catalytic results, and was especially highly selective to C_{5+} hydrocarbons and least selective for propylene.

(iii) SEM

SEM images in the following figures show affect of potassium dopants on the structure and morphology of catalysts. There is no significant difference in the morphology of these catalysts. All these images show cauliflower shaped particles which were well arranged on the surface of catalyst.

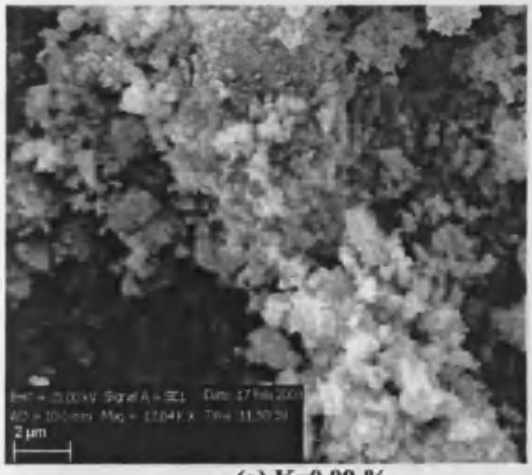

(a) K=0.09 %

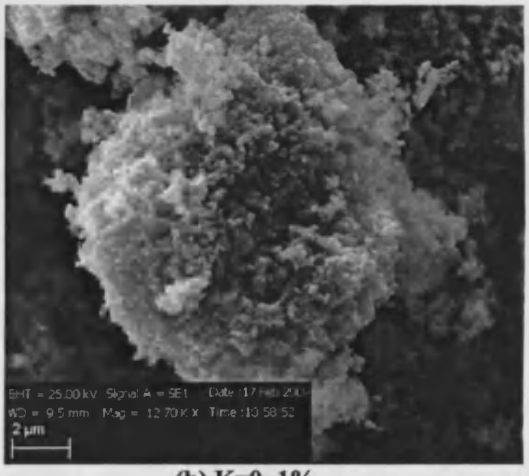

(b) K=0. 1%

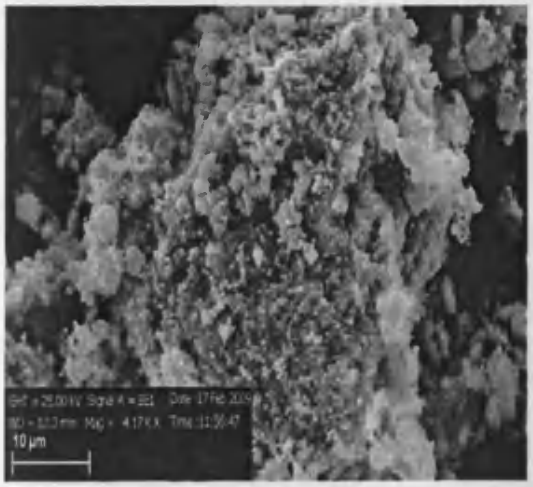

(c) K=0.12%

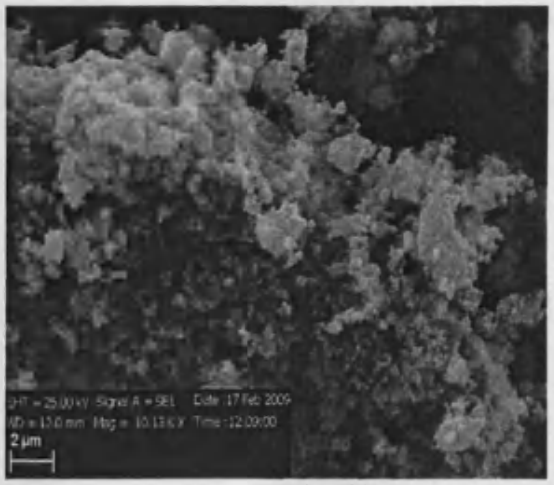

(d) 0.15%

Figure.4.2 SEM images of CoMnOx catalyst promoted with potassium

4.3.2 Mechanism of promoter (K) action

The effect of potassium promoter on the product spectrum is consistent with its effect on electronic properties of catalyst surface. Potassium, essentially affects the competition between dissociative CO chemisorption and H_2 chemisorption on active surface site of catalyst.

The CO adsorption mechanism during the FT reaction takes place via metal sigma bonding and the simultaneous back donation of transition metal valence electrons into anti bonding 2π orbitals of carbon in CO [39]. This back donation process causes a strengthening of metal-carbon bond, and a simultaneous weakening of carbon-oxygen bond. If there is sufficient weakening of C-O bond in the absorption process, then dissociative CO adsorption will occur which generates the building blocks for the formation of carbon chain.

Bonzel and Krebs [40, 41] have reported surface spectroscopic studies of CO adsorbed on alkali metal doped transition-metal surfaces. These studies have indicated a significant weakening of CO bond, and an increase in the extent of CO adsorption. A charge transfer has been reported to take place from the alkali metal to the vacant *d* orbitals of the active metal, as evidenced by the lowering of the work function [42]. The additional electron density imparted to the metal serves to increase the extent of back donation into 2π orbitals of CO, which causes a weakening of CO bond. This trend was observed by a noticeable decrease in the CO stretching frequency upon addition of alkali promoters [43, 44]. An increase in ΔH_{ads} was indicated from measurement of heat of adsorption of CO on Fe + K surface, with an increase in alkali metal content [45].

The presence of an electron-donating species on the catalyst surface can suppress the adsorption of hydrogen because hydrogen itself donates an electron to metal upon adsorption [46]. It has been reported by Dry and Koel [45, 47] that the presence of CO and surface carbide decreases the adsorption of hydrogen on metals. Furthermore, heat of adsorption of hydrogen decreases with an increase in alkali metal [45, 48, 49] which confirms that alkali-metal addition suppresses adsorption of hydrogen. Assuming that K has a similar effect on the chemisorptive properties of the present $CoMnO_x$ catalyst, then the observed reduction in methane formation and increase in selectivity of ethylene (K=0.1%) can be attributed to the suppression in relative concentrations of H_2 with respect to CO. This decrease in H_2 concentrations decreases the hydrogenating properties of catalyst surface.

4.4 Ruthenium

Ruthenium metal has been reported to be a good promoter for an enhancement of reduction of cobalt oxides and can inhibit the carbon deposition during FT reaction [50, 51]. Initially ruthenium catalysts were observed to be effective for "Polyethylene synthesis" [52], later it was found that typical products of FT can be formed by using ruthenium catalysts [51-56]. Ruthenium has been reported as a promoter which is not negatively affected by water (a by product in FT) [57, 58], and inactive ruthenium oxides are not formed. However, the exact reaction mechanism of Ru-promoted catalysts in FT reaction has not been clear.

In the present studies ruthenium doped (0.05, 0.1 and 0.15%) catalysts with $CoMnO_x$ were prepared and tested under similar conditions as detailed in experimental section 4.2. Ruthenium nitrocyl nitrate was used as a salt precursor.

4.4.1 Results

4.4.1.1 Catalytic activity results

Catalytic results for $CoMnO_x$ promoted with ruthenium are shown in table 4.3. Catalytic activity increased with an addition of small quantity of ruthenium promoter along with a considerable increase in methane selectivity. There was corresponding decrease in the selectivity of olefins. But selectivity of C_{5+} hydrocarbons was increased with addition of ruthenium. 0.1% addition of ruthenium showed highest catalytic activity with an enhanced selectivity to C_{5+} hydrocarbons. Interestingly, alcohols selectivity increased with an addition of 0.05% ruthenium in $CoMnO_x$, (ethanol was dominant).

Table 4.3 CO hydrogenation over $CoMnO_x$ doped with Ru (0.1%)

	$CoMnO_x$ + Ru (wt %)			
	0	0.05	0.1	0.15
Conversion of CO	12	11.5	16.8	14.4
Selectivity/wt% (normalized using mass balance)				
CH_4	16.8	16.3	14.2	20.8
C_2H_4	3.2	1.3	2.4	2.6
C_2H_6	9.1	3.6	3.6	2.9
C_3H_6	28.4	12.3	16.2	13.4
C_3H_8	7.4	1.9	2.5	2.1
C_4	17.6	14.5	19.3	15.3
C_{5+}	15	39	41	38.7
CO_2	tr	tr	tr	tr
Alcohols	2.6	11.1	0	4.4

Reaction conditions: Catalyst wt = 0.5g, Time online 86h, 220°C, 6 bar, CO/H_2 (1:1 mol ratio), GHSV = 600 h^{-1} C_{6+} = Gaseous, liquid and solid C_6-C_9 + liquid oxygenates, tr = trace quantity

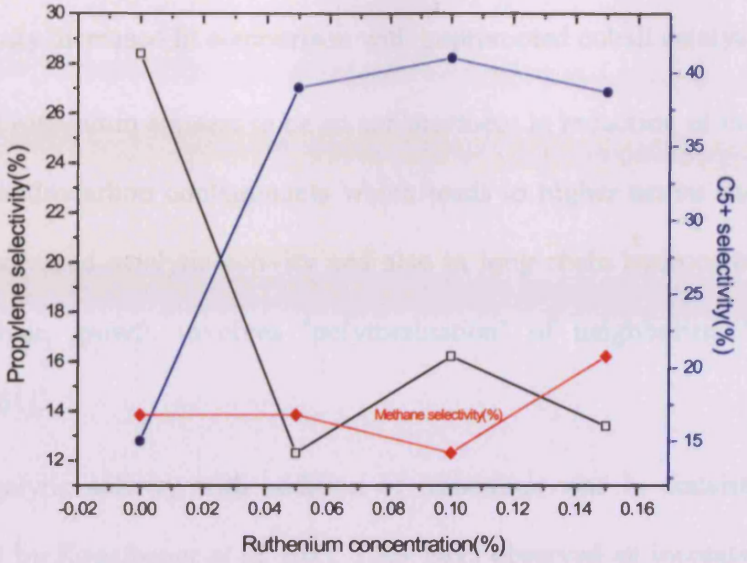

Figure 4.3 Effect of ruthenium promoter on selectivity of hydrocarbons

Figure 4.3 shows a clearer effect of ruthenium promoter on selectivity of methane, propylene and C_{5+} hydrocarbons. C_{5+} hydrocarbons get enhanced with addition of ruthenium and propylene selectivity decreases significantly. Methane selectivity remained same for pure $CoMnO_x$ catalyst and Ru=0.05%, decreased for 0.1% but it was enhanced with an increase in ruthenium to 0.15%.

Ruthenium is a very active catalyst for the CO hydrogenation. Its activity at lower temperature is higher than Co and Fe. It is a versatile catalyst, in that at higher temperature it is an excellent methanation catalyst (most active group VIII metals), while at lower temperatures it produces large amounts of high molecular waxes [59]. The addition of small quantity of ruthenium has been found to enhance both the initial reduction and in-situ regeneration of the cobalt catalyst [60]. The influence of low level of Ru promotion of Co on supports (TiO_2, SiO_2) has been thoroughly studied by Dry [60].

From these studies, it was found that (at Ru/Co atomic ratios of 0.008) the overall activity and C_{5+} selectivity increased in comparison with unpromoted cobalt catalysts.

The key role of ruthenium appears to be an enhancement in reduction of bulk and surface oxides and of hydrocarbon contaminants which leads to higher active sites. This effect results in an increased catalytic activity and also in long-chain hydrocarbon selectivity, because FT chain growth involves 'polymerization' of neighboring 'CH_2' surface intermediates [61].

Increase in catalytic activity with addition of ruthenium was in consistence with the results reported by Kogelbauer *et al.* [62]. They have observed an increase in number of reduced atoms in catalysts promoted with ruthenium resulting in an enhancement in catalytic activity during CO hydrogenation. Tsubaki *et al.* [63] have studied effect of 0.2% Ru on the catalytic activity of Co/SiO_2 catalyst. They have reported an increase in catalytic activity with addition of Ru promoter by improving the reducibility of cobalt. Li *et al.* [64] have reported an increase in CO conversion and a significant decrease in methane selectivity upon addition of Ru with Co/TiO_2 catalyst. The difference in selectivity of methane can be attributed to the different catalyst system. Cobalt has different interactions with MnO system which is affected in slightly different ways when promoted with ruthenium which can lead to new changes in catalyst system. Increased CO conversion with ruthenium promoted catalyst has been reported mainly because of an increased number of surface cobalt atoms [65].

Xiong *et al.* [66] have very recently studied effect of ruthenium promotion on Co-based catalysts for FT reaction. The addition of a small amount of ruthenium promoter to Co-

based catalyst shifted the reduction temperature of cobalt oxide to cobalt metal in two steps and decreased the amount of Co^{+2} species.

$$(Co_3O_4 \rightarrow CoO \text{ and } CoO \rightarrow Co^{o})$$

After reduction, ruthenium atoms were partially encapsulated within cobalt clusters with ruthenium in direct contact with cobalt atoms. A part of the ruthenium atoms took part in hydrogen spillover from ruthenium to cobalt oxide clusters. With increase in content of ruthenium catalyst reducibility gets increased and cobalt atoms become enriched at the surface.

4.4.1.2 Characterization of catalyst promoted with ruthenium

(i) BET

Surface area of catalysts promoted with different concentrations of ruthenium are shown in table 4.4. There is no apparent affect of ruthenium addition on BET surface area measurements.

Table 4.4 Surface area of catalysts promoted with ruthenium

$CoMnO_x$ +Ru%	Surface area (m^2/g)	
	Before calcination	After calcination
0	15	11
0.05	15	12
0.1	17	13
0.15	14	12

(ii) XRD

A comparison of XRD pattern for catalyst doped with ruthenium and undoped $CoMnO_x$ catalyst is shown in figure 4.4. Catalysts promoted with ruthenium show change in shapes of XRD peaks. There is a slight broadening of some phases and decrease in the intensity of peaks. All phases of typical mixed spinel oxides are present in catalysts promoted with ruthenium. Different catalytic results with addition of ruthenium into $CoMnO_x$ catalyst can be related to these differences in XRD patterns.

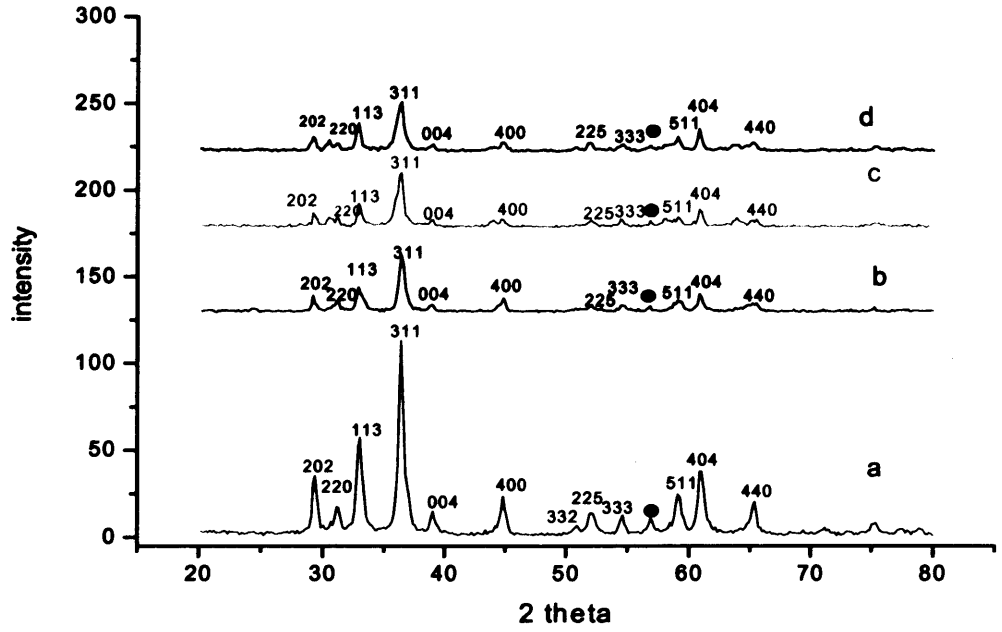

Figure 4.4 XRD comparison of catalyst promote with ruthenium, (a). Unpromoted $CoMnO_x$, (b).$CoMnO_x$+Ru=0.05%, (c).$CoMnO_x$+Ru=0.1%, (d).$CoMnO_x$+Ru=0.15% (○) Mn_3O_4

4.5 Primary alcohols selectivity

Both ruthenium (Ru=0.05 and 0.15%) and potassium (0.09, 0.12 and 0.15%) promoters have shown an enhancement in the selectivities of alcohols. The formation of these was consistent with an observed shift of selectivity pattern towards longer chain hydrocarbons coupled with the presence of increased concentrations of CO which is available for possible CO insertion in the formation of alcohols [67, 68].

It is reported that the addition of alkali salts to methanol synthesis catalysts often increase yields of higher alcohols [69]. It has been suggested that selectivity of alcohols during CO hydrogenation on Rh catalysts varies with the basicity or acidity of support [70]. Storch *et al.* [71] also have reported an increase in the content of oxygenated products with potassium promoter while studying Fe/Al_2O_3 catalysts.

Ruthenium has been reported to enhance the selectivity of alcohols when used as a promoter with Co catalysts [72, 73]. An enhancement in selectivity of alcohols has been reported when using ruthenium and other transition metal promoters with Co-based catalysts [74]. On the bases of extensive characterization studies it is noticed that highly dispersed cobalt metal is the main active site in catalysts promoted with transition metals, and that transition metals can promote the reduction of Co^{+2} cation to a metallic state by hydrogen spillover mechanism.

4.6 Conclusions

Effect of two different promoters on the catalytic performance of $CoMnO_x$ catalyst for CO hydrogenation activity has been studied using potassium and ruthenium.

Promotion of cobalt manganese catalyst with potassium in the range of 0.09, 0.12 and 0.15% increased CO conversion and C_{5+} selectivity. Addition of 0.1% potassium increased selectivity of light alkenes with decrease in methane selectivity.

From a literature survey the mechanism of promoter action was thought to be through the influence of potassium on electronic properties of catalyst surface, which creates a competition between dissociative CO chemisorption and H_2 adsorption on active catalyst surface. An increase in CO dissociative adsorption accompanied by a suppression of H_2 adsorption was due to the enhancement of electron-donating character of active metal with alkali promotion.

Addition of ruthenium promoter increased catalytic activity with corresponding increase in methane selectivity. Light alkenes selectivity was decreased with an addition of ruthenium metal and selectivity of C_{5+} hydrocarbons was enhanced.

4.7 Future work

Various aspects of addition of alkali and transition metal promoters (K and Ru) can be further modified by detailed investigation of actual mechanisms involved. Ru has been reported to affect the reduction behaviour of cobalt catalysts; TPR studies will be useful to get an idea of change in reduction temperature with addition of various concentrations

of Ru. CO chemisorption studies can provide an evidence of change in metal dispersion of these promoted catalysts which may have an effect on catalytic behaviour.

CO chemisorption studies on potassium and ruthenium doped catalysts will be very useful for explanation of increased selectivity of alcohols.

4.8 References:

[1]. Y.T. Shah, and A. J. Perrotta, *Ind. Eng. Chem. Prod. Res. Develop.*, 1976, **15**, 23

[2]. S. E. Colley, "*Hydrogenation of Carbon monoxide over modified cobalt-based catalysts*", PhD thesis, University of Witwatersrand, Johannesburg, South Africa, 1991

[3]. G.V. Lee, G. T. M. Bastein, I. V. Boogert, B. Schuller, H. Y. Luo, and V. Ponec, *J. Chem. Soc. Farad. Trans.*, 1987, **83**, 2013

[4]. G. W. Huber, S. J. M. Butala, M. L. Lee, and C. H. Bartholomew, *Catal. Lett.*, 2001, **74**, 45

[5]. H. K. Woo, R. Srinivasan, L. Rice, R. J. Deangelis, and P. J. Reucroft, *J. Mol. Catal.*, 1990, **59**, 83

[6]. J. E. Baker, R. Burch, S. J. Hibble, and P. K. Loader, *Appl. Catal.*, 1990, **65**, 281

[7]. S. E. Colley, M. J. Betts, R. J. Copperthwaite, G. J. Hutchings, and N. J. Coville, *J. Catal.*, 1992, **134**, 186

[8]. A. F. Y. Alshammary, I. T. Caga, A. Y. Tata, J. M. Winterbottom, and I. R. Harris, *J .Chem. Tech. Biotech.*, 1992, **55**, 275

[9]. I. R. Harris, I. T. Caga, A. Y. Tata, and J. M. Winterbottom, *Stud. Surf. Sci. Catal.*, 1993, **75**, 2801

[10]. A. G. Ruiz, A. S. Escribano, and I. R. Ramos, *Appl. Catal.*, 1994, **120**, 71

[11]. S. Bessel, *Stud. Surf. Sci. Catal.*, 1994, **81**, 479

[12]. E. Kikuchi, R. Sorita, H. Takahashi, and T. Matsuda, *Appl. Catal.*, 1999, **186**, 121

[13]. A. Frydman, D. G. Castner, C. T. Cambell, and M. Schmal, *J. Catal.*, 1999, **188**, 1

[14]. S. Sun, N. Tsubaki, and K. Fujimoto, *Chem. Lett.*, 2000, **2**, 176

[15]. J. L. Li, L. G. Xu, R. A. Keogh, and B. H. Davies, in "*Book of abstracts*", 219th ACS National Meeting, San Francisco, 2000

[16]. D. G. Wei, J. G. Goodwin, R. Oukaci, and A. H. Singleton, *Appl. Catal.*, 2001, **210**, 137

[17]. G. Jacobs, T. Das, P. M. Patterson, Y. Q. Zhang, J. L. Li, G. Racoillet, and B. H. Davies, *Appl. Catal.*, 2002, **233**, 263

[18]. J. L. Li, G. Jacobs, Y. Q. Zhang, T. Das, and B. H. Davies, *Appl. Catal.*, 2002, **223**, 195

[19]. R. V. Belosludov, S. Skahara, K. Yajima, S. Takami, M. Kubo, and A. Miyamoto, *Appl. Surf. Sci.*, 2002, **189**, 245

[20]. T. Riedel, and G. Schaub, *Top. Catal.*, 2003, **26**, 145

[21]. A. Martinez, C. Lopez, F. Marquez, and I. Diaz, *J. Catal.*, 2003, **220**, 486

[22]. M. Wei, K. Okabe, and H. Arakawa, *J. Jap. Petrol. Inst.*, 2003, **46**, 339

[23].W. S. Yang, D. H. Yin, J. Chang, H. W. Xiang, Y. Y. Xu, and Y. W. Li, *Acta, Chim. Sinica.*, 2003, **61**, 681

[24]. N. N. Madikizela-Mnqanqeni, and N. J. Coville, *J. Mol. Catal.*, 2005, **225**, 137

[25]. Y. Zhang, M. Koike, and N. Tsubaki, *Catal. Lett.*, 2005, **99**, 193

[26]. F. M. T. Mendes, C. A. C. Perez, F. B. Noronha, and M. Schmal, *Catal. Today.*, 2005, **101**, 45

[27]. Y. H. Zhang, H. F. Xiong, K. Y. Liew, and J. L. Li, *J. Mol. Catal. Chem.*, 2005, **237**, 172

[28]. H. F. Xiong, Y. H. Zhang, K. Liew, and J. L. Li, *J. Mol. Catal. Chem.*, 2005, **231**, 145

[29]. T. K. Das, G. Jacobs, and B. H. Davies, *Catal. Lett.*, 2005, **101**, 187

[30]. A. I. Molina, J. M. Robles, E. R. Catellon, B. Pawelec, J. L. G. Fierro, and A. Jimenez-Lopez, *Appl. Catal.*, 2005, **286**, 239

[31]. http://igitur-archive.library.uu.nl/dissertation/2006-0906-201148/c2.pdf

[32]. R. B. Anderson, in "*The Fischer Tropsch Synthesis*", Academic press, Orlando, FL, 1984

[33]. M. E. Dry, in "*The Fischer Tropsch Synthesis*", Springer-Verlag, New York, 1981, 159

[34]. Y. Yang, H. W. Xiang, Y. Y. Xu, L. Bai, and Y. W. LI, *Appl. Catal.*, 2004, **266**, 181

[35]. D. B. Bukur, D. Mukesh, and S. A. Patel, *Ind. Eng. Chem. Res.*, 1990, **29**, 194

[36]. D. G. Miller, and M. Moskovits, *J. Phys. Chem.*, 1988, **92**, 6081

[37]. G. H. Yang, and A. G. Oblad, *Am. Chem. Soc. Div. Pet. Chem. Prepr.*, 1978, **23**, 513

[38]. M. E. Dry, and G. J. Oosthuizen, *J. Catal.*, 1968, **11**, 18

[39]. C. T. Campbell, and D. W. Goodman, *Surf. Sci.*, 1982, **123**, 413

[40]. H. P. Bonzel, *J. Vac. Sci. Technol.*, 1984, **2**, 866

[41]. H. P. Bonzel, and H. J. Krebs, *Surf. Sci.*, 1981, **109**, 527

[42]. N. D. Lang, and A. R. Williams, *Phys. Rev. Lett.*, 1976, **37**, 212

[43]. E. L. Garfunkel, J. E. Crowell, and G. A. Somorjai, *J. Phys. Chem.*, 1982, **86**, 310

[44]. J. E. Crowell, E. L. Garfunkel, and S. A.Somorjai, *Surf. Sci.*, 1982, **121**, 203

[45]. M. E. Dry, T. Shingles, L. J. Boshoff, and G. J. Oosthuizen, *J. Catal.*, 1969, **15**, 190

[46]. M. E. Dry, in "*Catalysis, Science and Technology*" Vol. 1, Springer Verlag, Berlin, 1981, **4**, 159

[47]. B. E. Koel, D. E. Peebles, and J. M. White, *Surf. Sci.*, 1981, **107**, 367

[48]. C. H. Bartholomew, *Catal. Lett.*, 1990, **7**, 27

[49]. J. L. Rankin, and C. H. Bartholomew, *J. Catal.*, 1986, **100**, 533

[50]. E. Iglesia, S. L. Soled, and R. A. Fiato, US Patent, 1988, **4794099**

[51]. J. Panpranot, J. G. Goodwin, and A. Sayari, *J. Catal.*, 2002, **211**, 530

[52]. D. L. King, *J. Catal.*, 1978, **51**, 316

[53]. D. S. Jordan, and A. T. Bell, *J. Phys. Chem.*, 1986, **90**, 4797

[54]. D. S. Jordan, and A. T. Bell, *J. Catal.*, 1987, **107**, 338

[55]. E. Iglesia, S. Reyes, R. Madon, and S. Soled, *Adv. Catal.*, 1993, **39**, 221

[56]. M. A. Vannice, *Catal. Rev.*, 1976, **14**, 153

[57]. C. S. Kellner, and A. T. Bell, *J. Catal.*, 1981, **70**, 418

[58]. M. Clayes, and E. S Van, *Catal. Today.*, 2002, **71**, 419

[59]. M. A. Vannice, *J. Catal.*, 1975, **37**, 449

[60]. M. E. Dry, *Stud. Surf. Sci. Catal.*, 2004, **152**, 560

[61]. E. Iglesia, S. L. Soled, R. A. Fiato, and G. H. Via, *J. Catal.*, 1993, **143**, 345

[62]. A. Kogelbauer, J. G. Goodwin, and R. Oukaci, *J. Catal.*, 1996, **160**, 125

[63]. N. Tsubaki, S. Sun, and K. Fujimoto, *J. Catal.*, 2001, **199**, 236

[64]. J. Li, G. Jacobs, Y. Zhang, T. Das, and D. Davies, *Appl. Catal.*, 2002, **223**, 195

[65]. S. Vada, A. H. off, E. Adnanes, D. Schanke, and A. Holmen, *Top. Catal.*, 1995, **2**, 155

[66]. H. Xiong, Y. Zhang, K. Liew, and J. Li, *Fuel Proc. Tech.*, 2009, **90**, 237

[67]. D. A. Wesner, G. Linden, and H. P. Bonzel, *Appl. Surf. Sci.*, 1986, **26**, 335

[68]. G. Ertl, S. B. Lee, and M. Weiss, *Surf. Sci.*, 1981, **92**, 6081

[69]. S. C. Chuang, J. G. Goodwin, and I. Wender, *J. Catal.*, 1985, **95**, 435

[70]. J. R. Katzer, A. W. Sleight, P. Gajardo, J. B. Michel, E. F. Gleason, and S. McMillan, *Farad. Discuss.*, 1979, **72**, 72

[71]. H. H. Storch, N. Golumbic, and R. B. Anderson, in "*The Fischer Tropsch and related synthesis*" John Wiley and Sons, New York, 1951

[72]. B. H. Davies, *Top. Catal.*, 2005, **32**, 143

[73]. M. E. Dry, *J. Chem. Tech. Biotech.*, 2002, **77**, 43

[74]. K. Takeuchi, T. Matsuzaki, T. Hanaoka, and K. Wei, *J. Mol. Catal.*, 1989, **55**, 361

Chapter 5

Fischer Tropsch Synthesis on activated carbons combined with cobalt/iron and manganese; the effect of preparation and reaction conditions on CO hydrogenation

5.1 Introduction

Activated carbon is a form of carbon which is extremely porous and has a large surface area available for chemical reactions. Sufficient activation for useful applications may come solely from the high surface area, though further chemical treatment often enhances the adsorbing properties of the material.

Earlier studies indicated that using carbon as a support could alter catalytic behavior of metals in Fischer Tropsch reaction [1, 2]. In addition studies utilizing glassy carbons (carbon molecular sieves) showed that the ultramicroporosity in these carbons could affect selectivity in certain reactions [3, 4]. This lead to an initial study focused on the preparation and catalytic behavior of iron/glassy carbon catalysts [5-7]. It rapidly became apparent that these carbon-supported iron systems were quite interesting and a broader base was required for comparison, so catalysts composed of iron dispersed on graphitic carbon, carbon blacks and activated carbons were also prepared. In contradiction to earlier studies of Fe/carbon CO hydrogenation catalysts, these carbon supported iron catalysts were very active, and they typically had higher activities and olefin/paraffin ratios than unpromoted Fe/Al_2O_3 catalysts [5, 6].

Recently Van Steen and Prinsloo [8] have used catalysts composed of iron supported on carbon nano tubes for synthesis of C_1-C_5 hydrocarbons from syngas hydrogenation. However, the activity of these catalysts was quite low and declined quickly (from 45% to 15%) within 50h of testing.

In the last 20 years activated carbon has been widely used as a heterogeneous catalyst support but it was not commonly applied in the FTS field [9-13]. Vannice *et al.* [14-17] were pioneers of the use of activated carbon for supported FTS catalysts. They found that only CH_4 and C_2-C_4 olefins were produced selectively from syngas on activated carbon supported catalysts. Ma *et al.* [18] have studied the FTS with activated carbon supported iron catalysts. They found that catalyst activity was increased with increase in reduction temperatures between 350 and 420°C and gas and liquid hydrocarbons were formed on the catalysts with a C_{5+} weight percentage of about 35%.

In recent years, studies over molecular sieves indicate that meso-porous materials are very promising for primary production of diesel range hydrocarbons by FTS [19-22]. Production of hydrocarbons up to C_{28} has been reported by supported cobalt on these materials at typical FT conditions. Activated carbon has been found to be another promising catalyst support for restriction of hydrocarbon chain length [23-25].

The effect of molybdenum loading and four different types of activated carbon support on activity, stability and selectivities to hydrocarbons and oxygenates during Fischer-Tropsch synthesis have been studied by Ma *et al.* [26]. Addition of Mo promoter to the Fe/Cu/K catalyst supported on peat derived activated carbon leads to improved catalyst stability and selectivity. Carbon support type has been reported to affect both catalyst activity and selectivity.

In the present study two different types of activated carbons (peat and wood) have been investigated in combination with cobalt and iron/manganese catalysts for CO hydrogenation. The particular aim of these studies was to obtain:

– Low methane and CO_2 yield

– High selectivity of hydrocarbons

– High conversion of CO

5.2 Experimental

The detailed preparation of catalysts and their testing has been discussed in chapter 2. Two methods of preparation (Insipient wetness impregnation and co-precipitation) were adopted for preparation of carbon supported/combined catalysts.

Impregnation method was used for the preparation of wood and peat derived activated carbon supported catalysts with weight ratio of Co/Mn/C=20/20/60%. Weighed quantities of cobalt and manganese nitrates were dissolved in water and impregnated on carbon supports. Impregnated materials were dried at 110°C for 16h and calcined at 500°C under continuous flow of helium for 24h.

Activated carbon combined with cobalt manganese catalysts (Co/Mn/C = 40/40/20%) were prepared by co-precipitation from a solution of mixed nitrates at 80°C. Carbon was added in the mixed metal nitrate solutions (Co/Mn=1/1). Precipitation was done with aqueous solution of ammonium hydroxide at 80°C. pH was varied from 4 to 8.0. Precipitates were filtered and dried at 110°C and calcined at 500°C under continuous flow of helium for 24h.

Exactly similar method was adopted for the synthesis of iron manganese catalysts with activated carbons (Fe/Mn/C =40/40/20%). Iron nitrate was used as a salt precursor. pH was varied from 0.21-8.00.

The calcined catalysts were pelleted and sieved (0.65-0.85mm). Catalysts (0.5g) were loaded into six fixed-bed laboratory reactors (Appendix 4). Catalysts were subsequently reduced *in situ* at 400°C for 16h in a hydrogen atmosphere (GHSV = $600h^{-1}$). All catalysts were tested under almost identical reaction conditions (CO/H_2 = 1/1, T = 220°C,

P = 6bar, and GHSV = 600h^{-1}). A stabilization period of ~100h after initiation of FT synthesis was allowed before mass balance data collection. Analysis of gas products was determined by on-line gas chromatography capable of analysis of hydrocarbons (FID) and CO,H_2,CO_2,N_2 (TCD detector) detailed in appendix 5 and 6.

5.3 Results

5.3.1 Co/Mn supported on wood and peat derived activated carbons

Two catalysts were prepared with wood and peat derived activated carbons (Co/Mn/C=20/20/60%) using incipient wetness impregnation method. Weighed quantities of cobalt and manganese nitrates were dissolved in distilled water and impregnated on wood derived activated carbon. Impregnated material was dried at 110°C for 16h and calcined at 500°C under helium for 24h.

5.3.1.1 Catalytic testing results of Co/Mn supported on wood and peat activated carbons

Table 5.1 shows a comparison of supported cobalt and manganese on wood and peat derived activated carbon with a pure $CoMnO_x$ catalyst (prepared by co precipitation method and calcined in an air atmosphere). All three catalysts were tested at 240°C. Catalyst supported with 60% wood derived activated carbon was found to be more active compared with pure $CoMnO_x$ catalyst along with an increase in selectivity of C_{5+} hydrocarbons. Interestingly CO_2 selectivity was less with wood supported catalyst compared with pure $CoMnO_x$ catalyst.

Co, Mn catalyst supported on peat derived carbon has shown similar trend of activity and selectivity during CO hydrogenation reaction. These results of CO hydrogenation with wood and peat carbon supported catalysts are in good agreement with the results reported by Ma *et al.* [26]. They have observed that catalysts supported on peat and wood derived activated carbons are very active for CO conversion and increase the production of higher hydrocarbons. An increase in reaction temperature from 220°C to 240°C increases CO_2 selectivity for pure $CoMnO_x$ catalyst (discussed in chapter 3). Co/Mn supported on wood and peat carbons have added a positive effect to enhance the CO conversion and have decreased the CO_2 selectivity along with a significant increase in C_{5+} hydrocarbons.

Table 5.1 Catalytic testing results of Co and Mn combined with wood and peat derived carbon

		Co/Mn/C=20/20/60%	
	Pure $CoMnO_x$	Wood	Peat
Reaction Temp(°C)	240	240	240
Conversion of CO	36	41.8	43.5
Selectivity / wt% (normalized using mass balance)			
CH_4	8	15.7	12.8
C_2H_4	0.1	0.4	0.3
C_2H_6	3	7.9	5.9
C_3H_6	7	13.2	10.4
C_3H_8	2	4.8	3.8
C_4	5	2.9	2.5
C_{5+}	17	32.2	38.1
CO_2	51	14.9	18.8
Alcohols	7	8	7.5

Reaction conditions: Catalyst wt = 0.5g, Time online 116h, 6 Bar, CO/H_2 (1:1 mol ratio), GHSV = 600 h^{-1} C_{6+} = Gaseous, liquid and solid C_6-C_9 + liquid oxygenates, Alcohols = C_1-C_3 (gas phase)

5.3.1.2 Characterization of Co/Mn supported on wood derived activated carbon

(i) BET

Surface area of catalyst prepared by impregnation of cobalt and manganese on wood derived activated carbon with combination of Co/Mn/C=20/20/60% was 495m^2/g before calcination which was decreased to 397m^2/g after calcination. Surface area of wood derived activated carbon itself was 1055m^2/g.

Surface area of catalyst prepared by impregnation of cobalt and manganese on peat derived activated carbon with combination of Co/Mn/C=20/20/60% was 315m^2/g before calcination which was decreased to 225m^2/g after calcination. Surface area of peat derived activated carbon itself was 459m^2/g. Decrease in surface area of these catalysts shows filling of pores with addition of metal precursors.

(ii) XRD

Catalysts prepared by impregnation of cobalt and manganese nitrates on wood and peat derived activated carbon show some phases of mixed Co, Mn spinel oxides. Peak width of these phases is increased in the impregnated catalyst compared with pure $CoMnO_x$ catalyst.

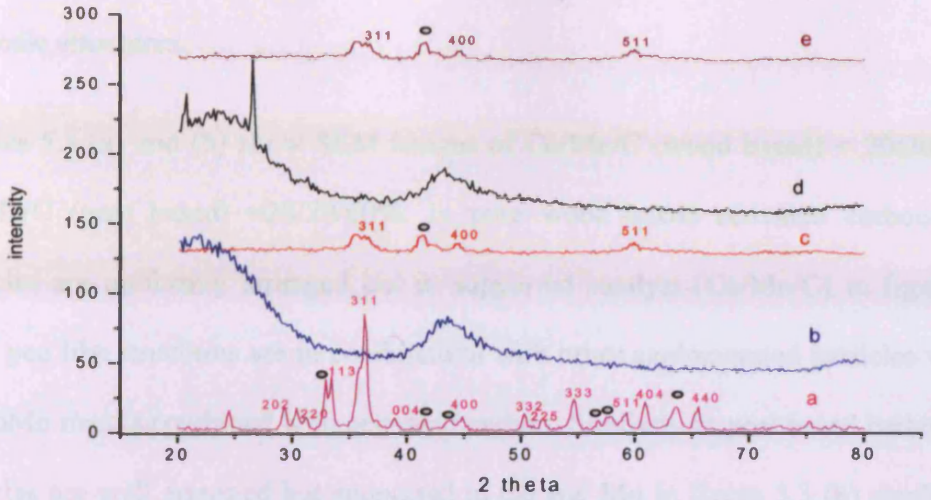

Figure 5.1 XRD pattern comparison of CoMnOx with Co/Mn/C=20/20/60% (a)Pure $CoMnO_x$ (b)peat derived activated carbon (c)Co/Mn/C(peat)=20/20/60% (d)wood derived carbon (e) Co/Mn/C(wood)=20/20/60% (○) Mn_3O_4

(iii) SEM

Figures 5.2 (a) and (b) show SEM images of peat and wood carbons that allow a qualitative comparison of morphologies of the supported materials.

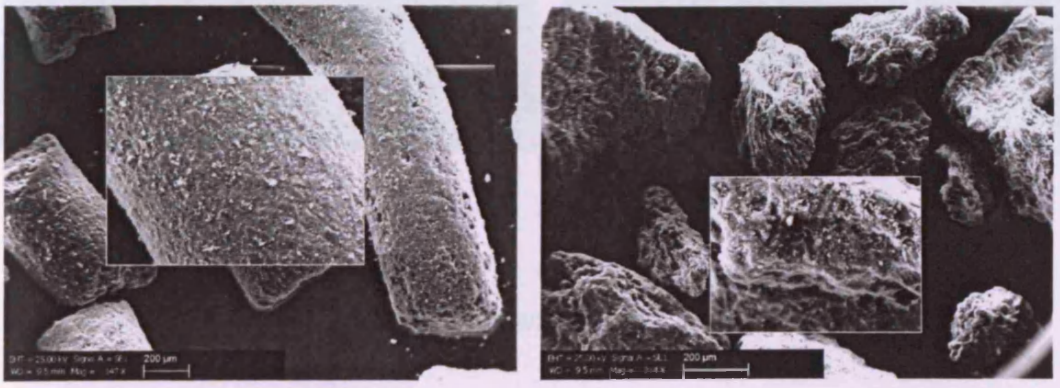

(a) **(b)**

Figure 5.2 a) wood-based activated carbon b) peat based activated carbon

The peat based carbon has slit like pores and the wood carbon has small pan like particles in needle structures.

Figures 5.3 (a) and (b) show SEM images of Co/Mn/C (wood based) = 20/20/60% and Co/Mn/C (peat based) =20/20/60%. In pure wood based activated carbon pan like particles are uniformly arranged but in supported catalyst (Co/Mn/C) in figure 5.3 (a) these pan like structures are in combination with other agglomerated particles which can be CoMn metals combined with activated carbon. Similarly in peat based carbon slit like particles are well arranged but supported in Co and Mn in figure 5.3 (b) small particles appear along with original slit shaped particles of peat carbon.

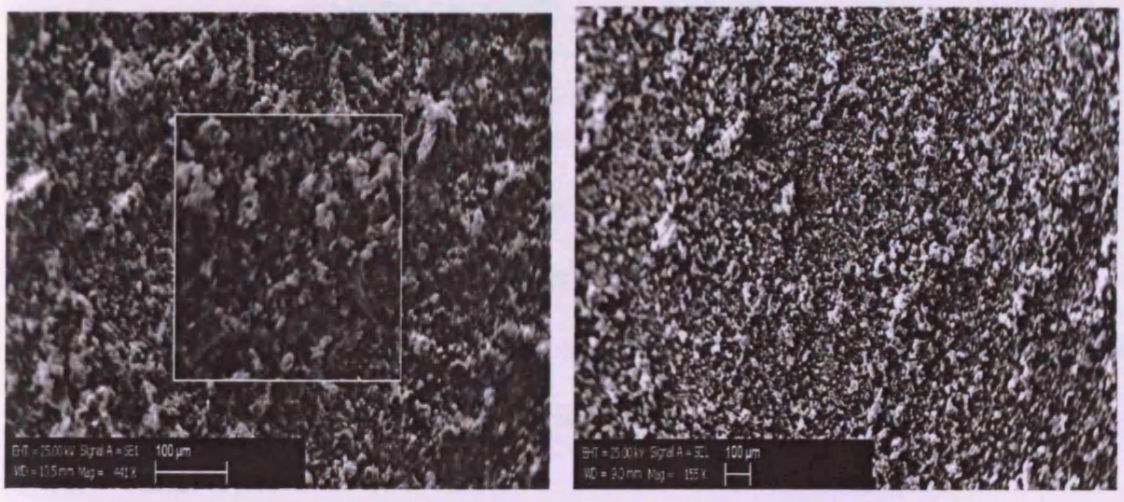

(a) **(b)**

Figure 5.3 (a) Co/Mn/C (wood-based) =20/20/60% (b) Co/Mn/C (peat based) =20/20/60%

(iv) EDX

Table 5.2 summarizes EDX results of wood and peat based carbons.

Table 5.2 Elements observed on activated carbon on EDX in order of abundance

Activated carbon type	Elements
Wood	C,S,Na,Si,K
Peat	C,Mg,S,Si,Al,Fe,K,P

Wood-based carbon shows C in abundance along with trace amounts of S, Na, Si, and K while peat-based carbon has shown additional Mg, Al, Fe, K and P.

Table 5.3 summarizes EDX results of supported Co/Mn/C (wood and peat) catalysts.

Table 5.3 Elements observed on supported Co/Mn activated carbon on EDX in order of abundance

Co/Mn/C=20/20/60%	Elements
Wood	C,O,Co,Mn
Peat	C,O,Co,Mn,Mg,S,Si,

Co/Mn supported on wood carbon has shown C, O as major elements in addition to Co and Mn. Other metals detected in wood carbon shown in table 5.2 could not be detected in catalysts. On the other hand Co/Mn supported on peat based carbon has shown C, O, Co, Mn and Mg as major elements and S, Si are in trace amounts. Al, Fe, K and P could not be detected in the supported peat carbon catalyst.

5.3.2 Co/Mn/C (wood and peat derived) by co-precipitation method

Further two more catalysts were prepared with higher ratios of Co and Mn metals combined with wood and peat derived activated carbons using co precipitation method. The ratio of Co/Mn/C was 40/40/20%. Detailed preparation procedure has been discussed in experimental. 0.5 g of each of catalyst was tested in 6-bed reactors (appendix 4).

Reduction was done with pure hydrogen at 400°C for 16h followed by syngas reaction at 6 bar pressure and 220°C as reaction temperature.

5.3.2.1 Results

5.3.2.1.1 Catalytic testing results

Table 5.4 shows catalytic testing results of Cobalt and manganese prepared in combination with wood and peat derived activated carbons in comparison with pure $CoMnO_x$ catalyst prepared and tested under similar conditions.

Co/Mn/C catalyst prepared with wood based carbon was less active for CO conversion and showed higher selectivity to CO_2. Other selectivity pattern was similar to pure $CoMnO_x$ catalyst. Catalyst prepared with peat based carbon was more active for CO conversion and was highly selective to CO_2.

Table 5.4 Catalytic testing results of Co and Mn combined with wood and peat derived carbon

	Pure CoMnOx	Co/Mn/C=40/40/20%	
		wood	peat
Reaction Temperature(°C)	220	220	220
Conversion of CO	12	3.8	14.6
Selectivity / wt% (normalized using mass balance)			
CH_4	16.8	19.8	19.6
C_2H_4	3.2	2.6	1.2
C_2H_6	9.1	7	5.8
C_3H_6	28.4	20.5	15.5
C_3H_8	7.4	4.1	3.5
C_4	17.6	7.9	7.3
C_{5+}	14.6	18	9.3
CO_2	tr	20	31.7
Alcohols	2.6	0	6.3

Reaction conditions: Catalyst wt = 0.5g, Time online 86h, 6 Bar, CO/H_2 (1:1 mol ratio), GHSV = 600 h^{-1} C_{6+} = Gaseous, liquid and solid C_6-C_9 + liquid oxygenates, Alcohols = C_1-C_3 (gas phase)

Ideally, comparison of Co/Mn/C (peat) catalysts presented in table 5.2 and 5.4 cannot be made because of different catalysts and reaction conditions. But, it can be argued that Co/Mn supported on wood and peat activated carbons by method of incipient wetness impregnation are better with respect to CO conversion and CO_2 selectivity compared with catalysts prepared with both types of carbons in combination with Co and Mn by method of co-precipitation.

5.3.2.1.2 Characterization of Co and Mn precipitated with peat and wood derived activated carbon

(i) XRD

Figure 5.4 shows XRD pattern of Co/Mn/C =40/40/20% in combination with peat and wood based carbons. Both catalysts (Co/Mn/C, with wood and peat carbons) show typical phases of Co, Mn mixed spinel oxides along with carbon.

Interestingly, XRD pattern of Co/Mn/C supported catalysts shown in figure 5.2 shows more phases of Co, Mn spinel oxides compared with higher loadings of Co, Mn with carbons shown in figure 5.4.

It can be argued that metals were more homogeneously dispersed on carbons by impregnation method compared with co-precipitation of Co and Mn with activated carbons. This is worth mentioning here that during co-precipitation of metal salts, although carbon was mixed and stirred with solutions but most of the carbon particles were not mixed thoroughly with precipitates.

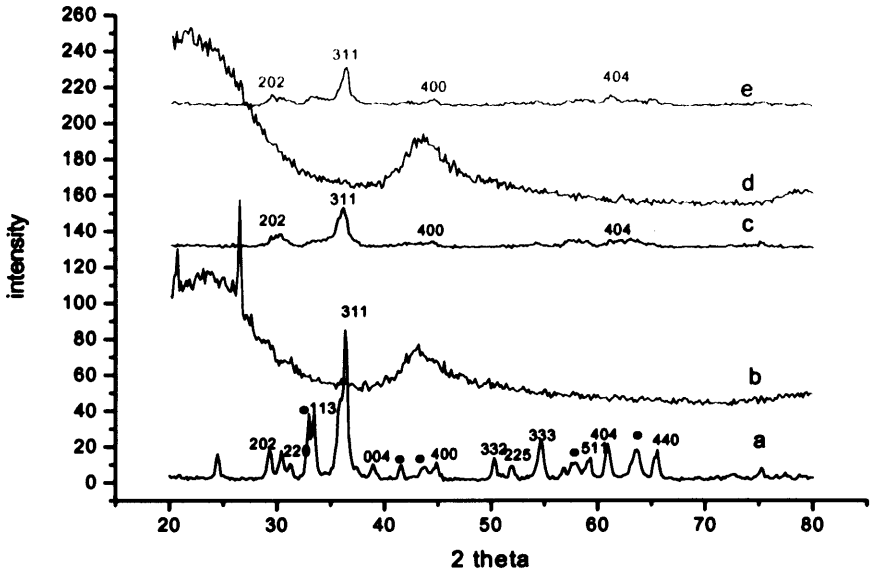

Figure 5.4. XRD pattern comparison of (a) Pure $CoMnO_x$ (b) peat derived activated carbon (c) Co/Mn/C(peat)=40/40/20%(d)wood carbon (e)Co/Mn/C(wood)=40/40/20%(○)Mn_3O_4

(ii) BET

Surface area of Co/Mn/C (wood) was 187m^2/g which increased to 260m^2/g after calcination. And surface area of Co/Mn/C (peat) was 93 m^2/g which increased to 120 m^2/g after calcination. Surface area of pure $CoMnO_x$ is 12m^2/g. These results of BET show that addition of carbon has affected surface of catalyst but there is no particular effect observed relevant to catalytic activity.

5.3.4 Iron/manganese/carbon (wood and peat derived)

At the end stage of project iron was used with manganese precipitated along with peat and wood based activated carbons. Iron has been an important Fischer Tropsch catalyst, mostly active in the form of reduced or promoted bulk oxides [27-29]. Activity of various small iron particles dispersed on oxide supports has been studied for CO hydrogenation.

It has been observed that strong interactions of iron with oxide surfaces prevent the complete reduction of iron [30-33]. Jung *et al.* [34, 35] have reported that the use of carbon support can prevent the reducibility problem and can also provide high dispersion of iron. They have reported very interesting activity results of iron/carbon catalysts for CO hydrogenation.

Two catalysts were prepared using Fe/Mn/C (wood and peat) = 40/40/20% by co precipitation method. Briefly carbon was added into mixed solutions of iron and manganese nitrates and precipitated with aqueous ammonia solution at 80°C. pH was varied from 0.21-8.00. Precipitates were filtered, washed, dried and calcined under standard conditions. Both catalysts were pelleted and sieved to 0.65-0.85mm, reduced under pure hydrogen at 400°C for 16h followed by syngas reaction. Iron catalysts were found to be inactive at 220°C and were tested at 300°C.

Fe/Mn catalyst prepared with wood based carbon was not very active even at 300°C compared with peat based carbon catalyst. Major product with Fe/Mn/C (wood based carbon) was CO_2. Fe/Mn/C (peat based carbon) was very active for CO conversion and showed CO_2 as main product along with alkanes selectivity pattern similar to wood based carbon catalyst. Iron has been reported to be an active water gas shift catalyst which results in higher CO_2 formation during FT reaction. Relatively very few studies have been published to discuss the formation of CO_2 in the FT synthesis. There are different phases of iron in iron-based catalysts. i.e., magnetite and carbide. XRD pattern of Fe/Mn/C catalysts in present studies has shown magnetite phases along with mixed phases of Fe and Mn.

5.3.4.1 Results

5.3.4.1.1 Testing results

Table 5.5 Catalytic testing results of Fe and Mn combined with wood derived carbon

	Fe/Mn/C=40/40/20%	
	wood	peat
Reaction Temperature(°C)	300	300
Conversion of CO	2.3	31
Selectivity / wt% (normalized using mass balance)		
CH_4	16.4	19.9
C_2H_4	1	0.2
C_2H_6	10.2	9.4
C_3H_6	2.4	1.7
C_3H_8	3.7	6.2
C_4	1	2.4
C_{5+}	1	2.9
CO_2	64.2	54
Alcohols	0	3.1

Reaction conditions: Catalyst wt = 0.5g, Time online 76h, P = 6 Bar, CO/H_2 (1:1 mol ratio), GHSV = 600 h^{-1} C_{6+} = Gaseous, liquid and solid C_6-C_9 + liquid oxygenates, Alcohols = C_1-C_3 (gas phase)

Some studies have assumed CO_2 formation as a secondary reaction which mainly takes place at magnetite phase [36, 37]. Although magnetite phase has been assumed to be responsible for water gas shift reaction but it is not clear from literature whether or not CO_2 is formed by water gas shift reaction of water, a main by product in FT synthesis.

5.3.4.1.2 Characterization of Fe and Mn precipitated with peat and wood derived activated carbon

(i) XRD

Figure 5.5 shows a comparison of Fe/Mn/C (wood and peat based carbons).Both catalysts show presence of $FeMn_3O_8$ along with carbon phases. There are some additional phases

of magnetite (Fe_3O_4) indicated with small circles. Presence of magnetite phases of Fe_3O_4 can be related to an increase in CO_2 selectivity with iron manganese and carbon catalysts during CO hydrogenation [37].

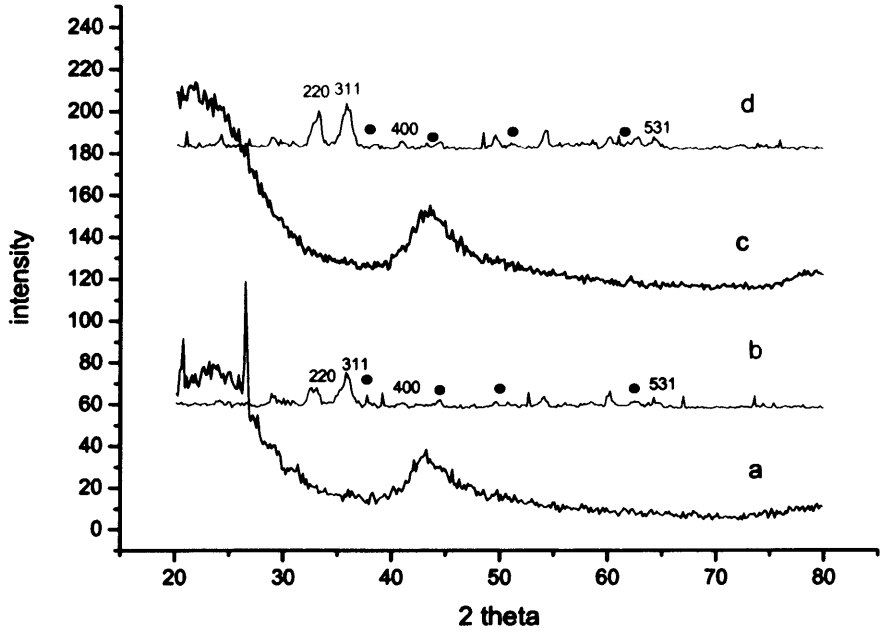

Figure 5.5. XRD pattern comparison of a) peat derived activated carbon b) Fe/Mn/C(peat)=40/40/20%c)wood carbon d)Fe/Mn/C(wood)=40/40/20%, (○) =magnetite Fe_3O_4

(ii) BET

Surface area of Fe/Mn/C (wood-based carbon) was 225 m^2/g which decreased to 217m^2/g after calcination while surface area of Fe/Mn/C (peat-based carbon) was 175 m^2/g which decreased to 158m^2/g after calcination.

5.4. Conclusions

Effect of two different types of carbon (wood and peat derived) on the catalytic performance (activity and selectivity) of cobalt and manganese catalysts is discussed in this chapter. Impregnation method was used for supporting cobalt and manganese on peat and wood carbons and their catalytic activity was compared under similar reaction conditions. Both types of carbons combined with metals were found to be more selective to the production of C_{5+} hydrocarbons with far higher CO conversion and low selectivity to CO_2 in comparison with pure $CoMnO_x$ at 240°C.

Further metal concentrations were increased along with both wood and peat carbons and were tested at lower temperature. Catalysts with higher concentrations of cobalt and manganese with 20% carbons were found to be less active at 220°C along with very high selectivity to CO_2 and low productivity of hydrocarbons compared with pure $CoMnO_x$ at 220°C.

Two iron catalysts have been prepared and tested with wood and peat based carbons and are found to be highly selective for CO_2 formation. Over all cobalt and manganese catalysts supported with wood based carbon, Co/Mn/C = 20/20/60% has been found to be less selective to CO_2 and more selective to hydrocarbons, particularly propylene, at higher temperature. Present studies have shown that increase in temperature from 220°C to 240°C with pure $CoMnO_x$ catalyst shifts the selectivity pattern to CO_2 but very interesting character for reduction for CO_2 formation with Co/Mn and wood based carbon has been observed. There is very limited literature available on effect of wood based carbon with FT catalysts, particularly cobalt catalysts. EDX analysis of wood and peat

carbons has shown different combination of metals present along with carbon which can lead to difference in catalytic activity.

5.5. Future work

A different catalyst system for CO hydrogenation reaction has been studied with cobalt, manganese in combination with wood and peat based carbons. Main emphasis was catalytic activity. Very big differences have been observed in the testing results. There is further need of detailed studies on actual mechanism involved with particular types of activated carbons. CO chemisorptions can provide good information on dispersion of active sites present with these particular catalysts. TPR studies can give an idea about the change in reduction behavior of carbon supported catalysts. XPS studies will be useful for an identification of oxidation states of cobalt and manganese before and after the reaction. TPR studies of Fe/Mn/C catalysts will be interesting to see if carbon has changed the reducibility of iron.

5.6 References:

[1]. M. A. Vannice, *Cat. Rev. - Sci. Eng.*, 1976, **14**, 153

[2]. K. Aika, H. Hori, and A. Ozaki, *J. Catal.*, 1972, **27**, 424

[3]. L. J. Schmitt, and P. L.Walker, *Carbon.*, 1971, **10**, 791

[4]. L. J. Schmitt, and P. L.Walker, *Carbon.*, 1972, **10**, 87

[5]. C. Moreno-Castilla, O. P. Mahajan, H. J. Jung, M. A.Vannice, and P. L.Walker, *Jr. Absts.*, 14th Amer. Carbon Conf. Penn State, 1979

[6]. M. A. Vannice, P. L. Walker, H. J. Jung, C. Moreno-Castilla, and O. P. Mahajan., Proc. VII, Int. Cong. Catal. Tokyo, 1980

[7]. C. Moreno-Castilla, O. P. Mahajan, P. L.Walker, H. J. Jung, and M. A. Vannice, *Carbon.*, 1980, **18**, 271

[8]. E. Van Steen and F. F. Prinsloo, *Catal. Today.*, 2002, **71**, 327

[9]. F. Rodriguez-Reinoso, *Carbon.*, 1998, **36**, 159

[10]. H. Tamon, and M. Okazaki, *Carbon.*, 1996, **34**, 741

[11]. B. Singh, S. Madhusudhanau, V. Bubey, R. Nath, and N. B. S. N. Rao, *Carbon.*, 1996, **34**, 327

[12]. J. Barrault, A. Guilleminot, J. C. Achard, V. Paul-Boncour, A. Percheron-Guegan, and L. Hilaire, M. Coulon, *Appl. Catal.*, 1986, **22**, 273

[13]. A. Guerrero-Ruiz, A. Sepulveda-Escribano, and I. Rodriguez-Ramos, *Appl. Catal.*, 1994, **120**, 71

[14]. J. J. Venter, and M. A. Vannice, *Catal. Lett.*, 1990, **7**, 219

[15]. J. J. Venter, M. Kaminsky, G. L. Geoffrroy, and M. A.Vannice, *J. Catal.*, 1987, **103**, 450

[16]. M. A. Vannice, P. L.Walker, H. J. Jung, C. Moreno-Castilla, and O. P. Mahajan, *Stud. Surf. Sci. Catal.*, 1981, **7**, 460

[17]. A. A. Chen, M. Kaminsky, G. L.Geoffroy, and M. A.Vannice, *J. Phys. Chem.*, 1986, **90**, 4810

[18]. W. P. Ma, Y. J. Ding, H. Y. Lou, and L. W. Lin, in. "*The 7th China-Japan Symposium on coal and C_1 chemistry*" 2001

[19]. D. H. Yin, W. H. Li, W. S. Yang, H. W. Xiang, Y. H. Sun, B. Zhong, and S. Y. Peng, *Microp. Mesop. Mater.*, 2001, **47**, 15

[20]. A. Y. Khodakov, A. Griboval-Constant, R. Bechara, and V. L. Zholobenko, *J. Catal.*, 2002, **206**, 230

[21]. M. Agustin, L. Carlos, M. Francisco, and D. Isabel, *J. Catal.*, 2003, **220**, 486

[22]. Y. Ohtsuka, Y. Takahashi, M. Noguchi, T. Arai, S. Takahashi, N. Tsubouchi, and Y. Wang, *Catal. Today.*, 2004, **89**, 419

[23]. W. P. Ma, Y. J. Ding, and L. W. Lin, *Ind. Eng. Chem. Res.*, 2004, **43**, 2391

[24]. W. P. Ma, Y. J. Ding, J. Yang, X. Liu, and L. W. Lin, *React. Kinet. Catal. Lett.*, 2005, **84**, 11

[25]. E. L. Kugler, L. Feng, X. Li, and D. B. Dadyburjor, *Stud. Surf. Sci. Catal.*, 2000, **130**, 299

[26]. W. Ma, E. L. Kugler, and D. B. Dadyburjor, *Stud. Surf. Sci. Catal.*, 2004, **163**, 125

[27]. R. B. Anderson, *Catalysis.*, 1956, **4**, 119

[28]. M. E. Dry, in "*Catalysis: Science and Technology*" 1981, **1**

[29]. V. Ponec, *Coal Sci.*, 1984, **3**, 1

[30]. M. A. Vannice, *J. Catal.*, 1975, **37**, 449

[31]. M. A. Vannice, *J. Catal.*, 1977, **50**, 228

[32]. M. A. Vannice, and R. L. Garten, *J. Mol. Catal.*, 1975, **1**, 201

[33]. M. A. Vannice, *J. Catal.*, 1982, **74**, 199

[34]. H. J. Jung, P. L. Walker, and M. A. Vannice, *J. Catal.*, 1982, **75**, 416

[35]. H. J. Jung, L. N. Mulay, M. A. Vannice, R. M. Stanfield, and W. N. Delgass, *J. Catal.*, 1982, **76**, 208

[36]. E. S. Lox, and G. F. Formette, *Ind. Eng. Chem. Res.*, 1993, **23**, 71

[37]. G. P. Van der Lann, and A. A. C. M. Beenackers, *Appl. Catal.*, 2000, **193**, 39

Chapter 6

An investigation of synthesis of higher alcohols from syngas using modified molybdenum sulphide catalysts

6.1 Introduction

Much attention has been given to the synthesis of mixed alcohols due to its properties as the gasoline blend or alternative motor fuel for the reduction of exhaust emission in the last 20 years. The addition of alcohols and other oxygenates into gasoline gives rise to decreases toxic exhaust gases (CO, NO_x) and in some cases increases octane number. Use of methyl tent-butyl ether (MTBE) has been prohibited recently in some countries as additive of oil-based fuel due to the new legal requirements in environmental protection.

So, the catalyst conversion of synthesis gas to mixed alcohols is attracting renewed interest for industrial applications as well as fundamental research.

6.2 Alkali-doped molybdenum sulfide based catalysts

Molybdenum based catalyst was first discovered by Dow [1, 2] and Union Carbide [3]. These catalysts are highly selective to C_{2+} alcohols synthesis and are naturally resistant against sulphur. Molybdenum sulphide based catalyst system has been studied by various researchers [4-6].

First of all Dow investigated Co-MoS_2 catalysts for the synthesis of higher alcohols from syngas. This catalyst was prepared by the method of co precipitation. They presented effects of different reaction parameters on the catalytic activity and selectivity of these catalysts. Alcohols selectivity was reported to be increased by an increase in reaction pressure and decreased feed ratio of syngas. Iranmahboob *et al.* [7, 8] have also reported an investigation of Co-MoS_2 catalysts. They have reported effect of temperature on selectivity of alcohols and they have concluded a temperature range of 563-583K as suitable condition for clay to act as a modifier which increases the activity and selectivity of catalysts [6]. They have also studied an effect of potassium and cesium promoters on Co-MoS_2/clay catalyst. They found that an increase in reaction temperature increased the alcohols yield but decreased alcohol selectivity [7].

Attempts have been made to develop new catalysts to improve the catalytic performance for selectivity of mixed alcohols. Recent studies have revealed that both the activity and selectivity to higher alcohols can be improved by addition of effective promoters, such as

Fischer-Tropsch components and alkali metals into MoS_2-based catalysts [9-11], change in nature of supports [12-17] and modification in catalyst preparation method [18,19].

Murchison *et al.* [1] and Xie *et al.* [20] have studied effect of potassium promoter on MoS_2 based catalyst. They have reported a decrease in catalytic activity upon addition of potassium and a shift of products to alcohols from higher hydrocarbons.

Very recently other new catalysts were also developed and a good activity and selectivity could also be obtained. For example, Kaliaguine *et al.* [21, 22] reported conversion of syngas to higher alcohols over nanocrystalline Co-Cu-based perovskites as catalysts. Xiang *et al.* [23, 24] have reported synthesis of higher alcohols from syngas over Fischer Tropsch elements modified molybdenum carbides. However up till now, alkali doped catalysts are still considered the most promising catalysts due to their resistance to sulphur poisoning and higher activity for the water-gas shift reaction.

Basically the function of cobalt in Co-MoS_2 catalyst is considered to modify the selectivity to the products (alcohols). This can be related to the capability of cobalt to enhance the chain growth [25-27].

In the design of unsupported Mo-S_2 based catalysts, it is important to properly introduce the modifier and preparation method to improve its catalytic activity. In literature [28-31] the 3rd row transition metals such as Co, Fe, Ni, Rh, have been introduced into alkali-doped MoS_2 catalyst systems. It has been considered that at least two forms of transition metal promoters simultaneously existed in MoS_2 based catalysts, namely, separate phases of transition metals and mixed phases such as so-called " Mo-M-S "(M=transition metals) [32,33]. It has been concluded that the close interaction between Mo and promoter atoms

also exerted a strong effect on the promotion effects for mixed alcohols synthesis from syngas. Moreover, the structure and morphology of metal promoter and MoS_2 support was closely related to the promotion effects. It has been reported that the addition of La or Ce, into supported Ni and supported cobalt catalysts gave an increase in catalytic activity [34-36].

In present studies, $CoMoS_2$ catalyst has been doped with three metal promoters, namely, Ni, Ti and Zr and their effect on morphology and catalytic performance has been studied for the synthesis of alcohols from syngas.

6.3 Experimental

Alkali-promoted cobalt molybdenum sulfide solid (Co-MoS_2/K_2CO_3) mixed with bentonite clay and sterotex® lubricant was used for the Co-MoS_2 based catalyst in this study. The Co-MoS_2 (Mo: Co = 2:1) solid was prepared by co-precipitation as described in Chapter 2.

Catalytic tests were carried out using high pressure reactor which is described in Chapter 2. The dilution of catalyst was performed by intimate mixing of the catalyst with silicon carbide (4.8 ml/5.2 ml for Co-MoS_2 based catalyst).

Prior to the catalytic run, system leakage test was carried out using nitrogen (Oxygen free, BOC). After the system was found safe and leak-free, syngas was gradually introduced to the system, replacing the nitrogen. Following the complete replacement, the system was brought up to the required pressure, followed by heating with a ramping rate of 1 K/min until it reached the desired temperature.

All catalysts were studied under identical reaction conditions. Reaction pressure was 75 bar and temperature of reaction was 580K.

6.4 Results on Co-MoS_2 based catalyst system

6.4.1 Catalytic testing results

The present section describes the CO hydrogenation activity of Co-MoS_2/K_2CO_3/clay/lubricant catalyst. Silicon carbide intimately mixed with catalyst was used for the catalytic reaction. Before catalytic test, a blank run with silicon carbide was carried out. There was no catalytic activity observed with the blank run. This suggests that silicon carbide is an inert material with respect to CO hydrogenation and hence can be used as diluent for catalytic test. Reasons of diluting the catalyst bed are: 1) to achieve and maintain an isothermal regime for the reaction; and 2) to avoid possible hot spot developing in the catalyst bed.

Table 6.1 shows catalytic testing results of pure $CoMoS_2$ mixed with K_2CO_3/bentonite clay/sterotex and SiC. This catalyst showed very high activity and it took almost 45h to get stabilized. Methane selectivity was high and hydrocarbon selectivity was less when compared with previously reported results of same catalyst under similar reaction conditions [37]. Selectivity of ethanol was similar as was reported earlier. Interesting characteristic of present catalyst preparation was increased CO conversion and selectivity to propanol. Better activity of catalyst can be attributed to the improved preparation conditions like controlled flow rate of reagents with the help of peristaltic pump, use of a proper reaction vessel instead of beaker and mechanical stirrer instead of magnetic stirrer.

Table 6.1 Comparison of CO hydrogenation over Co-MoS_2/K_2CO_3/clay/lubricant catalyst (previous [37] and present)

	a	b
Conversion of CO (exclusive CO_2)	48.5	18.9
Product (mol %)		
CH_4	25.62	24.9
C_2H_4	0	0.24
C_2H_6	0.35	8.87
C_3H_6	0	1.03
C_3H_8	0.32	4.91
C_4H_8	0	0.15
C_4H_{10}	0.03	1.53
C_5H_{10}	0.17	0.12
C_5H_{12}	0.17	0.43
CO_2	2.16	c
Methanol	13.78	26.7
Ethanol	32.4	23.3
1-Propanol	13.78	6.28
2-methyl,1-Propanol	0.27	0.55
1-butanol	8.26	0.91
Carbon mole selectivity (%)		
CH_4	39.53	14.1
$C_{>2}$	0.55	25.9
Methanol	21.28	15.2
Ethanol	25	26.5
1-Propanol	7.09	10.7
2-methyl,1-Propanol	0.1	1.26
1-Butanol	2.55	2.07
CO_2	3.33	c

Reaction conditions: 580 K, 75 Bar, CO/H_2 (1:1 mol ratio), GHSV = 1225 h^{-1}
(a) Present data (b) Previous data (c) Not reported

Figure 6.1 shows CO conversion after every 2 hours of reaction over period of 60h. From the CO conversion data, it can be seen that there were circa 40 – 45 hours needed for the reaction to reach stable condition. This induction period was different than was reported by Woo *et al.* [38] and Iranmahbood and Hill [39]. They have observed that 20-30h was induction time period for stabilization. The induction period could be the time required

for the alkali promoters and/or clay to spread onto the Co-MoS_2 surface. After this period, both catalytic systems show rather stable activities during entire catalytic run.

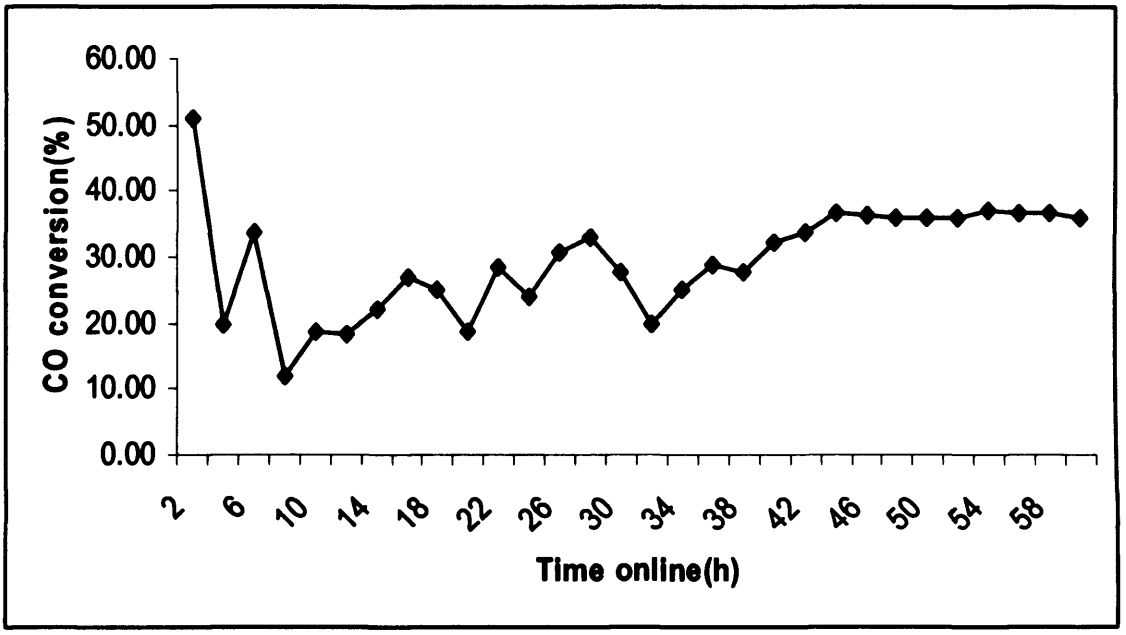

Figure 6.1 Time online data of CO hydrogenation on $CoMoS_2$ catalyst

Due to the restriction of current set-up, it was not possible to obtain online liquid analysis. All the liquid was analyzed together after the reaction completed. There was no hydrocarbon detected in the liquid product. It mainly consisted of alcohols and water.

This work was a repetition of previously reported catalyst [37]. Further modification of this catalyst was done by addition of various metal promoters like Zr, Ni and Ti. The effect of addition of these promoters on the catalytic activity of $CoMoS_2$ catalyst will be discussed in the following paragraphs.

6.5 Effect of metal promoters on catalytic performance of $CoMoS_2$

$CoMoS_2$ catalyst has never been reported in combination with Zr, and Ti. There is some patent literature specifically with Co/activated carbon and various bimetallic catalysts promoted with Zr, Ti and various other metals [40- 42].

Nickel is active catalyst for methanation reaction in the Fischer Tropsch Synthesis. The development of Co and Ni catalysts was reviewed by Anderson [43]. Fraga and Jordao [44] have reported the bulk AlNiCu catalysts being extremely selective for the synthesis of higher alcohols in the syngas reaction. They have also observed that change in salt concentration changes the selectivity pattern to greater extent. In 1934, Fischer and Meyer [45] reported active catalysts from alloys of 50% Co or Ni and 50% Al or Si with NaOH. Similar Si alloys with half Ni and half Co gave catalysts producing larger yield of liquid hydrocarbons. Lucero *et al.* [46] have patented a crystalline Mo_2C catalyst with Ni for the production of alcohols from syngas. Similarly, Zr is an effective promoter for Co-based catalysts which can improve the reducibility of cobalt-based catalysts. Zr-promoted Co catalysts were found to have higher activity and C_{5+} selectivity for FTS than unpromoted catalysts [47]. Ali *et al.* [48] reported that zirconium promotion possibly creates an active surface with cobalt that increases activity and selectivity to hydrocarbons. Titanium has also been reported to be a good promoter for FTS leading to high catalytic activity [49, 50]. Because of positive effects of Ni, Ti and Zr on FTS performance these metal promoters were used in combination with $CoMoS_2$ catalyst for reaction of CO hydrogenation. The details of their effect on activity and selectivity of alcohols is detailed in the following section.

6.5.1 Experimental

Pure $CoMoS_2$ catalyst was prepared by co precipitation method. Detailed procedure has been mentioned in chapter 2 and above. Catalyst precursor was promoted with Ni, Zr and Ti (0.2%) using nitrates (acetyl acetone for Ti) as salt precursors by impregnation method. Briefly, weighed quantity of metal salt was dissolved in distilled water and was impregnated on $CoMoS_2$. This impregnated material was dried at 110°C for 16h followed by calcination at 500°C for 1h under continuous flow of nitrogen. Catalysts were mixed with potassium carbonate (K_2CO_3), bentonite clay and sterotex® lubricant.

6.5.2 Results

6.5.2.1 Catalytic testing results

Table 6.2 shows a comparison of catalytic testing results of Ti, Zr and Ni doped on $CoMoS_2$. All these catalysts were premixed with K_2CO_3/Bentonite clay/sterotex lubricant, diluted with SiC and were tested under similar conditions.

$CoMoS_2$ doped with nickel (0.2%) was very active for CO conversion. The major product with this catalyst was CO_2. $CoMoS_2$ doped with titanium was more active compared with pure $CoMoS_2$ catalyst (results shown in table 6.1) but was highly selective to CO_2 like nickel. $CoMoS_2$ impregnated with zirconium was found to be less active in comparison with other catalysts. This is worth mentioning here that all these catalysts were premixed with potassium carbonate.

Table 6.2 CO hydrogenation over Co-MoS_2 + Ni, Ti, Zr/K_2CO_3/clay/lubricant catalyst

	$CoMoS_2$ doped with		
	Ni	Ti	Zr
Conversion of CO (exclusive CO_2) /%	74.11	54.7	23.52
Products (mol %)			
CH_4	16.40	24.5	28.79
C_2H_4	0.01	0.005	0.02
C_2H_6	5.09	2.97	8.53
C_3H_6	0.03	0.49	0.28
C_3H_8	3.87	11.02	13.95
C_4H_8	0.13	0.053	3.63
C_4H_{10}	0.08	0.31	9.55
C_5H_{10}	10.63	0	8.68
C_5H_{12}	11.95	0	8.68
C_6H_{12}	0.03	0.002	0.02
C_6H_{14}	0.08	0.6	0.06
CO_2	46.84	59.8	6.64
Methanol	1.48	0	2.35
Ethanol	1.61	0	2.56
1-Propanol	1.87	0	2.98
2-methyl,1-Propanol	0.98	0	1.55
1-butanol	0.90	0	1.43
Carbon mole Selectivity (%)			
CH_4	21.98	27.12	50.64
$C_{>2}$	10.71	6	28.03
Methanol	1.99	0	4.26
Ethanol	1.08	0	2.27
1-Propanol	0.84	0	1.76
2-methyl,1-Propanol	0.33	0	0.69
1-Butanol	0.24	0	0.51
CO_2	62.79	66.18	11.74

Reaction conditions: 580 K, 75 Bar, CO/H_2 (1:1 mol ratio), GHSV = 1225 h^{-1}

Alcohols selectivity was less compared with pure $CoMoS_2$ but was found to be more selective for hydrocarbons synthesis. The combined effect of alkali addition along with nickel, zirconium and titanium can add into selectivity pattern.

Nickel is considered a good methanation catalyst and can also dissociate hydrogen very fast and forms stable carbides [51, 52]. Ponec [53] has reviewed effect of Rh based catalysts on alcohol selectivity. An enhancement in alcohols selectivity (particularly ethanol) was reported over Rh/supported SiO_2 catalysts doped with titanium and zirconium. Recently Ni doped β-MoC_2 catalysts have been reported for syngas conversion to higher alcohols [54, 55]. The undoped and unmodified β-MoC_2 exhibited a high CO conversion but produced CO_2 and hydrocarbons as a major product. But alcohols selectivity was improved upon addition of K and Ni promoters. Conversely doping the same catalyst (K-Ni- β-MoC_2) with cobalt instead of nickel increased the selectivity of hydrocarbons.

Present studies have shown an enhancement in hydrocarbons and CO_2 selectivity upon addition of nickel promoter into $CoMoS_2$ catalyst. This catalyst has been mixed with potassium carbonate. A combined effect of Co, Ni and K along with MoS_2 leads to many possible reactions during CO hydrogenation.

Although undoped MoS_2 produces only hydrocarbons, commonly methane, the selectivity dramatically shifts to alcohols upon addition of alkali promoters. The role of alkali promoters into these catalysts is to shift the products from hydrocarbons to alcohols. Several researchers have studied MoS_2-based catalyst for higher alcohols synthesis (HAS) [56-65]. The selectivity of hydrocarbons and alcohols varies depending on type of metal promoters used. A combination of Ni with MoS_2 catalyst has been studied along with K_2CO_3 [66]. This catalyst has been found to be highly reactive for CO conversion and has shown good selectivity to hydrocarbons. CO_2 selectivity data is not available for these catalysts. Alcohols selectivity has been found to be very low compared with pure

$CoMoS_2$ catalyst. Present studies have shown similar trend with respect to hydrocarbons selectivity. This trend is expected, taking into account the fact that nickel is a very well known methanation catalyst [67].

From the present studies it can be argued that the promotional activity of nickel in these catalysts is due to the bifunctionality of Ni; one is catalyzing the formation of alcohols and second is CO insertion reactions. Depending on the dominant reaction, product stream shifts to CO_2 or alcohols.

Titanium addition into $CoMoS_2$ has resulted in formation of CO_2, while addition of zirconium in $CoMoS_2$ has shown an increase in the formation of hydrocarbons, methane being the main product.

In CO hydrogenation, it is reported generally that CO molecules adsorbed in a dissociative pattern are responsible for the synthesis of hydrocarbons while those adsorbed associatively result in the formation of alcohols [68]. In alcohols synthesis catalysts, alkali metals can reduce availability of active hydrogen by blocking the active sites for dissociative chemisorption of CO. This blockage of active sites decreases the interaction of CO with catalyst surface. The associatively adsorbed CO will be directly hydrogenated to alcohols. From the present results (of $CoMoS_2/K_2CO_3$ + doped with Ti, Ni, Zr), none of these catalysts was found active for alcohols synthesis compared with pure $CoMoS_2/K_2CO_3$. This can be argued that K combined with $CoMoS_2$ pure catalyst blocks the active sites for CO to adsorb dissociatively and leads to direct hydrogenation for alcohols formation. But addition of transition metals affects the basicity of surface species leading to different reaction. Again it is hard to emphasize the existence of a

single possible reaction responsible for alcohols or hydrocarbons formation because of a lot of possibilities of various other reactions.

6.5.2.2 Characterization of $CoMoS_2$ doped with various metal promoters

(i) XRD

A comparison of XRD patterns of $CoMoS_2$ catalyst doped with Ni, Zr and Ti has been shown in figure 6.2.

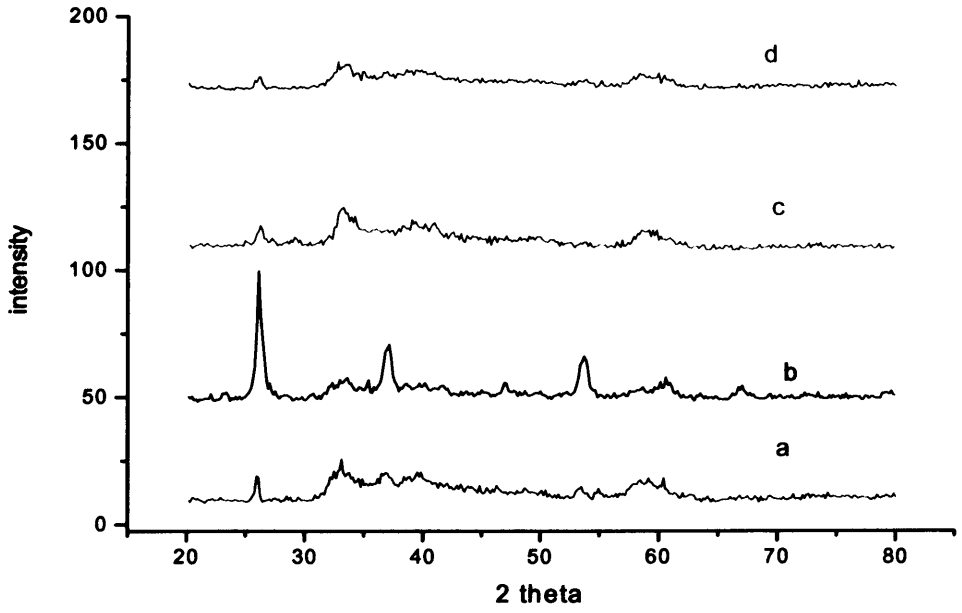

Figure 6.2 XRD comparison of $CoMoS_2$ doped with various metals a) pure $CoMoS_2$ b) Ni c) Zr d) Ti

The solid pure sample was identified as belonging to MoS_2.This was concluded because of the characteristic reflections at 2 theta of 33.4, 39.4,50 and 59. There is one peak at 26.2 which is characteristic of cobalt molybdenum oxide sulphide (CoMoOS). XRD

pattern of catalyst doped with nickel is different than others. All peaks get more intense and crystalline compared with pure $CoMoS_2$. Catalysts with Zr and Ni do not show any change in XRD patterns when compared with pure $CoMoS_2$.

(ii) BET

Table 6.3 shows BET surface area measurements for $CoMoS_2$ doped with Ti, Ni and Zr. Catalysts promoted with Ni and Ti have shown an increase in surface area compared with pure $CoMoS_2$ catalyst. $CoMoS_2$ impregnated with zirconium has shown lowest surface area in comparison with other catalysts. Zr doped with $CoMoS_2$ has shown the lowest activity for CO conversion while Ni doped with $CoMoS_2$ was highly active for conversion of CO.

Table 6.3 BET surface areas of $CoMoS_2$ doped with various metals

Catalysts	Surface area (m^2/g)	
	Before calcination	After calcination
$CoMoS_2$	48	35
$CoMoS_2$+Zr	35	24
$CoMoS_2$+Ti	55	49
$CoMoS_2$+Ni	67	59

(iii) SEM

Figure 6.3 shows a comparison of pure $CoMoS_2$ and doped catalysts. Addition of promoters has definitely affected the surface morphology and geometry of catalysts. Some remarkable differences can be observed in these images. For pure catalyst $CoMoS_2$, spongy like structures were observed. Size and geometry of these particles was uniform. There were big lumps of particles and various small sized particles were arranged on top of them. For the zirconium doped catalyst the morphology of surface was completely

changed. It consisted of various particles of different sizes and shapes. Catalyst doped with Ti has shown a uniform distribution of very big particles along with small spherical objects scattered on the surface. Catalyst doped with nickel was completely different compared with other three catalysts. It consisted of spongy shaped structures of different sizes.

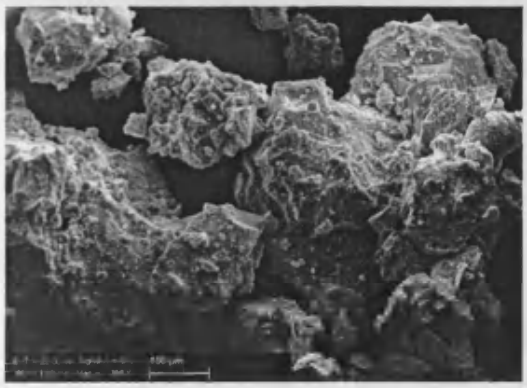

(a) Pure $CoMoS_2$

(b) $CoMoS_2$+Zr

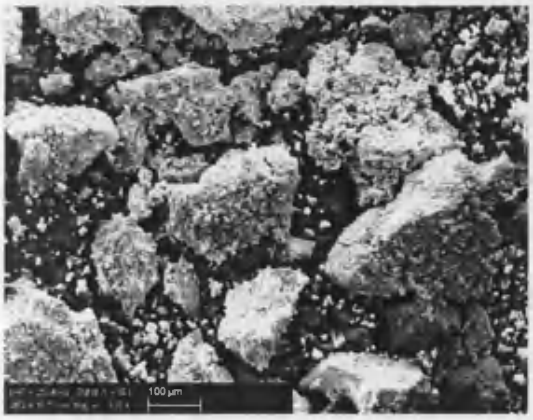

(c) $CoMoS_2$+Ti

(d) $CoMoS_2$+Ni

Figure 6.3 SEM images of $CoMoS_2$ and doped $CoMoS_2$ with various metals

The evident morphological differences between pure $CoMoS_2$ and doped $CoMoS_2$ suggest that addition of Zr, Ni and Ti addition has effectively changed the surface composition. Similar differences were observed in BET measurements. Although XRD patterns were similar for Zr and Ti doped catalysts and pure $CoMoS_2$ but there was clear difference in XRD of nickel promoted catalyst. These similarities in surface characterization suggest that addition of Zr and Ti have affected the surface composition while it can be argued that addition of Ni can modify the surface and bulk both.

6.6 Conclusions

One particular catalyst system of $CoMoS_2$ has been reproduced under improved preparation conditions. This catalyst has shown very good activity along with similar selectivity of alcohols as was reported earlier. Further this catalyst system has been modified by addition of various metal promoters. $CoMoS_2$ promoted with 0.2% Ni was found to be highly active for CO conversion but was more selective to hydrocarbons. Titanium addition shifted the products completely to hydrocarbons instead of alcohols. Zirconium addition into $CoMoS_2$ catalyst has shown low water gas shift reaction and major product was methane, along with other hydrocarbons(C>2).Nickel promoter was found to be highly active for water gas shift reaction. Combined effect of alkali (K from K_2CO_3) along with these transition metal promoters lead to a change in surface composition leading to a big shift of product stream from alcohols to CO_2 and hydrocarbons. SEM images and BET measurements of promoted catalysts have shown clear differences between doped and pure $CoMoS_2$ catalysts. These differences in characterization of promoted catalysts can be related to the differences in catalytic activity.

6.7 Future work

This work was a continuation of previously reported catalyst ($CoMoS_2$). Further modification was done by addition of metal promoters but the reaction conditions were not changed. Variation in reaction pressure, temperature and syngas ratio can be studied in future. Testing pure catalysts (without mixing with potassium carbonate) can give different activity. Surface composition has a strong effect on selectivity pattern which can be studied and related by XPS. CO chemisorption studies will be useful for understanding the active sites on catalyst surface. TPR will be useful for further information about the reduction behavior of these catalysts. Only one particular concentration (0.2%) has been studied so far, it can be useful to vary the concentrations of these metals which can influence the surface basicity or acidity leading to different reaction pathways. Further, a combination of different metals can be studied on $CoMoS_2$ catalyst, e.g. the hydrocarbon formation from $Ni/CoMoS_2$ can be suppressed by addition of lanthanum. The promotional effect of La metal with Ni has been reported that leads to a strong interaction of Ni and La improving the Ni dispersion on surface of catalyst [67]. Addition of lanthanum has been reported to enhance the selectivity for higher alcohols.

6.8 References:

[1]. C. B. Murchison, M. M. Conway, R. R. Stevens, and G. J. Quarderer, *Proc. 9th Int. Congr. Catal.*, 1988, **2**, 626

[2]. R. R. Stevens, European Patent, 1986, **172431**

[3]. N. E. Kinkade, European Patents, 1985, **0149255** and **0149256**

[4]. J. G. Santiesteban, C. E. Bogdan, R. G. Herman, and K. Klier, *Proc. 9th Int. Congr. Catal.*, 1988, **2**, 561

[5]. X. Youchang, B. M. Naasz, and G. A. Somorjai, *Appl. Catal.*, 1986, **27**, 233

[6]. J. Iranmahboob, H. Toghiani, D. O. Hill, and F. Nadi, *Fuel Proc. Tech.*, 2002, **79**, 71

[7]. J. Iranmahboob, D. O. Hill and H. Toghiani, *Appl. Catal.*, 2002, **231**, 99

[8]. J. Iranmahboob, D. O. Hill, and H. Toghiani, *Appl. Surf. Sci.*, 2001, **185**, 72

[9]. K. Fujimoto, and T. Oba, *Appl. Catal.*, 1985, **13**, 289

[10]. T. Tatsumi, A. Muramatsu, and H. Tominaga, *Appl. Catal.*, 1987, **60**, 3157

[11]. D. B. Li, C. Yang, H. R. Zhang,W. H. Li,Y. H. Sun, and B. Zhong, *Top. Catal.*, 2005, **32**, 233

[12]. D. B. Li, C.Yang, H. R. Zhang, W. H. Li, Y. H. Sun, and B. Zhong, *Stud. Surf. Sci. Catal.*, 2004, **147**, 391

[13]. Z. R. Li,Y. L. Fu, J. Bao, M. Jiang, T. D. Hu, T. Liu, and Y. N. Xie, *Appl. Catal.*, 2001, **220**, 21

[14]. X. M. Ma, G. D. Lin, and H. B. Zhang, *Catal. Lett.*, 2006, **111**, 141

[15]. X. M. Wu, Y. Y. Guo, J. M. Zhou, G. D. Lin, X. Dong, and H. B. Zhang, *Appl. Catal.* 2008, **340**, 87

[16]. X. Dong, H. B. Zhang, G. D. Lin, Y. Z. Yuan, and K. R. Tsai, *Catal. Lett.*, 2003, **85,** 237

[17]. H. B. Zhang, X. Dong, G. D. Lin, X. L. Liang, and H. Y. Li, *Chem. Commun.*, 2005, **40**, 5094

[18]. Z. R. Li, Y. L. Fu, M. Jiang, T. D. Hu, T. Liu, and Y. N. Xie, *J. Fuel. Chem. Tech.*, 2001, **29**, 149

[19]. X. G. Li, L. J. Feng, Z. Y. Liu, B. Zhong, D. B. Dadyburjor, and E. L. Kugler, *Ind. Eng. Chem. Res.*, 1998, **37,** 3853

[20]. Y. Xie, B. M. Naasz, and G. A. Somorjai, *Appl. Catal.*, 1986, **27**, 233

[21]. N. Tien-Thao, M. H. Zahedi-Niaki, H. Alamdari, and S. Kaliagine, *J. Catal.*, 2007, **245**, 348

[22]. N. Tien-Thao, M. H. Zahedi-Niaki, H. Alamdari, and S. Kaliagine, *Appl. Catal.*, 2007, **326**, 152

[23]. M. L. Xiang, D. B. Li, H. J. Qi, W. H. Li, B. Zhong, and Y. H. Sun, *Fuel.*, 2007, **86**, 1298

[24]. M. L. Xiang, D. B. Li, H. J. Qi, W. H. Li, B. Zhong, and Y. H. Sun, *Fuel.*, 2006, **85**, 2662

[25]. G. Herman, in: Guczi, L. Ed., in "*Studies in Surface Science and Catalysis*" 1991, **64**, 265

[26]. P. Courty, D. Durand, E. Fruend, and A. Sugier, *J. Mol. Catal.*, 1982, **17**, 241

[27]. D. J. Elliot, F. Pennella, *J. Catal.*, 1986, **102**, 464

[28]. K. J. Smith, R. G. Herman, and K. Klier, *Chem. Eng. Sci.*,1990, **45**, 2693

[29]. Z. R. Li, Y. L. Fu, and M. Jiang, *Appl. Catal.*, 1999, **187**, 187

[30]. H. C. Woo, and Y. G. Kim, *Catal. Lett.*,1993, **20**, 221

[31]. Z. R. Li, Y. L. Fu, M. Jiang,Y. Xie, T. Hu, and T. Liu, *Catal. Lett.*, 2000, **65**, 43

[32]. H. Topsoe, B. S. Clausen, R. Candia, C. Wivel, and S. Morup, *J. Catal.*,1981, **68**, 433

[33]. B. H. Upton, C. C. Chen, N. M. Rodriguez, and R. T. K. Baker, *J. Catal.*, 1993, **141**, 171

[34]. D. Z. Wang, X. P. Cheng, Z. R. Huang, X. Z. Wang, and S. Y. Peng, *Appl. Catal.*, 1991, **77**, 109

[35]. H. J. G. Rotgerink, R. P. A. M. Paalman, J. G. V. Ommen, and J. R. H. Ross, *Appl. Catal.*, 1988, **45**, 257

[36]. D. B. Li, C. Yang, H. J. Qi, H. R. Zhang, W. H. Li, Y. H. Sun, and B. Zhong, *Catal. Commun.*, 2004, **5**, 605

[37]. Y. Zhao "*On the investigation of alcohol synthesis via the Fischer Tropsch reaction*", PhD Thesis, University of Cardiff, 2007

[38]. H. C. Woo, I. Nam, J. S. Lee, J. S. Chung, and Y. G. Kim, *J. Catal.*, 1993, **142**, 672

[39]. J. Iranmahboob, and D. O. Hill, *Catal. Lett.*, 2002, **78**, 49

[40]. Y. H. Zhu, T. Wang, G. Jiao, and Y. Lv, U. S. Patent, 2008, **891263**

[41]. M. K. Carter, U. S. Patent, 2008, **797666**

[42]. H. Danjo, N. Fukuoka, and T. Mimura, 2008, W.O. **52905**

[43]. R. B. Anderson in "*Catalysis*", Vol 4. Van Nostrand Reinhold, Princeton, New Jersey, 1956

[44]. M. A. Fraga, and E. Jordao, *React. Kinet. Catal. Lett.*, 1998, **64**, 331

[45]. F. Fischer, and K. Meyer, *Brennst.-Chem.*, 1934, **107**, 84

[46]. J. A. Lucero, K.V. Sethi, and H. W. Tuminello, U.S. Patent, 2007, **10342**

[47]. G. R. Moradi, M. M. Basir, A. Taeb, and A. Kiennemann, *Catal. Commun.*, 2003, **4**, 27

[48]. S. Ali, B. Chen, and J. G. Goodwin. *J. Catal.*, 1995, **157,** 35

[49]. P. Chaumette, O. Clause, and H. Azib, European patent, 1997, **400730**

[50]. S. Hinchiranan, Y. Zhang, S. Nagamori, T. Vitidsant, and N. Tsubaki, *Fuel Proc. Tech.*, 2008, **89**, 455

[51]. A. Barbier, E. B. Pereira, and G. A. Martin, *Catal. Lett.*, 1997, **45,** 221

[52]. A. M. Kraan, *Hyperf. Interac.,* 1998, **111**, 23

[53]. V. Ponec, *Stud. Surf. Sci. Catal.*, 1991, **64**, 117

[54]. M. Xiang, D. Li, W. Li, B. Zhong, and Y. Sun, *Catal. Commun.*, 2007, **8**, 503

[55]. M. Xiang, D. Li, W. Li, B. Zhong, and Y. Sun, *Catal. Commun.*, 2007, **8**, 513

[56]. L. Gang, Z. Chengfang, C. Yanqing, Z. Zhibin, N. Yianhui, C. Linjun, and Y. Fong, *Appl. Catal.*, 1997, **150**, 243

[57]. Y. T. Park, I. Nam, and G. Y. Kim, *Ind. Eng. Chem. Res.*, 1997, **36**, 5246

[58]. G. Bian, L. Fan, Y. Fu, and K. Fujimoto. *Appl. Catal., 1998*, **170**, 255

[59]. G. Bian, L. Fan, Y. Fu, and K. Fujimoto. *Ind. Eng. Chem. Res.*, 1998, **3**, 1736

[60]. Z. Li, Y. Fu, and M. Jiang, *Appl. Catal .A. Gen.,* 1999, **187**, 187

[61]. D. Li, C. Yang, W. Li, Y. Sun, and B. Zhong, *Top. Catal.,* 2005, **32**, 233

[62]. D. Li, C. Yang, N. Zhao, H. Qi, W. Li, Y. Sun, and B. Zhong, *Fuel Proc. Tech.*, 2007, **88**, 125

[63]. J. Iranmehboob, H. Toghiani, and D. O. Hill, *Appl. Catal., 2003*, **247**, 207

[64]. J. Bao, Y. Fu, and Z. Sun, *Chem. Commun.*, 2003, **6**, 746

[65]. N. Koizumi, K. Murai, T. Ozaki, and M. Yamada, *Catal. Today.*, 2004, **89**, 465

[66]. D. Li, C. Yang, H. Qi, H. Zhang, W. Li, Y. Sun, and B. Zhong, *Catal. Commun.*, 2004, **5**, 605

[67]. J. Shested, S. Dahl, J. Jacobsen, and J. R. Rostrup-Nielsen, *J. Phys. Chem.*, 2005, **109**, 2432

[68]. X. Xiadong, E. B. M. Doesburg, and J. J. F. Scholten, *Catal. Today.*, 1987, **2**, 125

Chapter 7

Conclusions

An increased interest to develop non-petroleum based alternative methods for the production of fuels and chemical feedstock has led to a need for Fischer Tropsch (F-T) technology. The production and sales of chemical feedstock (by products of the FT synthesis) have significantly increased the economic viability of the FT process.

This thesis has attempted to examine some important advances in Fischer Tropsch reaction since its initial development. A historical review is provided in first chapter in which a detailed comparison of the commonly used catalysts is given along with proposed mechanisms for CO hydrogenation. Chapter 2 is devoted to a detailed description of the equipment and methods used during this study.

One of the main objectives of the current thesis was synthesis of a catalyst which is highly selective to hydrocarbons with a lower selectivity to methane and longer life time. We have investigated an already studied $CoMnO_x$ catalyst. Various preparation variables for this catalyst have been studied in detail in order to find out the best preparation conditions. Variable pH method of co-precipitation has been found to be better compared with an already studied method of constant pH. Precipitation of cobalt and manganese metals at pH=2.8 - 8.00 at 80°C with 0 h ageing was found to be the best method for synthesis of $CoMnO_x$ catalyst. A detailed investigation has been done for the optimization of reaction conditions. Best reaction temperature was found to be 220°C and the best reaction pressure was 6 bar. It has been observed that CO_2 selectivity was very low (almost negligible) for the reactions done at 220°C. While an increase in temperature from 220°C to 240°C increases methane and CO_2 along with an increase in selectivity towards C_{5+} hydrocarbons.

A strong requirement for improved catalysts for the synthesis of more selective products from syngas encouraged an investigation of the effects of metal promoters on an existing but modified $CoMnO_x$ catalyst. Three different concentrations of ruthenium with $CoMnO_x$ catalyst have also been studied. Methane selectivity has been found to be enhanced by the addition of 0.15% Ru, this also giving an increase in the formation of higher hydrocarbons. A small change in concentration of ruthenium gave a large difference in catalyst behavior. Addition of ruthenium, overall, has shown an enhancement in the formation of hydrocarbons.

We have also studied an effect of different concentrations of potassium addition on $CoMnO_x$ catalyst. A particular concentration of 0.15% has found to be good for synthesis

of light hydrocarbons along with the lowest selectivity to methane. Most of the results of potassium addition were found to be similar to the previously reported results. A detailed investigation of the effect of addition of these promoters has been discussed in chapter 4.

The effect of the use of two different types of activated carbons (peat, wood) as support for Co/ Mn and Fe/ Mn catalysts was reported in chapter 5. Co/Mn with addition of both wood and peat derived carbons was found to be more active compared with our pure $CoMnO_x$ catalyst. Co/Mn/C (peat source) was found to be highly selective to synthesis of propylene with higher catalytic activity compared with Co/Mn/C (wood source).

A comparison of Co/Mn and Fe/Mn along with peat and wood carbons has also been given in chapter 5. Fe/Mn/C had low activity at low temperature so these catalysts were tested at 300°C. Fe/Mn/C (peat source) has been found to be highly active with dominant products of alkanes along with high CO_2 and methane compared with Co/Mn/C (peat source).

A combination of activated carbon derived from wood with Fe/Mn (300°C) and Co/Mn (220°C) showed very low activity for CO conversion. Co/Mn/C (wood source) was more selective to propylene with less CO_2 compared with Fe/Mn/C (wood source) which was highly selective to CO_2.

An additional effort has been made for the study of alcohols synthesis from syngas using the well known $CoMoS_2$ catalyst for this reaction. The $CoMoS_2$ catalyst has been prepared under improved conditions and was tested under similar reaction conditions as have already been reported in patent literature. This catalyst has been found to be more active with respect to CO conversion and has shown higher selectivity to 1-propanol and

was less selective to methanol and hydrocarbons. Further $CoMoS_2$ has been modified with Zr, Ti and Ni metals. One particular concentration (0.2%) of these metals has been tested. All three metal promoters have shown low selectivity for alcohols formation. Ni and Ti have been found to be very active for water gas shift reaction while Zr doped catalyst was more active for hydrocarbons synthesis (methane being the main product). Clear differences have been observed in the surface geometry and morphology of these doped catalysts along with a change in surface area measurements. Actual mechanism of these catalysts cannot be argued because of lack of characterization of these catalysts.

An important characteristic of the present studies is that a lot of effort has been made to collect all the products, including liquids and waxes. CO_2 is included in the products and attempts have been made to get a catalyst with the lowest possible selectivity of CO_2. Most of the reported studies do not include liquids, waxes and CO_2.

The reaction of CO hydrogenation by FT technology has provided an indirect route for the production of fine petrochemicals from syngas. This fact alone makes the process very important for future investigation of synthetic fuels production. Since the development of the first methanation catalyst 106 years ago, the Fischer Tropsch process has reached a stage when researchers are able to operate it on the commercial scale. However, there is very little understanding about the actual mechanism of reactions leading to final products.

APPENDIX

Appendix 1

Single bed reactor

A schematic representation of the single bed reactor rig is shown in figure 2.3. This was a simple lab-reactor made of a stainless steel tube (3/16-in i.d.) housed within a single zone furnace. The furnace controlled the temperature of the reactor through a thermocouple dipped inside the catalyst bed.

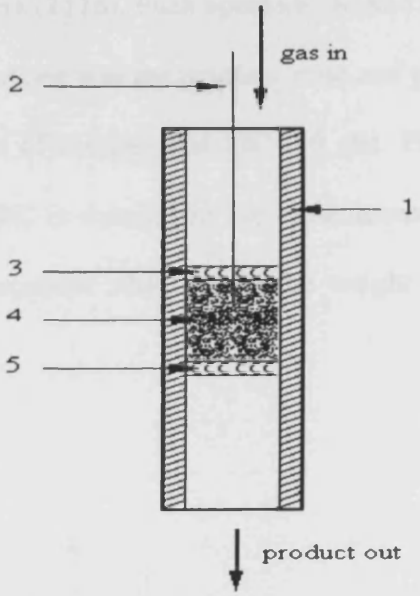

Figure 2.3 Single bed reactor, 1: reactor chamber; 2: thermocouple; 3, 5: quartz wool; 4: catalyst bed.

In this reactor, the catalyst bed was sandwiched between quartz wool plugs.

Appendix 2

High pressure reactor for alcohols synthesis

Flow diagram of high pressure reactor and single bed reactor was exactly similar which is shown in figure 2.5, while schematic of this reactor was different (figure 2.4). It consisted of a stainless steel tube (3/8-in i.d., 27-in length) and a thermo-well (3/16-in o.d.) fitted with an axial thermocouple. The reactor fitted inside a three-heating-zone heated furnace. Temperature control of the furnace was achieved by a control panel that consisted of three Eurotherm controllers (2116). Each controller linked to a single zone.

The middle zone of the reactor was the reaction zone and placed within it the catalyst bed which typically consisted of catalyst and SiC (80 grit, Fischer Scientific). The ratio of volume of catalyst and SiC is detailed in the experimental part of the relevant chapter. The bottom zone had a support tube to hold the weight of the materials in the middle zone above.

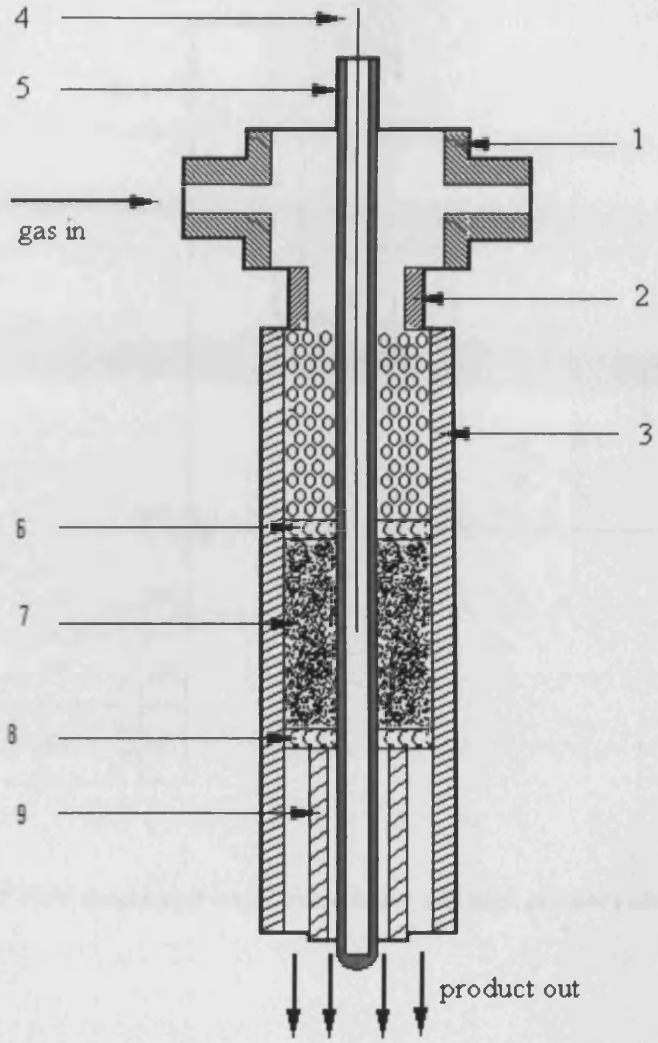

Figure 2.4 Schematic representation of high pressure reactor; 1: cross fitting; 2: connector; 3: reactor chamber; 4: thermocouple; 5: thermowell; 6, 9: quartz wool; 7: catalyst bed; 9: support tube.

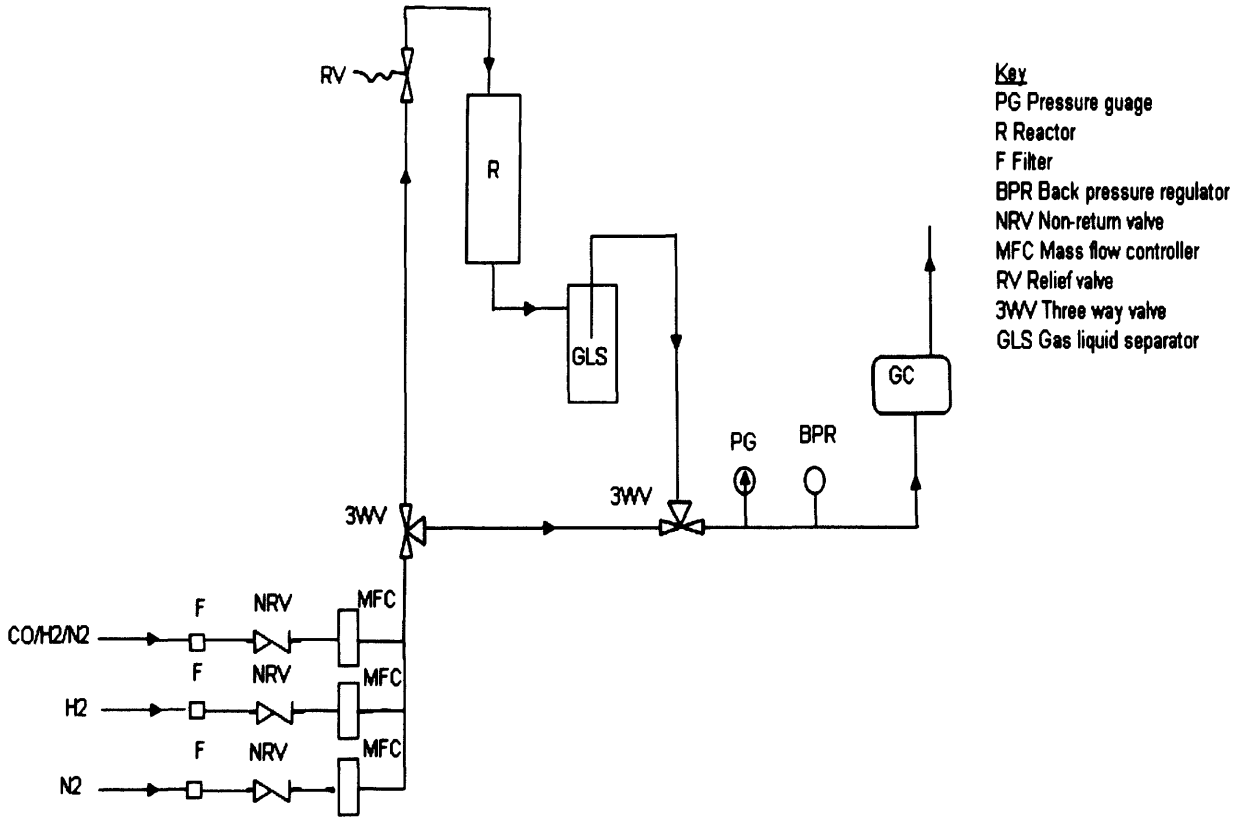

Figure 2.5 Flow diagram of single bed reactor and high pressure alcohols reactor

Appendix 3

Product Analysis for catalysts tested in single bed and high pressure alcohol reactor

Analysis of gaseous product was achieved by an online gas chromatograph (GC, Varian 3800). A 5m*1/8 inch stainless steel Porapak-Q column (mesh size 80-100) was used to separate the reactants and products. Concentrations of hydrogen, carbon monoxide, carbon dioxide and nitrogen were analyzed by a thermal conductivity detector (TCD). The TCD compares the conductivity of the analyzed gas to that of a reference gas. Conversion was determined using an internal standard, nitrogen. Organic compounds such as hydrocarbons and oxygenates were determined by a flame ionization detector (FID). By using a hydrogen and air flame, the FID burns the organic compounds into ions whose amounts are roughly proportional to the number of carbon atoms present.

Liquid products from alcohols reactor were identified by gas chromatography mass spectrometer (GC-MS, Perkin Elmer TurboMass). Quantification of liquid products was determined by an offline GC equipped with a Chrompack capillary column (CP-Sil 8CB, 30m, 0.32mm, 1μm) and an FID detector.

Appendix 4

6-bed reactors

CO hydrogenation for most of the catalysts for light alkenes synthesis was carried out using six fixed-bed laboratory reactors as shown schematically in figure 2.6, which enabled the testing of catalysts under identical experimental conditions.

The reactors were constructed from 316 stainless steel with an internal diameter of 14mm. Test experiments showed that blank thermal reactions in the absence of catalysts were negligible at and below 300°C. The reactor consisted of two main parts: (i) the reactor section containing 0.5g of catalyst and (ii) a post reactor liquid and wax trap. Overall, figure of these reactors was similar to the single bed reactor presented in figure 2.3. Preheated gas and catalyst temperatures were measured using K-type thermocouple positioned in the centre of catalyst bed. Premixed synthesis gas (typically CO 47.5%, H_2 47.5%, N_2 5% v/v) and H_2 (for reduction) were fed to the combined reactors at flow rates controlled using mass flow controllers (BROOKS 5850S). The pressure was controlled using a back pressure regulator (Pressure rang 1-30 bar) located down stream of the reactor and wax/liquid trap. High boiling wax products were trapped in the post-reactor trap which was held at about +/- 140°C reaction temperature. Lower boiling waxes and liquids passed through into the trap which was held at room temperature.

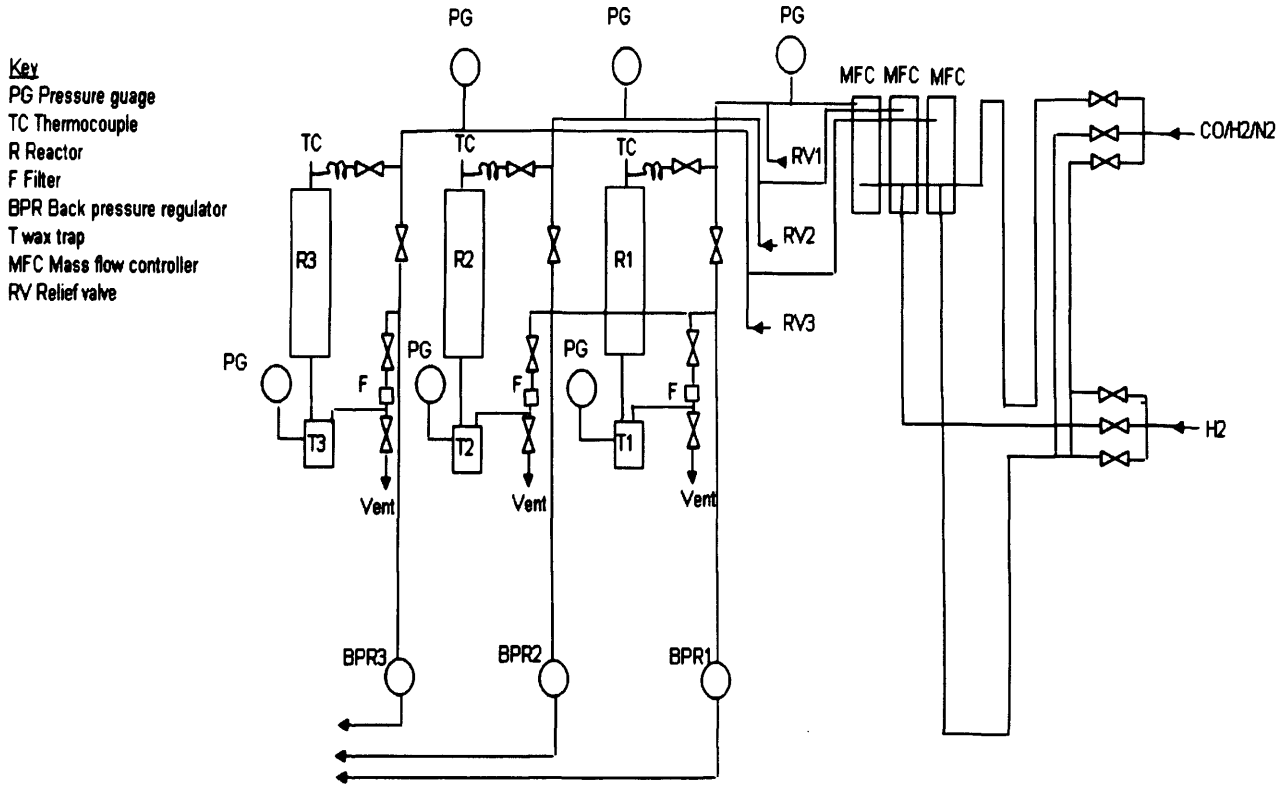

Fig.2.6 Schematic of one set of 6-bed reactors

Six reactors were arranged in set of 2 ovens, three reactors in each oven. Figure 2.6 presents one set of these reactors and the other one was exactly similar to this.

Appendix 5

Data Evaluation

A procedure of data manipulation was required, in order to obtain quantitative data in the form of individual product selectivities from the integrated response of the respective gas chromatographs. Two types of calculation methods were used for the evaluation of data. One method was based on used of a correction factor, outlined by Dietz [4], while the other method was based on use of online response factors of particular products in gas phase. Both of these methods have been detailed below:

i) Data collection by use of Dietz's correction factors

The varying response of the detector to each product component was corrected by multiplying each component's area counts by Dietz's correction factors. Since the selectivity of each component of the product yield from a catalyst was quoted in percent mass derived from equation (1).

Selectivity of component i = mass of i/ total mass of all components*100/1 (1)

Gas product's concentration was converted from mass percent into volume percent, using standard gas mixtures with known volume percent; with the method detailed by Mike [5], as detailed in eq. (2) and (3). The volume percent of gas components was then converted into grams per component shown in eq (4).

Factors for correcting %m/m to %v/v

$$\varepsilon = (\%v/v * M_w)/\%m/m \qquad (2)$$

where M_w = molecular weight of the component

ε factor was calculated by using a standard gas calibration for a 1%v/v for a given gas.

Volume percent of the gas components can be calculated from eq (3).

$$\%v/v = (\%m/m^* \varepsilon)/M_w \qquad (3)$$

Ideal gas law was used for calculation of grams of gas products per component

$$n = PV/RT$$

where n (the number of moles) is used to calculate the mass percent per component using the following equation

$$\text{mass of component i} = N_i * M_{wi}$$

and V= inlet flow rate (ml/hr)*mass balance period (hrs)*%v/v

After addition of weight of liquids and solid masses, the percentage of each compound was calculated.

Calculation of conversion

An indication of the activity of the catalyst was determined by the extent of conversion of the carbon monoxide or for more active catalysts by the extent of volume reduction of the reagent gases (using nitrogen as internal standard). The basic equation used was

$$\text{Conversion \%} = \text{Moles of } CO_{in} - \text{moles of } CO_{out}/\text{moles of } CO_{in} * 100/1$$

ii) Data collection by using the online response factors

First of all, the varying response of the detector to each product component was converted into %v/v by, multiplying them with online calibration factors. Then these were converted into moles by taking account the flow out of internal standard, moles of feed in and time in hours. Moles of each product were converted into moles% and selectivity % was measured by taking carbon numbers into account. Mass of gas products was measured by multiplying the number of moles with molecular weight of particular product. Mass of gas products was combined with the mass of liquids and solids. Selectivity by mass was calculated for all products by normalization with the total mass of gases, liquid and solids.

A simplistic example is presented below for data evaluation of hydrocarbons by using both methods.

i) Dietz's factors

Total catalyst run time=58 hours; mass of liquids accumulated =0.09 g'mass of solids accumulated = 0.1g; gaseous flow rate = 5ml/min

Gas analysis:

Components	Area	C.F.	Corrected area	%m/m	%v/v[b]	Actual mass(g)[c]
CH_4	51566.2	0.97	53161	26.4	2.4	0.49
C_2H_6	18941.7	0.97	19527.5	9.6	0.2	0.18
C_2H_4	8184.1[a]	1.07	7648.7	3.8	0.4	$7*10^{-2}$
C_3H_8	22566.7	0.98	23027.2	11.3	0.3	0.21
C_3H_6	75396.2	1.02	76934.9	38.2	1.3	0.71
C_4 hydrocarbons	13358.1	1.09	12255.1	6.06	0.15	0.11
C_5 hydrocarbons	10216.8	1.03	9823.8	4.85	0.1	$9*10^{-2}$
CO_2	267	44	6.07	0.05	$1.2*10^{-3}$	$2*10^{-3}$

Mass of gases'liquids'solids = 1.862 + 0.09 + 0.01 = 1.962g. Therefore final mass distribution (%m/m) is:

CH_4	24.9%
C_2H_4	3.6%
C_2H_6	9.1%
C_3H_6	36.1%
C_3H_8	10.8%
C_4 hydrocarbons	5.7%
C_5 hydrocarbons	10.1%
CO_2	0.12%

Factor for correcting %m/m to %v/v, $\acute{\varepsilon} = (\%v/v * M_w)/\%m/m$ - (1), where M_w = molecular weight of component.

(a) 1% v/v C_2H_4 has an integrated peak area of 252847 unit from calibrations.

Therefore from eq. (1)

$\acute{\varepsilon} = ((8184.1 / 252847) * 28.1)/2.4 = 0.38$

(b) From (1), $\%v/v = \%m/m * \acute{\varepsilon} / M_w$

(c) Using mass = n * M_w, where n=number of moles = PV/RT (Ideal gas equation), and V is calculated from

Total gas volume * %v/v = 10ml/min * 58 hours *%v/v

Definitions: C.F. = Correction factor; Area=integrated GC response; %m/m=% by mass'%v/v=%by volume.

ii) Calculations using the online GC calibration factors:

Components	Area	V/V (%)	Mole (%)	Selectivity (%)	mass of gas produced (g)
CH_4	51566.2	2.68	40.29	22.55	$8.1*10^{-2}$
C_2H_6	18941.7	0.48	7.26	8.12	$6.2*10^{-3}$
C_2H_4	8184.1	0.09	1.35	1.51	$1.0*10^{-3}$
C_3H_8	22566.7	0.41	6.28	10.55	$7.5*10^{-3}$
C_3H_6	75396.2	1.34	20.23	33.96	$2.3*10^{-2}$
C_4 hydrocarbons	13358.1	0.22	3.39	7.58	$5.6*10^{-3}$
C_{5+} hydrocarbons	10216	0.11	1.72	4.82	$2.7*10^{-3}$
CO_2	267	1.30	19.48	10.90	$2.4*10^{-2}$

Mass of gases'liquids'solids = 0.089 + 0.09 + 0.01 = 0.19g. Therefore final mass distribution (%m/m) is:

CH_4	9.8
C_2H_4	0.6
C_2H_6	3.3
C_3H_6	12.2
C_3H_8	4.0
C_4 hydrocarbons	3.0
C_{5+} hydrocarbons	54.2
CO_2	12.98

Calculations for data evaluation of alcohols

For gas phase product, the concentration (v %) of component i at time x (x = 1-60) can be obtained from GC analysis. The flow rate at time x (x = 1-60) of effluent out gas can be calculated using internal standard (N_2). With these two parameters known, the molar rate of component i at time x can be obtained. For example, at time 20 hour, the concentration of CO is 45.1% and the calculated flow rate (out) is 89.3 ml/min, the molar rate of CO at time 20 hour can be obtained as below.

Molar rate of component CO = 45.1% * (89.3 ml/min)*(60 min/hour)

*(1liter/1000ml) *(1 mole/24.2liter)

= 0.10 mole/hour

The molar rate of other components at 20 hours can be calculated in a similar way. Method of online response factors was used for calculation of alcohols selectivity. For liquid phase product, composition of the liquid can be obtained from GC. With the total weight known (for example weight of total liquid collected = y g), the moles of each component can be calculated. With the moles of gas product and liquid product known, the total moles of carbon out of system can be calculated.

$$\text{Carbon mole (out)} = \sum_{j=1}^{60} CO(mole)_{out} + \sum_{j=1}^{60} CO_2(mole) +$$

$$\sum_{j=1}^{60} CH_4(mole) + 2^* \sum_{j=1}^{60} C_2H_4(mole) +$$

$$2^* \sum_{j=1}^{60} C_2H_6(mole) + 3^* \sum_{j=1}^{60} C_3H_6(mole) +$$

$$3^* \sum_{j=1}^{60} C_3H_8(mole) + \ldots + CH_3OH\ (mole) +$$

$$2^* C_2H_5OH\ (mole) + 3^* C_3H_7OH\ (mole) + \ldots$$

$$= z \text{ mole}$$

$$\text{Error percentage} = \frac{Carbon(in) - Carbon(out)}{Carbon(in)} * 100$$

Gas analysis:

Components	Area counts	V/V (%)	moles
CH_4	3813988	30.91	0.70
C_2H_4	475	$1.96*10^{-3}$	$4.49*10^{-5}$
C_2H_6	69098	0.46	$1.1*10^{-2}$
C_3H_6	3980	0.02	$4.1*10^{-4}$
C_3H_8	95388	0.99	$2.3*10^{-2}$
C_4H_8	1125	$4.2*10^{-3}$	$9.6*10^{-4}$
C_4H_{10}	53777	0.21	$5.1*10^{-3}$
C_5H_{10}	666	0.08	$2.3*10^{-3}$
C_5H_{12}	25698	1.39	$3.2*10^{-2}$
C_6H_{12}	1999	0.01	$1.7*10^{-4}$
C_6H_{14}	3958	0.01	$3.3*10^{-4}$
CO_2	42267	11.20	0.25

Liquids analysis:

Components	Area counts	Moles
Methanol	1667982	52124.43
Ethanol	645511	14002.40
1-Propanol	261344	4348.48
2-methyl,1-propanol	19395	261.67
1-butanol	120823	1369.87

In next step, moles of all products can be converted into moles% in order to calculate selectivity%.

Components	Moles (%)	Carbon moles	Carbon mole selectivity (%)
CH_4	45.17	0.70	50.8
C_2H_4	$2.8*10^{-3}$	$2.2*10^{-4}$	$1.61*10^{-3}$
C_2H_6	0.68	$5.29*10^{-3}$	0.4
C_3H_6	0.03	$1.36*10^{-4}$	$9.8*10^{-3}$
C_3H_8	1.44	$8.1*10^{-3}$	0.5
C_4H_8	0.01	$2.4*10^{-5}$	$1.7*10^{-3}$
C_4H_{10}	0.30	$1*10^{-2}$	0.1
C_5H_{10}	0.11	$3.5*10^{-4}$	$2.5*10^{-2}$
C_5H_{12}	0.11	$3.58*10^{-4}$	$2.6*10^{-2}$
C_6H_{12}	0.01	$2.8*10^{-4}$	$2.0*10^{-3}$
C_6H_{14}	0.02	$5.5*10^{-4}$	$3.9*10^{-3}$
CO_2	16.3	0.25	18.4
Methanol	19.42	0.3	21.8
Ethanol	10.43	$8.2*10^{-2}$	5.9
1-propanol	4.23	$2.2*10^{-2}$	1.6
2-methyl1-propanol	0.22	$1*10^{-3}$	0.1
1-butanol	1.40	$4*10^{-3}$	0.3

Appendix 6

Product Analysis of catalysts tested in 6-bed reactors

Analysis of gaseous product was achieved by an online gas chromatograph (GC, Varian 3800). Three columns were used for analysis of gaseous products, (Front-Varian CP-Al_2O_3/KC, 25m, 0.32mm, 5μm, CP7519, Middle-Mol sieve 13X, 60-80 Mesh, Rear-Hayesep C, 80-100 Mesh).

Concentrations of hydrogen, carbon monoxide, carbon dioxide and nitrogen were analyzed by a thermal conductivity detector (TCD). Conversion was determined using an internal standard, nitrogen. Organic compounds such as hydrocarbons and oxygenates were determined by a flame ionization detector (FID).

Appendix

Appendix

6 BED FISCHER TROPSCH REACTOR GC SCHEMATIC.
INSTALLATION JUNE 2006
SABIC PROJECT
T. DAVIES
K. COLE
S. IQBAL.

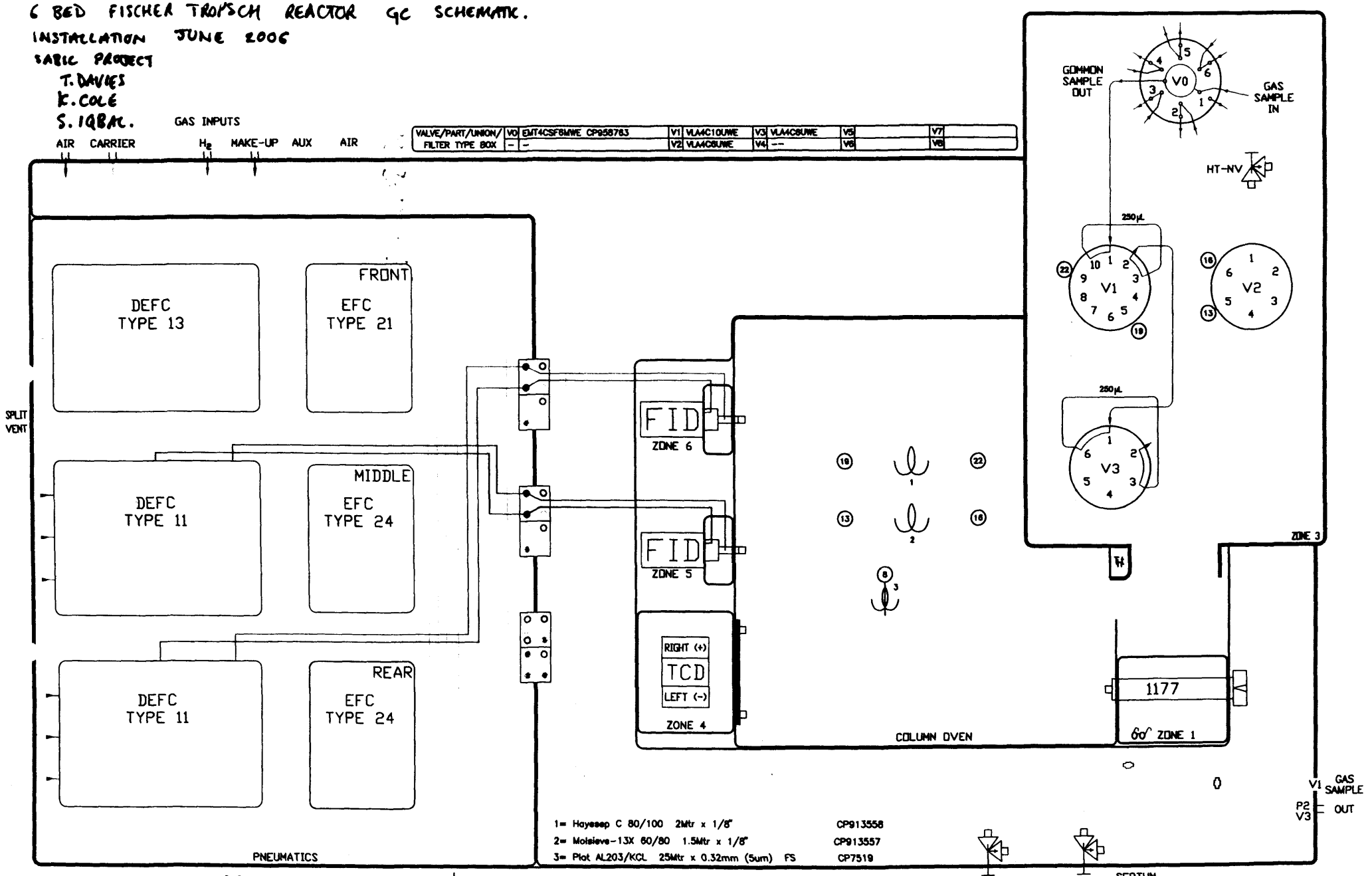

60° = Note: Physical located on ZONE 2 | ⊬ = All column and other transfers through heated transit

FITTINGS: 1=1/16" 2=1/8" 3=3/16" 4=1/4"
FLOW CONTROLLER
ON/OFF & METERING VALVE
PRESSURE REGULATOR

HEATED ZONES

ZONE	TYPE	TEMP. LIMIT	LOCATION	COOLANT
COL. OVEN	COL. OVEN	200°C	COL. OVEN	NONE
1	1177	280°C	FRONT	NONE
2				
3	L.v.v OVEN	200°C	REAR	NONE
4	TCD	380°C	FRONT	NONE
5	FID	350°C	MIDDLE	NONE
6	FID	350°C	REAR	NONE

COLOR LEGEND
CARRIER
MAKE-UP
HYDROGEN
AIR
SAMPLE

VALVE AND EXTERNAL EVENT CONNECTIONS

V#	CCW or OFF(-)	CW or ON(+)	EE#
1	FILL+BACKFLUSH	INJECT	1
2	SERIES	BYPASS	2
3	FILL	INJECT	3
4			4
5			5
6			6
7			7

DRAWN BY	DATE	REVISED BY	DATE
VERMEULEN	28.11.06	–	
APPROVED	DATE	CHECKED	DATE
L.BOS	28.11.06	VERMEULEN	28.11.06

MODEL 3800 CUSTOM PLUMBING DIAGRAM
BASED ON CS-413 + CS-100

ORDER NUMBER	SERIAL NUMBER	
9494594	103499	0 ECR
		1 REV